INTER TURN FAULT ANALYSIS OF CAGE INDUCTION MOTOR

A DISSERTATION

Submitted in partial fulfillment of the requirements for the award of the degree of

INTEGRATED DUAL DEGREE

in

ELECTRICAL ENGINEERING

(With Specialization in Power Electronics)

By

SRIKONDA HARI KISHAN

DEPARTMENT OF ELECTRICAL ENGINEERING
INDIAN INSTITUTE OF TECHNOLOGY ROORKEE
ROORKEE - 247 667 (INDIA)

JUNE, 2012

I.D. No. MT/188/SPG/51

CANDIDATE'S DECLARATION

I hereby declare that the work that is being presented in this project entitled **"INTER TURN FAULT ANALYSIS OF CAGE INDUCTION MOTOR"** in partial fulfillment of the requirement for the award of the degree of **Integrated Dual Degree** in **Electrical Engineering** submitted to the **Department of Electrical Engineering, Indian Institute of Technology Roorkee, India** is an authentic record of my own work carried under the guidance of **Dr. S.P. GUPTA, Professor**, Department of Electrical Engineering, Indian Institute of Technology, Roorkee.

The matter embodied in this dissertation has not been submitted for the award of any other degree or diploma.

S. Hari Kishan

Date: 12 June 2012 **SRIKONDA HARI KISHAN**

Place ROORKEE

CERTIFICATE

This is to certify that the above statement made by the candidate is true to the best of my knowledge.

S.P. Gupta

Date: 12th June/12 **Dr. S.P. GUPTA**

Place: Roorkee Professor

Dept. of Electrical Engineering

Indian Institute of Technology Roorkee

Roorkee – 247667 (INDIA).

ACKNOWLEDGEMENT

I wish to acknowledge my deep sense of gratitude and indebtedness to my respected guide **Prof. Dr. S.P. GUPTA**, Department of Electrical Engineering, Indian Institute of Technology Roorkee, Roorkee for his intuitive and meticulous guidance and perpetual inspiration in completion of this dissertation work. I want to express my profound gratitude for his co-operation in scrutinizing the manuscript and his valuable suggestions throughout the work. I feel privileged to work under him during the course of work. His encouraging support and thorough involvement in the formulation of the research work and preparation of manuscript are gratefully acknowledged.

I convey my gratitude to the entire faculty for helping me to widen my knowledge through discussions at the time of seminar and project presentations.

I express my sincere thanks to all the research scholars of our department for helping me in revealing my doubts as when necessary.

I would like to mention my special thanks to my parents for their endless support and encouragement and for always believing, and helping me to believe, that I can succeed at anything.

S. Hari Kishan

Date: 12 June 2012 SRIKONDA HARI KISHAN

Place: Roorkee Enrol.no-071605

ABSTRACT

Increasing interest has been seen in condition monitoring techniques for rotating electrical machines in power plants, because condition monitoring has the potential to reduce operating costs, enhance the reliability of operation, and improve power supply and service to customers. For fault identification in induction motors, apart from locating specific harmonic components in the line current (popularly known as motor current signature analysis), other signals, such as speed, torque, noise, vibration etc., are also explored for their frequency contents. Sometimes, altogether different techniques, such as thermal measurements, chemical analysis, etc., are also employed to find out the nature and the degree of fault. In addition, human involvement in the actual fault detection decision making is being replaced now by automated tools, such as expert systems, neural networks, fuzzy-logic-based systems; to name a few. It is indeed evident that this area is potentially important.

Computer simulation of motor operation can be particularly useful in gaining an insight into its dynamic behavior and electro-mechanical interaction. With a suitable model, motor faults may be simulated and the change in corresponding parameters can be estimated. This can significantly reduce the computer simulation time and make model-based condition monitoring more reliable and easily achievable.

In the present work, two models with orthogonal axis are developed for simulation of three-phase induction motors having asymmetrical windings and inter-turn short circuits on the stator. The first model assumes that each stator phase winding has a different number of turns. To model shorted stator turns, the second model assumes phase *as* has two windings in series, representing the unaffected portion and the shorted portion. It uses the results of the first model to transfer phase *as* to *qd* so that shorted portion is transferred to the *q* axis. Simulations results from the models are in good agreement with other studies and are validated with the experimental results obtained. A third model has been developed with the same considerations which can incorporate the fault in an induction motor under operation. The models have been successfully used to study the transient and steady state behaviour of the induction motor with short-circuited turns. The study has been further extended to analyze the effect of voltage unbalance on the characteristics of an induction motor with inter turn fault.

CONTENTS

LIST OF FIGURES / TABLES

Table No.	Table Description	Page No.
1.1	Table: Comparison between induction machine models	4

CHAPTER 1
INTRODUCTION AND LITERATURE REVIEW

1. 1 Introduction

Electrical motors are the majority of the industry prime movers and are the most popular for their reliability and simplicity of construction. Although induction motors are reliable, they are subjected to some mode of failures. These failures may be inherent to the machine itself or due to operating conditions. The origins of inherent failures are due to the mechanical or electrical forces acting in the machine enclosure. Researchers have studied a variety of machine faults, such as winding faults, unbalanced stator and rotor parameters, broken rotor bars, eccentricity and bearing faults. Different methods for fault identification have been developed and used effectively to detect the machine faults at different stages using different machine variables, such as current, voltage, speed, efficiency, temperature and vibrations. Thus, for safety and economic considerations, there is a need to monitor the behaviour of large motors, as well as small motors, working in critical production processes.

Traditional maintenance procedures in industry have taken two routes; the first is to perform fixed time interval maintenance, where the engineers take advantage of slower production cycles to fully inspect all aspects of the machinery. The second route is to simply react to the plant failure as and when it happens. However, making use of today's technology, a new scientific approach is becoming a new route to maintenance management. One of the key elements to this new approach is predictive maintenance through condition monitoring, which depends upon the condition of the plant. Condition monitoring is used for increasing machinery availability and performance, reducing consequential damage, increasing machine life, reducing spare parts inventories and reducing breakdown maintenance. An efficient condition-monitoring scheme is capable of providing warning and predicting the faults at early stages. There are many ways to detect mechanical and electrical problems in induction motors, either directly or indirectly, such as vibration monitoring, motor current signature analysis (MCSA), electromagnetic field monitoring, chemical analysis, temperature measurability, infrared measurement, acoustic noise analysis, and partial discharge measurement. Among these

methods, vibration analysis and current analysis are the most popular due to their easy measurability, high accuracy, and reliability.

Directly, many parameters can be monitored to provide useful indications of incipient faults. These parameters include case vibration and noise, stator phase current, air-gap or external magnetic flux density.

Indirectly, modeling and simulation of electrical machine operation under healthy and faulty conditions will also provide useful information for fault prediction and identification. Computer simulation of motor operation can be particularly useful in gaining an insight into their dynamic behavior and electro-mechanical interaction. With a suitable model, motor faults may be simulated and the change in corresponding parameters can be simulated. It has been found that an accurate motor simulation can be achieved with a general model and accurate parameter selection, in spite of using a sophisticated model. This can significantly reduce the computer simulation time and make model-based condition monitoring more reliable and easily achievable [1], [2].

1.2 Literature review

A basic paper for induction machine analysis has been reported by Stanley [3]. The analysis made by Stanley is based on the direct three-phase model using phase variables and its presentation in shifted reference axis. Later on, many researchers made their contributions on the basis of the machine model given by Stanley with some modifications.

Patel et al. [4] have presented a quality mathematical model of induction machine based on the steady state and dynamic equations and D-Q transformation technique. This model can be used for steady state as well as transient analysis of squirrel cage or wound rotor structure. The model has been used to investigate the effects of variations in the machine size and parameter values on the dynamic performance of induction machine. Different operating conditions are simulated using MATLAB code. Also, the behavior of the induction machine is observed with and without supply harmonics. Pahwa and Sandhu[5] have proposed a q-d axis based modeling to analyze the transient performance of three-phase squirrel cage induction motor using stationary reference frame, rotor reference frame and synchronously rotating reference frame. Simulated results have been compared and verified with experimental results on a test machine. The proposed system has been developed using MATLAB/SIMULINK. Javed

and Izhar [6] have developed a method which relies on the continuous measurement of the phase difference between the terminal voltages of the machine. for the detection of phase failure faults in poly phase Induction machines. The proposed method has been simulated using MATLAB/SIMULINK. The simulated results show the reliability and usefulness of this method. Akpama et al.[7] have presented the simulation of induction machine performance under unbalanced source voltage conditions and the analysis of induction machines under balance and unbalanced conditions has been made. The models representing the machine under balance and unbalanced conditions were simulated with the help of MATLAB and the simulated results compared. The results proved that the operation performance of an induction machine can be studied using simulated result from MATLAB without going through the rigorous analytical method. Arkan et al. [8] have proposed two models for simulation of three-phase induction motors with inter-turn short circuits on the stator. The models have been successfully used to study the transient and steady state behaviour of the induction motor with short-circuited turns, and to test stator fault diagnostic algorithms operating in real time. Liang et al. [9] have presented both a theoretical and experimental analysis of asymmetric stator and rotor faults in induction machines. A three-phase induction motor was simulated and operated under normal healthy operation, with one broken rotor bar and with voltage imbalances between phases of supply. Vilas et al. [2] have reported a mathematical foundation and theoretical analysis of asymmetric stator faults in induction machines. A three-phase induction motor is simulated with simple differential equations. Experimental verification of excitation current under healthy condition is also been discussed.

Ueda et al. [10] have studied the effect of supplying the machine from variable frequency source from the point of view of stability. The effect of the machine parameter's variation on the machine stability has been discussed. Levi et al. [11,12]have reported the modelling of induction motor and synchronous machine considering sinusoidal and non-sinusoidal supply. The models are based on d-q axes and the analysis includes the effect of machine saturation and core loss. Different control strategies of induction motor are also considered. Neto et al. [13]have presented a mathematical model of three-phase induction motor using phase variables. The model is based on the harmonic impedance concept and accordingly, the voltage and torque equations are derived. Two cases are included in the analysis, supplying the machine from sinusoidal and non-sinusoidal supply using PWM inverter. Toliyat et al.

[14_16] have developed an analysis method for modelling the multiphase cage induction motor. The model considers the m.m.f harmonics using winding function approach. The model is used effectively to simulate different types of machine faults, such as asymmetry in the stator winding, air-gap eccentricity and rotor bar fault. Joksimovic and Penman[17]have presented an induction motor model based on the winding function approach to investigate the relation between the machine faults and the current harmonics. The simulation and analytical results are verified by experimental investigation. The developed algorithm is compatible with commercially available software.

A comparison of various reference frame models with phase variables based model is presented in Table 1.1 [18]. Although the complexity of phase variable model and the time needed for simulation of the machine behavior is high in comparison with the other models, it can be used to cover all the machine conditions with ease of implementation.

Table 1.1: Comparison between induction machine models

Machine model	Complexity	Characteristics
Phase variable model	6 x 6 matrix	Suitable for all machines conditions. Direct presentation of machine variables. Better suited for unbalanced condition of supply and stator.
Stationary reference frame	4 x 4 matrix	Better suited for unbalanced condition of supply and stator. Transformations needed of machine variable.
Rotor reference frame	4 x 4 matrix	Better suited for unbalanced condition of rotor faults. Transformations needed of machine variable.
Synchronously rotating reference frame	4 x 4 matrix	Better suited for non-sinusoidal supply. Transformations needed of machine variable.

When the machine is fed from voltage or frequency converters, or it is subjected to some mode of supply faults or unbalanced in stator and rotor circuits, some modifications in the machine model are needed. One of the common methods used to model such conditions under steady state is the symmetrical component method. The extension of this method is the instantaneous symmetrical components (InSC), which is used to formulate the dynamic equations of induction motors [19].

The induction machine health identification can be achieved with the aid of a high precision computer controlled on-line monitoring system based on-line machine modeling. In this system, three-phase currents, three-phase voltages and speed are recorded on-line and stored in the computer memory. The recorded three phase voltages are fed to the developed machine model in order to calculate the machine currents and to predict the machine conditions. By

comparing the actual recorded machine currents (recorded simultaneously with the machine voltages) with the simulated currents, the machine condition can be obtained qualitatively. One of the effective methods, which has been adopted recently to predict machine condition using machine currents, is Park's vector approach [20]. This approach is based on the rotating reference frame model of the induction machine. If the machine is healthy and the q axis current vector component i_q is drawn against d-axis current vector component i_d, a circular locus centered at the origin of the co-ordinates will be obtained. However, if the relation between i_q and i_d is not producing a regular circle, the induction machine health or the supply conditions are questionable. Monitoring of the relation between Park's vector components can identify different types of machine faults.

Modelling of induction motors with shorted turns is the first step in the design of turn fault detection systems [21].Simulation of transient and steady state behaviour of motors with these models enable correct evaluation of the measured data by diagnostic techniques. The asymmetrical induction machine has been a subject of considerable interest. Brown and Butler [22] have utilized symmetrical component theory to establish a general method of analysis for operation of poly phase induction motors having asymmetrical primary connection. Jha and Murthy [23] have utilized rotating field concepts to develop a generalized theory of induction machines having asymmetrical windings on both stator and rotor. Winding-function-based models presented in Refs. [24,25],and models presented in Refs. [26,27] need motor geometrical design parameters.

The generalized theory of electrical machines incorporating orthogonal or qd0 axis theory is generally accepted as the preferred approach to almost all types of transient and steady state phenomena [28]. The analysis of machines is greatly facilitated by the standard transformation to qd0 axis. The same transformation process can be applied to machines in which there are phase unbalances [29].Hence, it is useful to extend this approach to also incorporate problems encountered with asymmetrical induction motors.

1.3 Dissertation organization

The present **Chapter 1** presents an overview on the need for condition monitoring, the various condition monitoring techniques and states the advantages of computer simulation for fault analysis. Brief Literature review on the previous work in the area of fault analysis has been presented.

The **Chapter 2** discusses about the common faults present in an induction motor. The causes for these various faults and the ease with which they can be detected are also presented. In order to identify the weakest component in electrical motors that is subjected to failure, some statistical studies about the machine failure were also discussed.

The **Chapter 3** presents a review of existing induction motor condition monitoring methods. This covers a variety of topics, techniques, methods, and approaches. The practical use of various condition monitoring methods for fault diagnosis of electric machines were also presented.

The **Chapter 4** discusses the development of simulation models of induction motor with different number of turns and with stator inter turn fault using the motor equations transformed to stationary reference frame (qd axis).

The **Chapter 5** discusses the simulation results that have been obtained from the developed models and the inter-turn fault analysis has been carried out. The variations in the torque characteristic, speed, positive and negative sequence current and the short circuit current have been observed. The variation of the negative sequence current and the short circuit current with the number of shorted turns at different values of external resistance has been observed. The effect of unequal winding temperature due to voltage unbalance on the negative sequence current has been considered. Also, the effect of voltage unbalance on the various characteristics of an induction motor with inter turn fault has been observed.

The **Chapter 6** highlights the main conclusions drawn from the work done. Future scope for the improvements to get better performance is presented.

CHAPTER 2

INDUCTION MOTOR FAULTS

2.1 Induction Motors

Electrical machines are extensively used and are the core of most engineering systems. These machines have been used in all kinds of industries. An induction machine is defined as an asynchronous machine that comprises a magnetic circuit which interlinks with two electric circuits, rotating with respect to each other and in which power is transferred from one circuit to the other by electromagnetic induction. It is an electromechanical energy conversion device in which the energy converts from electric to mechanical form. The energy conversion depends upon the existence in nature of phenomena, interrelating magnetic and electric fields on the one hand, and mechanical force and motion on the other. The rotor winding in induction motors can be squirrel-cage type or wound-rotor type. Thus, the induction motors are classified into two groups:

- Squirrel-cage and
- Wound-rotor induction motors.

The squirrel cage induction motor consists of conducting bars embedded in slots in the rotor iron and short circuited at each end by conducting end rings. The rotor bars are usually made of copper, aluminum, magnesium or alloy placed in slots. Standard squirrel cage rotors have no insulation since bars carry large currents at low voltages. Another type of rotor, called a form-wound rotor, carries a poly phase winding similar to three phase stator winding. The terminals of the rotor winding are connected to three insulated slip rings mounted on the rotor shaft. In a form-wound rotor, slip rings are connected to an external variable resistance which can limit starting current and associated rotor heating. During start-up, inserting external resistance in the wound-rotor circuit produces a higher starting torque with less starting current than squirrel-cage rotors. This is desirable for motors which must be started often.

The squirrel-cage induction motor is simpler, more economical, and more rugged than the wound-rotor induction motor. A squirrel-cage induction motor is a constant

speed motor when connected to a constant voltage and constant frequency power supply. If the load torque increases, the speed drops by a very small amount. It is therefore suitable for use in constant-speed drive systems. On the other hand, many industrial applications require several speeds or a continuously adjustable range of speeds. DC motors are traditionally used in adjustable drive systems. However, since DC motors are expensive, and require frequent maintenance of commutators and brushes. Squirrel-cage induction motors are preferred because they are cheap, rugged, have no commutators, and are suitable for high-speed applications. In addition, the availability of solid state controllers has also made possible to use squirrel-cage induction motors in variable speed drive systems. The squirrel-cage induction motor is widely used in both low performance and high performance drive applications because of its roughness and versatility.

2.2 Induction Motor Faults

The Induction motor is considered as a robust and fault tolerant machine and is a popular choice in industrial drives. It is important that measures are taken to diagnose the state of the machine as and when it enters into the fault mode. It is further necessary to do so on-line by continuously monitoring the machine variables. The reasons behind failures in rotating electrical machines have their origin in design, manufacturing tolerance, assembly, installation, working environment, nature of load and schedule of maintenance. Induction motor, similar to other rotating electrical machines, is subjected to both electromagnetic and mechanical forces. The design of the motor is such that the interaction between these forces under normal condition leads to a stable operation with minimum noise and vibrations. When the fault takes place, the equilibrium between these forces is lost, leading to further enhancement of the fault.

The common internal faults can be mainly categorized into two groups:

- Electrical faults
- Mechanical faults

Electrical faults include faults caused by winding insulation problems, and some of the rotor faults. Mechanical faults include bearing faults, air gap eccentricity, load faults and misalignment of shaft.

2.2.1 Electrical faults

The following electrical faults are very common in three phase induction motor while operating in industries.

2.2.1.1 Rotor faults

Usually, lower rating machines are manufactured by die casting techniques whereas high ratings machines are manufactured with copper rotor bar. Several related technological problems can rise due to manufacturing of rotors by die casting techniques. It has been found that squirrel cage induction motors show asymmetries in the rotor due to technological difficulties, or melting of bars and end rings. However, failures may also result in rotors because of so many other reasons. There are several main reasons of rotor faults [30, 1].

- During the brazing process in manufacture, non uniform metallurgical stresses may be built into cage assembly and these can also lead to failure during operation.
- A rotor bar may be unable to move longitudinally in the slot it occupies, when thermal stresses are imposed upon it during starting of machine.
- Heavy end ring can result in large centrifugal forces, which can cause dangerous stresses on the bars.

Because of the above reasons, rotor bar may be damaged and simultaneously unbalance rotor situation may occur. Rotor cage asymmetry results in the asymmetrical distribution of the rotor currents. Due to this, damage of the one rotor bar can cause the damage of surrounding bar and thus damage can spread, leading to multiple bar fractures. In case of a crack, which occurs in a bar, the cracked bar will overheat, and this can cause the bar to break. Thus, the surrounding bar will carry higher currents and therefore they are subjected to even larger thermal and mechanical stresses which may also start to crack [1]. Most of the current which would have flowed in the broken bar now will flow in the two bars adjacent to it. Thus, the large thermal stresses may also damage the rotor laminations. The temperature distribution across the rotor lamination is also changed due to the rotor asymmetry. The cracking of the bar can be presented at various locations, including the slot portion of the bars under consideration and end rings of bar joints. The possibility of cracking in the region of the end rings of bar joints is the greatest when the start up time of the machine is long and when frequent starts are required [31].

2.2.1.2 Short turn faults

According to the survey, 35- 40 % of induction motor failures are related to the stator winding insulation [32]. Moreover, it is generally believed that a large portion of stator winding-related failures are initiated by insulation failures in several turns of a stator coil within one phase. This type of fault is referred as a "stator turn fault" [33]. A stator turn fault in a symmetrical three-phase AC machine causes a large circulating current to flow and subsequently generates excessive heat in the shorted turns. If the heat which is proportional to the square of the circulating current exceeds the limiting value the complete motor failure may occur. However, the worst consequence of a stator turn fault may be a serious accident involving loss of human life. The organic materials used for insulation in electric machines are subjected to deterioration from a combination of thermal overloading and cycling, transient voltage stresses on the insulating material, mechanical stresses, and contaminations. Among the possible causes, thermal stresses are the main reason for the degradation of the stator winding insulation. Stator winding insulation thermal stresses are categorized into three types: aging, overloading, and cycling [31]. Even the best insulation may fail quickly if motor is operated above its temperature limit. As a rule of thumb, the life of insulation is reduced by 50 % for every 10°C increase above the stator winding temperature limit [34]. It is thus necessary to monitor the stator winding temperature so that an electrical machine will not operate beyond its thermal capacity. For this purpose, many techniques have been reported [35]-[38]. However, the inherent limitation of these techniques is their inability to detect a localized hot spot at its initial stage.

A few mechanical problems that accelerate insulation degradation include movement of a coil, vibration resulting from rotor unbalance, loose or worn bearings, air gap eccentricity, and broken rotor bars [31]. The current in the stator winding produces a force on the coils that is proportional to the square of the current. This force is at its maximum under transient overloads, causing the coils to vibrate at twice the synchronous frequency with movement in both the radial and the tangential direction. This movement weakens the integrity of the insulation system [31]. Mechanical faults, such as broken rotor bar, worn bearings, and air-gap eccentricity, may be a reason why the rotor strikes the stator windings. Therefore, such mechanical failures should be detected before they fail the stator winding insulation [39, 40]. Contaminations due to foreign materials can lead to adverse effects on the stator winding

insulation. The presence of foreign material can lead to a reduction in heat dissipation [41]. It is thus very important to keep the motors clean and dry, especially when the motors operate in a hostile environment.

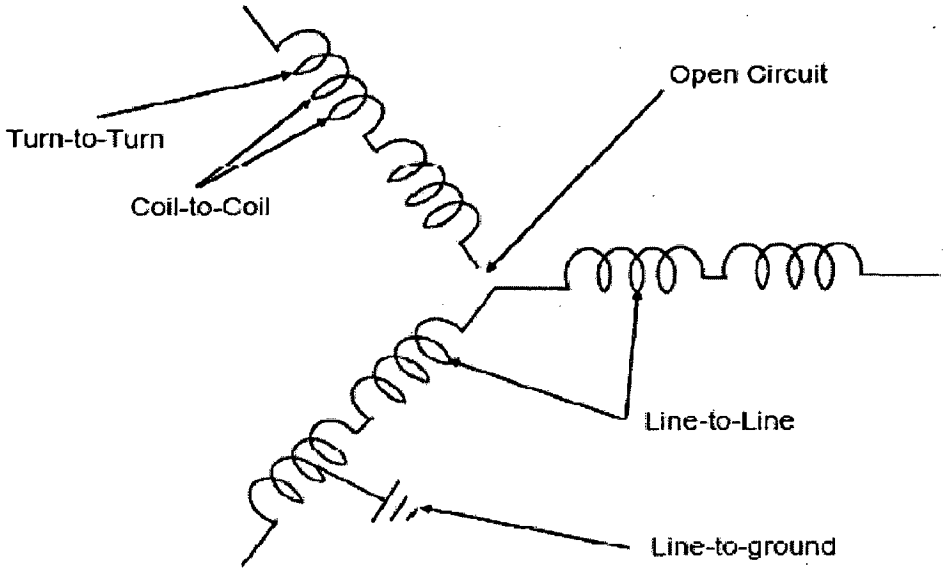

Figure 2.1. Various types of short winding faults

Regardless of the causes, stator winding-related failures can be divided into the five groups: turn-to-turn, coil-to-coil, line-to-line, line-to-ground, and open-circuit faults as presented in Figure 3.1. Among the five failure modes, turn-to-tur n faults (stator turn fault)have been considered the most challenging one since the other types of failures are usually the consequences of turn faults. Furthermore, turn faults are very difficult to detect at their initial stages. To solve the difficulty in detecting turn faults, many methods have been developed [42]-[48].

2.2.2 Mechanical faults

Common mechanical faults found in three phase induction motor are discussed below:

2.2.2.1 Air gap eccentricity

Air gap eccentricity is common rotor fault of induction machines. This fault produces the problems of vibration and noise. In a healthy machine, the rotor is center-aligned with the stator bore, and the rotor's center of rotation is the same as the geometric center of the stator

bore. When the rotor is not centre aligned, the unbalanced radial forces (unbalanced magnetic pull or UMP) can cause a stator-to-rotor rub, which can result in damage to the stator and the rotor [49, 50]. There are three types of air gap eccentricity [30, 1, 49]:

a) Static eccentricity
b) Dynamic eccentricity
c) Mixed eccentricity

Static eccentricity is a steady pull in one direction which create UMP. It is difficult to detect unless special equipment used [49, 51].

A dynamic eccentricity on the other hand produces a UMP that rotates at the rotational speed of the motor and acts directly on the rotor. This makes the UMP in a dynamic eccentricity easier to detect by vibration or current monitoring.

Actually, static and dynamic eccentricities tend to coexist. Ideal centric condition scan never be assumed. Therefore, an inherent grade of eccentricity is implied for any real machine. The combined static and dynamic eccentricity is called mixed eccentricity.

2.2.2.2 Bearing faults

Bearings are common elements of electrical machine. They are employed to permit rotary motion of the shafts. In fact, bearings are single largest cause of machine failures. According to some statistical data, bearing fault account for over 41% of all motor failures[52]. Bearing consists of two rings called the inner and the outer rings. A set of balls or rolling elements placed in raceways rotate inside these rings. A continued stress on the bearings causes fatigue failures, usually at the inner or outer races of the bearings. Small pieces break loose from the bearing, called flaking or spalling. These failures result in rough running of the bearings that generates detectable vibrations and increased noise levels. This process is helped by other external sources, including contamination, corrosion, improper lubrication, improper installation, and brinelling. The shaft voltages and currents are also sources for bearing failures. These shaft voltages and currents result from flux disturbances such as rotor eccentricities [53]. High bearing temperature is another reason for bearing failure. Bearing temperature should not exceed certain levels at rated condition. For example, in the petroleum and chemical industry, the IEEE 841 standard specifies that the stabilized bearing temperature rise at rated load should not exceed 45 degree. The bearing temperature rise can be

caused by degradation of the grease or the bearing. The factors that can cause the bearing temperature rise include winding temperature rise, motor operating speed, temperature distribution within motor, etc. Therefore, the bearing temperature measurement can provide useful information about the machine health and bearing health [54, 55].

A fault in bearing could be imagined as a small hole, a pit or a missing piece of material on the corresponding elements. Under normal operating conditions of balanced load and a good alignment, fatigue failure begins with small fissures, located between the surface of the raceway and rolling elements, which gradually propagate to the surface generating detectable vibrations and increasing noise levels [55]. Continued stress causes fragments of the material to break loose, producing localized fatigue phenomena known as flaking or spalling [56]. Once started, the affected area expands rapidly contamination the lubricant and causing localized overloading over the entire circumference of the raceway [55]. Some sources such as contamination, corrosion, improper lubrication, improper installation or brinelling reduce the bearing life. Contamination and corrosion are the key factors of bearing failure because of the harsh environments present in most industrial settings. The lubricants are contaminated by dirt and other foreign matter that are commonly often present in the environment of industries. Bearing corrosion is produced by the presence of water, acids, deteriorated lubrication and even perspiration from careless handling during installations [55, 56]. Once the chemical reaction has advanced sufficiently, particles are worn-off resulting in the same abrasive action produced by bearing contamination. Under and over-lubrication are also some other causes of bearing failure. In either case, the rolling elements are not allowed to rotate on the designed oil film causing increased levels of heating. The excessive heating causes the grease to break down, which reduces its ability to lubricate the bearing elements and accelerates the failure process. In addition, Installation problems are often caused by improperly forcing the bearing onto the shaft or in the housing. This produces physical damage in form of brinelling or false brinelling of the raceways which leads to premature failure. Brinelling is the formation of indentations in the raceways as a result of deformation caused by static overloading. While this form of damage is rare, a form of "false brinelling" occurs more often. In this case, the bearing is exposed to vibrations while even though lightly loaded bearings are less susceptible, false brinelling still happens and has even occurred during the transportation of uninstalled bearings [55]. Misalignment of the bearing is

also a common result of defective bearing installation. Regardless of the failure mechanism, defective rolling element bearings generate mechanical vibrations at the rotational speeds of each component. Imagine for a hole on the outer raceway: as rolling elements move over the defect, they are regularly in contact with the hole which produces an effect on the machine at a given frequency. Thus, these characteristic frequencies are related to the raceways and the balls or rollers, can be calculated from the bearing dimensions and the rotational speed of the machine.

2.2.2.3 Load faults

In some applications such as aircrafts, the reliability of gears may be critical in safeguarding human lives. For this reason, the detection of load faults (especially related to gears) has been an important research area in mechanical engineering for some time. Motors are often coupled to mechanical loads and gears. Several faults can occur in this mechanical arrangement. Examples of such faults are coupling misalignments and faulty gear systems that couple a load to the motor.

In order to identify the weakest component in electrical motors that is subjected to failure, some statistical studies about the machine failure are reviewed here. Three examples of separate studies conducted in different countries for motor faults are summarised as follow [18] :

- Under EPRI sponsorship on industry assessment, a study is conducted by General Electric Co. to evaluate the reliability of powerhouse motors and identify the operation characteristic. Part of this study is to specify the reason behind the motor failures. Fig. 2.2shows the results of the EPRI study on the reliability of powerhouse motors in the US. The study is made on the basis of actual motor failure.
- A similar study on the major component failure of powerhouse motors has been conducted by IEEEIGA. The study is carried out on the basis of opinion as reported by the motor manufacturer. The results of this study are presented in Fig. 2.3, where the failure is grouped according to major contributors.
- At Ronningen in Norway, four plants for production of poly olefins form an integrated industrial complex. High populations of electrical motors are used for high-pressure reactor, extruders, piston compressors, gas screw compressors and pumps. A survey of machine

faults was carried out by B&K experts in 1997. Fig. 2.4shows the results of the detected faults by vibration monitoring.

It can be noted from these studies that the major type of faults that the induction machine is subjected to is the bearing faults.

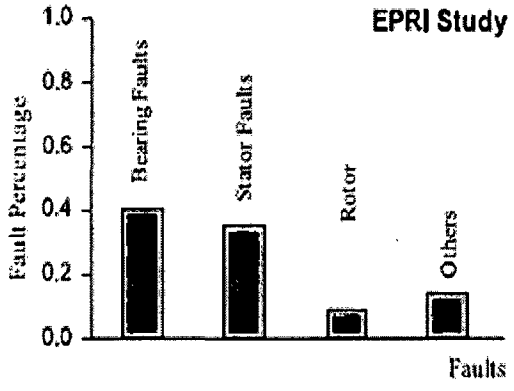

Fig 2.2: Results of EPRI study on induction motor reliability

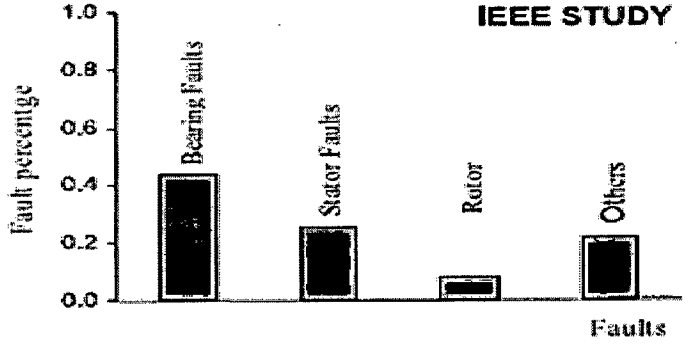

Fig 2.3: Results of IEEE study on Induction motor failure

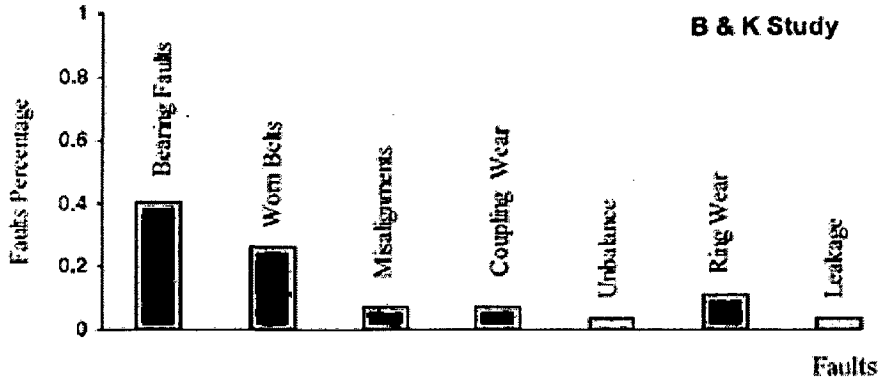

Fig 2.4: Results of a study conducted by B & K on the major faults detected in IM

2.3 Chapter Summary

The most prevalent faults in induction motor were described in detail in this chapter. The common internal faults can be mainly categorized into two groups: Electrical faults and Mechanical faults. Electrical faults include faults caused by winding insulation problems, and some of the rotor faults. Mechanical faults include bearing faults, air gap eccentricity, load faults and misalignment of shaft. In order to identify the weakest component in electrical motors that is subjected to failure, some statistical studies about the machine failure were also discussed.

CHAPTER 3

CONDITION MONITORING TECHNIQUES

3.1 General Concept of Condition Monitoring

Condition monitoring (CM) stands for the analysis of the condition of a machine to determine the types of faults and their severity while the motor is under a normal operating condition.

A CM system should be capable of monitoring the running machines with the existence of electrical interference, predicting the need for maintenance before serious deterioration or breakdown occurs, identifying and locating the defects in detail, and even estimating the life of machines. Four main parts should be contained in a CM system to practice these functions [57]:

1) Sensor: Sensors can convert a physical quantity to an electrical signal. Quantities and phenomenon will be monitored if they themselves or their detectable changes can reveal incipient faults long before catastrophic failures occur. Selection of sensors will rely on the monitoring method and come down to the knowledge on failure mechanisms of the machine. Commonly, the sensors should be suitable for on-line measurement. Sensitivity, cheapness, and non invasion are the key requirements and expectation to practise this task.

2) Data acquisition: A data acquisition unit will be built to realize amplification and pre-processing of the output signals from sensors, for example, conversion from analogue to digital and correction of sensor failures. Data communication technique and microcomputer may be needed.

3) Fault detection: The main purpose is to find out if there is an incipient fault appearing in the machine so that alarm can be given and further analysis can be exerted. There are two different methods for fault detection, named model-referenced method and feature extraction. The former detects faults by comparing the results of measurements with predictions of models that may be mathematical simulation models or artificial intelligence based. For most feature extraction methods, frequency and time-domain signal processing technologies will be used to obtain 'signatures' which can represent normal and faulty performance.

4) Diagnosis: The detected abnormal signals need be post processed to make out a prescription as a clear indication to maintenance. It used to be done by experts or offline analysis and now tends to be implemented online and automatically by computer combined with advanced technologies. The prescriptions presented to the user are expected to include name and location of each defect, status of the machine, advises for maintenance, and so on.

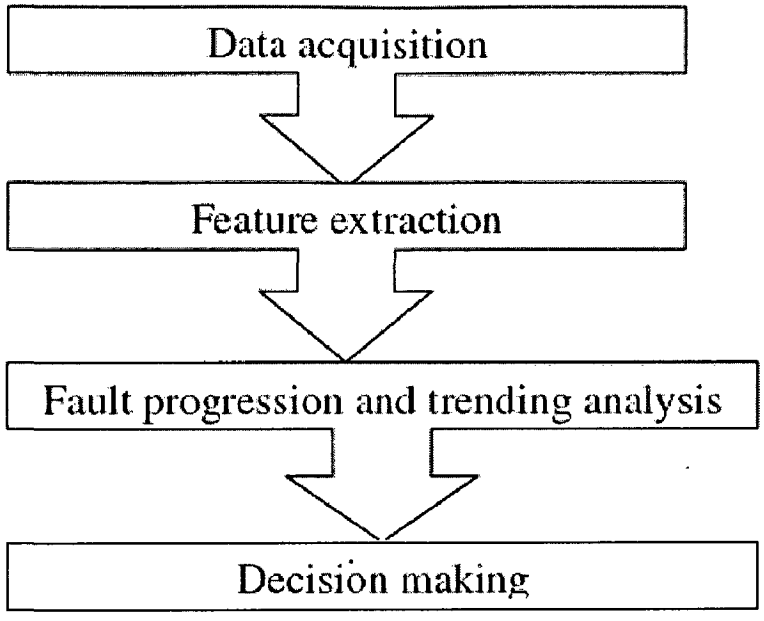

Fig.3.1 Process for Fault Diagnosis

3.1.1 Benefits of Condition Monitoring

The flow of fault current, detected by a protective relay, is the final part of an electrical machine failure, and involves consequential damage. Earlier warning of a failure could be provided by making relays especially sensitive so that they give an alarm. This is often done, for example, in the rotor earth fault relay of a generator, but the warning is relatively short. Damage must precede the flow of a fault current, so for monitoring to improve on relays it must detect this damage, as directly as possible, and give a clear indication that it has occurred. If warning is given early and the information is presented clearly enough, the machine can be removed from service for repair or a repair can be scheduled at a more convenient time. The benefits which condition monitoring can bring to a particular machine depend upon the following:

*(a)*the amount of warning monitoring can give of an impending failure

*(b)*the value of the machine itself

(c)the total cost incurred if the machine fails, which depends upon:

(i) the direct cost of the repair or replacement

(ii) the time to repair or replace the machine

(iii) the replacement generation costs per day for the generating unit in which the machine is operating

(iv) whether standby capacity or a spare for the machine is available

(d)the cost and reliability of the monitoring scheme itself.

As an example, taking these points into account, if reliable monitoring of a high value, strategic machine can detect a fault only 1 s before the protective relays would operate, the monitoring is hardly likely to be any benefit. On the other hand, if monitoring can reliably give 1 h or more warning on this same machine, that is likely to be of considerable value and if days or months of warning can be given on machines of less value, that can be beneficial in planning maintenance.

To summarize, condition monitoring of an electrical machine will yield benefits if a reliable monitoring system exists, which can provide sufficient warning of a typical failure mechanism, so that the machine can be taken out of service and repaired at a cost which is substantially less than if fault currents flowed. The net benefit will be positive if the cost of the monitoring system is less than the likely saving in cost of repairs following faults. At the moment, condition monitoring on electrical machines is in its infancy, largely because of the inherent reliability of electrical plant. Larger motors and generators are already fitted with a number of traditional monitoring sensors. However, a number of new monitoring techniques have been devised, and with the availability of cheap computing power, measurements from these and traditional techniques can now be processed and acted upon in a way that makes condition monitoring viable for large, strategically important machines. But effective condition monitoring must consist of all three of the following parts:

(a)measuring selected parameters to give early indication of damage

*(b)*processing and assessing the significance of these measurements

(c)taking action upon these measurements.

3.2 Existing Condition Monitoring Techniques

Different researchers have used various monitoring techniques for induction motors using different machine variables. These monitoring techniques have been classified into the following 13 categories using different parameters [58].

3.2.1. Vibration

All electric machines generate noise and vibration, and the analysis of the produced noise and vibration can be used to give information on the condition of the machine. Even very small amplitude of vibration of machine frame can produce high noise. Noise and vibration in electric machines are caused by forces which are of magnetic, mechanical and aerodynamic origin. The largest sources of vibration and noise in electric machines are the radial forces due to the air gap field. Since the air gap flux density distribution is product of the resultant m.m.f. wave and total permeance wave. The resultant m.m.f. also contains the effect of possible rotor or stator asymmetries, and permeance wave depends on the variation of the air gap as well , the resulting magnetic forces and vibrations also depends on these asymmetries. Thus, by analyzing the vibration signal of an electric machine, it is possible to detect various types of faults and asymmetries . Bearing faults, rotor eccentricities, gear faults and unbalanced rotors are the best candidates for vibration based diagnostics. The vibration monitoring of electric machines is accomplished through the use of broad-band, narrow-band, or spectral (signature) analysis of the measured vibration energy of the machine. Vibration-based diagnostics is the best method for fault diagnosis, but needs expensive accelerometers and associated wiring. This limits its use in several applications, especially in small machines where cost plays a major factor in deciding the condition monitoring method.

The major disadvantage of vibration monitoring is cost. For example, a regular vibration sensor costs several hundred dollars. A high product cost can be incurred just by employing the necessary vibration sensors for a large number of electric machines. Another disadvantage of vibration monitoring is that it requires access to the machine. For accurate measurements, sensors should be mounted tightly on the electric machines, and expertise is required in the mounting. In addition, sensors themselves may fail.

3.2.2. Current

Current Park's vector, zero-sequence and negative-sequence current monitoring and motor current signature analysis, all fall under the category of electrical monitoring. These methods use stator current to detect various kind of machine and inverter faults. In most applications, the stator current of an induction motor is readily available since it is used to protect machines from destructive over-currents, ground current, etc. Therefore, current monitoring is a sensor-less detection method that can be implemented without any extra hardware.

Motor current signature analysis (MCSA) is one of the most powerful methods of online motor diagnosis for detecting motor faults. Using MCSA has advantages such as no estimation of Motor parameters and the simplicity of current sensors and their installation. MCSA detects changes in a machine's permeance by examining the current signals. It uses the current spectrum of the machine for locating characteristic fault frequencies. When a fault is present, the frequency spectrum of the line current becomes deviated from healthy motor. Such fault modulates the air-gap and produces rotating frequency harmonics in the self and mutual inductances of the machine. It depends upon locating specific harmonic component in the line current. The spectrum may be obtained using frequency domain analysis by using signal processing techniques. The diagnostic analysis has been reported by various researchers using the sequence components of current, radio-frequency (RF) component of neutral current, and shaft currents.

3.2.3. Magnetic Flux

Any distortion in the air-gap flux density due to stator defects will set up an axial homopolar flux in the shaft, which can be sensed by a search coil fitted around the shaft. The air-gap flux can also be sensed by sensing the voltage across two properly located motor coils. One can get a signal by subtracting these two voltages, which is independent of stator '*ir*' drop and approximately independent of motor leakage reactance drop. By using a minimum of four search coils located axisymmetrically to the drive shaft, the location of shorted turn can be found out.

3.2.4. Instantaneous Angular Speed

Various asymmetry faults in induction motors can be detected by monitoring the stator core vibration using instantaneous angular speed (IAS) techniques. In case of stator winding fault or

unbalanced supply, the vibration signal will contain a significant component with twice the supply frequency. For phase imbalance, the fault symptom is a significant increase in the 100-Hz component (if the supply frequency is 50 Hz).

3.2.5. Temperature

A rugged temperature sensor can be mounted on the winding or embedded in the insulation, which is electrically isolated from its instrumentation. The temperature estimation can be based on the thermal model and stator resistance model if unobstructed ventilation is ensured, and ambient temperature is accounted for plus the effect of elevation on the motor temperature and cooling. The phenomenon of setting up of the space charge as a consequence of the aging of the stator insulation has been utilized for the thermal step method (TSM). The measurement of thermally stimulated discharge currents (TSDC) is also made which gives the energy levels of the traps. By associating TSM and TSDC, a complete study of the apparition and of the development of the space charges can be made and the stator insulation lifetime can be predicted. A nondestructive diagnostic apparatus using plastic-optical-fiber (POF) sensor has been developed for evaluating the aging of insulating resins for low-voltage induction motors. This apparatus measures the change of reflective absorbance ratio at two different near-IR wavelengths.

3.2.6. Air-Gap Torque

The air-gap torque is produced by the flux linkage and the currents of a rotating machine. It is sensitive to any unbalance created due to defects as well as by the unbalanced voltages. The zero frequency of the air-gap harmonics shows that the motor is normal. In case of an induction motor with single-phase stator winding, the angular speed (as observed from the rotor) of forward and backward stator rotating fields, the rotor and rotor rotating magnetic fields are $\pm\omega_s$, $\omega_s(1-s)$, and $s\omega_s$, respectively. The forward stator rotating field produces a constant torque while the backward stator field interacting with the rotor field produces a harmonic torque whose

Frequency = Stator field angular speed – (Rotor angular speed + Rotor field angular speed observed from rotor) $= -\omega_s - \{\omega_s(1-s) + s\omega_s)\} = -2\omega_s$.

This means the double fundamental frequency torque indicates the gap in the stator winding and/or voltage.

3.2.7. Noise/Acoustic Noise

The noise spectrum of induction machines is dominated by EM, ventilation, and acoustic noise. Ventilation noise is associated with air turbulence, which is produced by periodic disturbances in the air pressure due to rotating parts. The EM noise is due to the action of Maxwell's stresses that act on the iron surfaces in the presence of a magnetic field. These forces induce vibrations in the stator structure, which cause radiated noise. The sound power level due to aerodynamic and mechanical noise increases at a rate of 12 dB per doubling of the motor speed. Increased motor speed gives rise to EM noise. The ground wall insulation interrogation can be done by optimally launching an ultrasonic wave into a stator bar and using the conductor as a waveguide.

3.2.8. Induced Voltage

The voltage induced along the shaft of a machine (generator) is an indication of the stator core or winding degradation. Shaft voltage has not yet proved to be a useful parameter for continuous monitoring because it is difficult to measure in a reliable way. Moreover, it has also been shown that any damage to the core or the winding would need to be substantial before a significant variation in shaft voltage occurred. The changes in the root mean square (rms) magnitude of Vsum (Vsum,rms) can reveal the presence and severity of turn-fault diagnostics where Vsum is the sum of instantaneous phase voltages. The maximum turn-fault sensitivity is obtained after band pass filtering around the fundamental frequency.

3.2.9. Power

The instantaneous electric power has definite advantages in comparison to current as a detection parameter. The characteristic spectral component of the power appears directly at the frequency of the disturbance, independent of the synchronous speed of the motor. The utilization of the instantaneous power enhances the reliability of the diagnostics of the induction motors.

3.2.10. Partial Discharge

This is a small electrical discharge, which occurs due to insulation imperfection. For example, delaminations within the ground wall insulation, resulting from poor manufacturing or overheating, gives rise to voids or air pockets, which get discharged. The partial discharge analyzer (PDA) test, developed in 1976, is one of the first techniques to be used during normal machine operation of hydro generators. Other techniques have been developed using specialized sensors. A deteriorated winding has a PD activity approximately 30 times or even higher than a winding in good condition. The effectiveness of stator winding maintenance can be easily monitored with an online PD test.

3.2.11. Gas Analysis

The degradation of the electrical insulation within a motor produces carbon monoxide gas which passes into the cooling air circuit and can be detected by an infrared (IR) absorption technique . The high-frequency pulse width modulation (PWM) pulses generate excessive voltage peaks leading to the start of motor insulation breakdown. It occurs as a result of electrostatic fields surrounding oppositely polarized conductors that begin to strip electrons from the surrounding air gap, leaving molecules with positive electrical charge (ionization) producing ozone which get combined with nitrogen from the air to produce forms of nitrous oxides. It corrosively attacks the insulation causing embitterment and eventual fracture. Ozone sniffing techniques are used for the detection of ozone.

3.2.12. Surge Testing

The surge testing is an established method for diagnosing winding faults. In the surge comparison test, two identical high voltages, high-frequency pulses are simultaneously imposed on two phases of the motor winding with third phase grounded. An oscilloscope is used to compare the reflected pulses indicating the insulation faults between windings, coils, and group of coils. The pulse-pulse surge testing is a predictive field method to show the turn-turn insulation weakness before the turn-turn short occurs. An electronic and portable device "Surge Tester" is used to locate insulation faults and winding dissymmetry.

3.2.13. Motor Circuit Analysis

By measuring the electro-magnetic properties of the electric motor as an electric circuit, the motor circuit analysis (MCA) determines the variations within the motor and identifies the defects. In MCA, a low amount of energy with amplified responses is applied. The responses help in evaluating the condition of both the windings and rotor through the comparative readings.

3.2.14.AI-Based Fault Monitoring Approaches

Despite the various techniques mentioned above, the monitoring and fault detection of electrical machines have moved from the traditional techniques to AI techniques in recent years. The main steps of an AI-based diagnostic mechanism are signature extraction, fault identification, and fault severity evaluation. The various AI techniques, expert systems, artificial neural networks (ANNs), fuzzy logic, fuzzy neural networks (NNs), genetic algorithms, etc. for the fault diagnostics of stator faults have been reported in the literature.

3.2.14.1. Artificial Neural Networks

Artificial neural networks (ANNs) are one of the oldest AI paradigms that have been around the power engineering research arena for quite some time. ANNs mimic the human brain structure, which consists of simple arithmetic units connected in complex layer architecture. They are capable of representing highly nonlinear functions and performing multi-input, multi-output mapping. They learn these functions through examples. ANNs have been applied densely in the area of motor condition monitoring and fault diagnosis, performing one or more of the following tasks [59]:

- pattern recognition, parameter estimation, and nonlinear mapping applied to condition monitoring;
- training based on both time and frequency domain signals obtained via simulation and/or experimental results;
- real time, online unsupervised diagnosis;
- dynamic updating of the structure with no need to retrain the whole network;
- filtering out transients, disturbances, and noise;
- fault prediction in incipient stages due to operation anomalies;
- operating conditions clustering based on fault types.

3.2.14.2. Fuzzy and Adaptive Fuzzy Systems

Fuzzy logic and adaptive fuzzy systems are emerging as powerful AI techniques. Fuzzy logic is a more powerful variation of crisp logic; where knowledge representation is closer to the way humans think. Fuzzy inference systems employ powerful inferential engines on natural (linguistic) variables and build data bases via fuzzy *if—then* rules. Adaptive fuzzy systems utilize the learning capabilities of ANNs or the optimization strength of genetic algorithms to adjust the system parameter set in order to enhance the intelligent system's performance based on *a priori* knowledge. Some of the fuzzy and adaptive-fuzzy systems' applications to motor fault diagnosis include

- evaluating performance indices using linguistic variables;
- predicting abnormal operation and locating faulty element;
- utilizing human expertise reflected to fuzzy *if—then* rules;
- system modeling, nonlinear mapping, and optimizing diagnostic system parameters through adaptive fuzzy systems;
- fault classification and prognosis.

3.2.14.3. Expert Systems

Expert systems represent an attempt to emulate the human thought through knowledge representation and inference mechanisms. Within a bound domain of knowledge, expert systems are capable of decision making on a quality level comparable to human experts. Although they are expensive and time-consuming during evolvement, some research work dedicated to applying expert systems to machine fault diagnosis was reported in the literature. These applications include

- emulating and implementing human expertise;
- building and online updating system knowledge bases;
- signal filtering, information search, and feature extraction;
- data managing and information coding in knowledge bases;
- employment of users interactive sessions;
- fault classification, diagnosis, and location;
- knowledge base building through simulation and/or experimentation.

Applications of AI tools in condition monitoring and fault diagnosis of electric machines and drives have provided the automation of the diagnostic process. It also helped in utilizing the human expertise, and gaining early and precise detection. Artificial intelligence is expanding the horizon of the new research related to the topic in the coming years.

3.2.15. Modeling/Simulation for Faulty Motors

The development of "smart" condition monitoring systems is in full swing. Their success depends on their accuracy as well as on their ability to discriminate between normal/balanced and abnormal/unbalanced conditions. Hence, the possibility of simulating fault conditions becomes more attractive and important. Researchers have put in a lot of effort to predict the performance of induction machines using various modeling/simulation techniques and tools for various faults. The steady-state and transient state of healthy and faulty machines under different operating conditions like steady-state (no load and onload) and transient state (startup, loading, unloading, and shutting down) have been considered in the literature.

3.3 Chapter Summary

This chapter presented a review of existing induction motor condition monitoring methods. This covered a variety of topics, techniques, methods, and approaches. The practical use of various condition monitoring methods for fault diagnosis of electric machines was presented. The usage of electric motors is rapidly increasing in a wide variety of industrial and transit applications. Therefore, the demand for reliable fault detection methods for electric machines is increasing.

CHAPTER 4

INDUCTION MOTOR MODEL WITH STATOR WINDING FAULTS

4.1. Induction motor model with Asymmetrical Stator Winding

The model for a symmetrical three-phase induction motor is well known [60–63]. To derive equations for asymmetrical stator winding and rotor, the following assumptions have been made:

- Each stator phase of the motor has a different number of turns, but uniform spatial displacement is assumed;
- Magnetic saturation is not present.

With the appropriate subscripts *as*, *bs*, *cs*, *ar*, *br*, and *cr*, the voltage equations of the magnetically coupled stator and rotor circuits can be written as follows:

$$v^s_{abc} = r^s_{abc} i^s_{abc} + p\lambda^s_{abc}\,, \qquad 0 = r^r_{abc} i^r_{abc} + p\lambda^r_{abc} \tag{4.1}$$

Where $p = d/dt$. Applying a stationary reference frame transformation to this equation yields the corresponding *qd0* equations and Eq. (4.1) becomes

$$v^s_{qd0} = r^s_{qd0} i^s_{qd0} + p\lambda^s_{qd0}\,,$$

$$0 = r^r_{qd0} i^r_{qd0} - \omega_r \begin{bmatrix} 0 & 1 & 0 \\ -1 & 0 & 0 \\ 0 & 0 & 0 \end{bmatrix} \lambda^r_{qd0} + p\lambda^r_{qd0} \tag{4.2}$$

Where

$$r^s_{qd0} = \begin{bmatrix} r^s_{11} & r^s_{12} & r^s_{13} \\ r^s_{21} & r^s_{22} & r^s_{23} \\ r^s_{31} & r^s_{32} & r^s_{33} \end{bmatrix}$$

and matrix elements are given in Appendix A and assuming $r_{ar} = r_{br} = r_{cr} = r_r$, $r^r_{qd0} = r_r I_{3x3}$.

In matrix notation, the flux linkages of the stator and rotor windings may be written in terms of the winding inductances and the current as [8]

$$\begin{bmatrix} \lambda^s_{abc} \\ \lambda^r_{abc} \end{bmatrix} = \begin{bmatrix} L^{ss}_{abc} & L^{sr}_{abc} \\ L^{rs}_{abc} & L^{rr}_{abc} \end{bmatrix} \begin{bmatrix} i^s_{abc} \\ i^r_{abc} \end{bmatrix} \tag{4.3}$$

where stator and rotor inductances are

$$L_{abc}^{ss} = \begin{bmatrix} L_{asas} & L_{asbs} & L_{ascs} \\ L_{bsas} & L_{bsbs} & L_{bscs} \\ L_{csas} & L_{csbs} & L_{cscs} \end{bmatrix}$$

and

$$L_{abc}^{rr} = \begin{bmatrix} L_{arar} & L_{arbr} & L_{arcr} \\ L_{brar} & L_{brbr} & L_{brcr} \\ L_{crar} & L_{crbr} & L_{crcr} \end{bmatrix}$$

Because of symmetry, stator mutual inductances have $L_{asbs} = L_{bsas}$, $L_{ascs} = L_{csas}$ and $L_{bscs} = L_{csbs}$. Similarly rotor self- and mutual inductances have $L_{arar} = L_{brbr} = L_{crcr}$ and $L_{arbr} = L_{arcr} = L_{brar} = L_{brcr} = L_{crar} = L_{crbr}$ respectively.

Those of the stator-to-rotor mutual inductances are dependent on the rotor angle (orientated with respect to stator), therefore

$$L_{abc}^{sr} = \begin{bmatrix} L_{asar}\cos\theta_r & L_{asbr}\cos\left(\theta_r + \frac{2\pi}{3}\right) & L_{ascr}\cos\left(\theta_r - \frac{2\pi}{3}\right) \\ L_{bsar}\cos\left(\theta_r - \frac{2\pi}{3}\right) & L_{bsbr}\cos\theta_r & L_{bscr}\cos\left(\theta_r + \frac{2\pi}{3}\right) \\ L_{csar}\cos\left(\theta_r + \frac{2\pi}{3}\right) & L_{csbr}\cos\left(\theta_r - \frac{2\pi}{3}\right) & L_{cscr}\cos\theta_r \end{bmatrix} \tag{4.4}$$

and $L_{abc}^{rs} = L_{abc}^{sr'}$ where (') means the transpose of the matrix.

The coefficients L_{asar}, L_{asbr}, L_{ascr}, L_{bsar}, L_{bsbr}, L_{bscr}, L_{csar}, L_{csbr}, L_{cscr} are peak values of stator-to-rotor mutual inductances. Because of rotor symmetry $L_{asar} = L_{asbr} = L_{ascr}$, $L_{bsar} = L_{bsbr} = L_{bscr}$ and $L_{csar} = L_{csbr} = L_{cscr}$.

The stator and rotor *qd0* flux linkages are obtained by applying transformation to the stator and rotor *abc* flux linkages in Eq. (4.3), that is

$$\lambda_{qd0}^{s} = L_{qd0}^{ss} i_{qd0}^{s} + L_{qd0}^{sr} i_{qd0}^{r},$$

$$\lambda_{qd0}^{r} = L_{qd0}^{rs} i_{qd0}^{s} + L_{qd0}^{rr} i_{qd0}^{r} \tag{4.5}$$

where $L_{qd0}^{ss} = \begin{bmatrix} L_{11}^{ss} & L_{12}^{ss} & L_{13}^{ss} \\ L_{21}^{ss} & L_{22}^{ss} & L_{23}^{ss} \\ L_{31}^{ss} & L_{32}^{ss} & L_{33}^{ss} \end{bmatrix}$, $L_{qd0}^{sr} = \begin{bmatrix} L_{11}^{sr} & L_{12}^{sr} & 0 \\ L_{21}^{sr} & L_{22}^{sr} & 0 \\ L_{31}^{sr} & L_{32}^{sr} & 0 \end{bmatrix}$, $L_{qd0}^{rr} = \begin{bmatrix} L_{11}^{rr} & 0 & 0 \\ 0 & L_{22}^{rr} & 0 \\ 0 & 0 & L_{33}^{rr} \end{bmatrix}$, and

$L_{qd0}^{rs} = \begin{bmatrix} L_{11}^{sr} & L_{21}^{sr} & 0.5L_{31}^{sr} \\ L_{12}^{sr} & L_{22}^{sr} & -0.5L_{32}^{sr} \\ 0 & 0 & 0 \end{bmatrix}$. Matrix elements of L_{qd0}^{ss}, L_{qd0}^{sr}, L_{qd0}^{rr} and L_{qd0}^{rs} are given in Appendix A.

Normally, an induction machine is connected to a three phase supply by a three-wire connection (i.e. neutral current does not flow). Hence, for a squirrel cage induction machine and

three-wire connection, the stator and rotor flux linkages in Eq. (4.5) may be expressed compactly as

$$\begin{bmatrix}\lambda_q^s\\ \lambda_d^s\\ \lambda_q^r\\ \lambda_d^r\end{bmatrix}=\begin{bmatrix}L_{11}^{ss} & L_{12}^{ss} & L_{11}^{sr} & L_{12}^{sr}\\ L_{21}^{ss} & L_{22}^{ss} & L_{21}^{sr} & L_{22}^{sr}\\ L_{11}^{sr} & L_{12}^{sr} & L_{11}^{rr} & 0\\ L_{21}^{sr} & L_{22}^{sr} & 0 & L_{22}^{rr}\end{bmatrix}\begin{bmatrix}i_q^s\\ i_d^s\\ i_q^r\\ i_d^r\end{bmatrix} \tag{4.6}$$

4.2. Determination of inductances

In order to define asymmetrical machine inductances, assume stator phases *as*, *bs* and *cs* have numbers of winding turns given by N_a, N_b and N_c respectively, and that rotor phases *ar*, *br*and *cr* have winding turns given by $N_{ar} = N_{br} = N_{cr} = N_r$. If self- and mutual inductances are known for a symmetrical machine with reference number of turns N_s, new parameters for an asymmetrical machine can be defined from these inductance values as described in [60, 63, 64].

By using known parameters the stator self-inductances for phases *as*, *bs* and *cs* can be calculated as [8]

$$L_{asas} = \frac{N_a^2}{N_s^2}\left(L_{ls} + \frac{2}{3}L_m\right) = N_a^2 L_{mls} \tag{4.7}$$

$$L_{bsbs} = N_b^2 L_{mls} \tag{4.8}$$

$$L_{cscs} = N_c^2 L_{mls} \tag{4.9}$$

where $L_{mls} = \frac{1}{N_s^2}\left(L_{ls} + \frac{2}{3}L_m\right)$.

The stator mutual inductances between phases *as* and *bs*, *bs* and *cs*, and *cs* and *as* can be derived as

$$L_{asbs} = L_{bsas} = \left(-\frac{1}{2}N_a N_b\right)\left(\frac{2}{3}\frac{L_m}{N_s^2}\right) = -\frac{1}{3}\frac{N_a N_b}{N_s^2}L_m = N_a N_b L_{mss} \tag{4.10}$$

$$L_{ascs} = L_{csas} = N_a N_c L_{mss} \tag{4.11}$$

$$L_{bscs} = L_{csbs} = N_b N_c L_{mss} \tag{4.12}$$

where $L_{mss} = -\frac{1}{3}\frac{L_m}{N_s^2}$.

The rotor self- and mutual inductances can be found by a similar way. Because the rotor is assumed symmetric, the total self-inductances of rotor phases *ar*, *br*and *cr* are equal.

Therefore

$$L_{arar} = L_{brbr} = L_{crcr} = L_{lr} + \frac{2}{3}\frac{N_r^2}{N_s^2}L_m = L_{lr} + L_{mar} \tag{4.13}$$

where $L_{mar} = \frac{2}{3}\frac{N_r^2}{N_s^2}L_m$.

For the same reason, rotor mutual inductances are also equal to each other and given by

$$L_{arbr} = L_{arcr} = L_{brar} = L_{brcr} = L_{crar} = L_{crbr}$$

$$= -\left(\frac{1}{2}\right)\left(\frac{2}{3}\frac{N_r^2}{N_s^2}L_m\right) = -\frac{1}{2}L_{mar} \tag{4.14}$$

Previously defined stator-to-rotor mutual inductances can be defined in term of new parameters. Because of rotor symmetry (turn numbers for each rotor phase are equal) mutual inductances will be $L_{arar} = L_{asbr} = L_{ascr}$, $L_{bsar} = L_{bsbr} = L_{bscr}$, $L_{csar} = L_{csbr} = L_{cscr}$.

Referring to Fig. 4.1 , we can see that the rotor phase *ar* is displaced from stator phase *as* by the electrical angle θr, where θr is a variable [8].

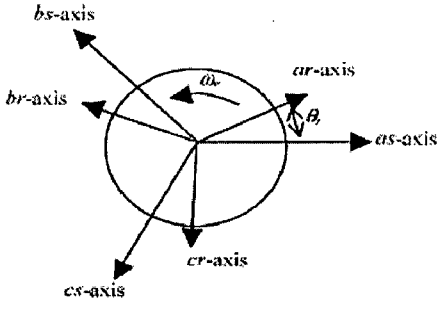

Fig.4.1. Induction Machine Winding Displacement.

The corresponding mutual inductances will vary with θr. The variable sine and cosine factors are already present in Eq. (4.4), so peak mutual inductances will be

$$L_{asar} = L_{asbr} = L_{ascr} = \frac{2}{3}\frac{N_a N_r}{N_s^2}L_m = N_a L_{msr} \tag{4.15}$$

$$L_{bsar} = L_{bsbr} = L_{bscr} = \frac{2}{3}\frac{N_b N_r}{N_s^2}L_m = N_b L_{msr} \tag{4.16}$$

$$L_{csar} = L_{csbr} = L_{cscr} = \frac{2}{3}\frac{N_c N_r}{N_s^2}L_m = N_c L_{msr} \tag{4.17}$$

where $L_{msr} = \frac{2}{3}\frac{N_r}{N_s^2}L_m$.

4.3. Simulation of the asymmetrical induction motors

In this subsection, equations are rearranged for the asymmetrical induction motor model that has been developed [8]. The *qd*-applied voltage in a reference frame fixed to the stator can be obtained from the stator phase voltage v_{as}, v_{bs} *and* v_{cs} by standard transformation [62]. The *qd* voltages will be

$$v_q^s = \frac{2}{3}\left[v_{as} - \frac{1}{2}(v_{bs} + v_{cs})\right] = \frac{2}{3}\left[v_{ag} - \frac{1}{2}(v_{bg} + v_{cg})\right],$$

$$v_d^s = \frac{1}{\sqrt{3}}(-v_{bs} + v_{cs}) = \frac{1}{\sqrt{3}}(-v_{bg} + v_{cg}) \tag{4.18}$$

Where v_{ag}, v_{bg} and v_{cg} are supply phase voltages. Flux linkages may be obtained from Eq. (4.2) for a three wire system to give

$$\lambda_q^s = \int (v_q^s - r_{11}^s i_q^s - r_{12}^s i_d^s)\, dt,$$

$$\lambda_d^s = \int (v_d^s - r_{21}^s i_q^s - r_{22}^s i_d^s)\, dt,$$

$$\lambda_q^r = \int (\omega_r \lambda_d^r - r_r^r i_q^r)\, dt,$$

$$\lambda_d^r = -\int (\omega_r \lambda_q^r + r_r^r i_d^r)\, dt \tag{4.19}$$

The current can be found by inverting Eq. (4.6).

The speed of the machine can be obtained from the torque equation as

$$\omega_r(t) = \frac{P}{2J}\int (T_{em} + T_{mech} - T_{damp})\, dt \tag{4.20}$$

T_{em} is the electromagnetic torque impressed on the shaft of the machine and can be expressed as

$$T_{em} = \frac{3}{2}\frac{P}{2}(\lambda_d^s i_q^s - \lambda_q^s i_d^s) \tag{4.21}$$

T_{mech} is the externally applied mechanical torque in the direction of the rotor speed, T_{damp} is the damping torque in the opposite direction of the rotor speed, and J is inertia.

By using Eqs.(4.18)–(4.21) with resistances and inductances that are defined in Appendix A, a motor with asymmetrical windings can be simulated. The compact model for the simulation of the asymmetrical motor is shown in Fig. 4.2.

Results of simulation in Fig. 4.2 are fed to a diagnostic block that uses negative sequence current to display motor condition. Supply voltage and motor current are decomposed into their positive and negative sequence components and the condition of the motor is analysed.

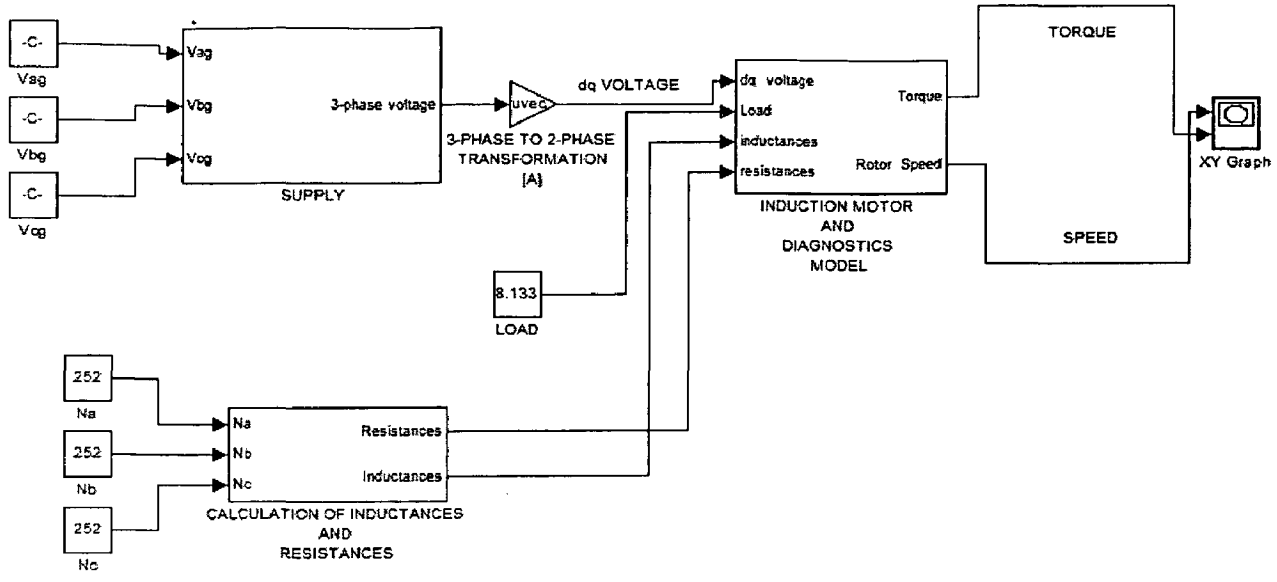

Fig.4.2.Simulation of Asymmetrical Induction Motor Model.

4.4 Induction motor model with Stator Inter turn Short circuit

In order to develop an induction motor model with a stator inter-turn short circuit, it has been assumed that phase *as* has two windings in series comprising N_{us} unshorted turns and N_{sh} shorted turn(s), where $N_{as} = N_{us} + N_{sh} = N_s$, the overall number of turns N_s. The phases *bs* and *cs* have $N_{bs} = N_{cs} = N_s$. By assuming the unequal numbers of stator turns, the first model can be used for induction motor model with inter-turn short circuit to transfer motor equation from *abc* axes to *qd0*axes. By doing this, the N_{sh} turn shorted winding can be introduced in *qd0* axes. The fault severity can be changed by varying the number of shorted turns, and by a current limiting resistance across the short circuit windings. The same assumptions that were made for the first model are valid for this model as well.

In the following, the modification of equations for the new model is presented [8].

The self-inductances for phase *as*, *bs*, and *cs* in Eqs.(4.7)–(4.9) will be

$$L_{asas} = \frac{N_{us}^2}{N_s^2}\left(L_{ls} + \frac{2}{3}L_m\right) + 2N_{us}N_{sh}\left(\frac{2}{3}\frac{L_m}{N_s^2}\right) + \frac{N_{sh}^2}{N_s^2}\left(L_{ls} + \frac{2}{3}L_m\right)$$

$$= (N_{us}^2 L_{mls} + N_{us}N_{sh}L_{msh}) + (N_{us}N_{sh}L_{msh} + N_{sh}^2 L_{mls})$$

$$= (L'_{asas} + L_{assh}) + (L_{assh} + L_{shsh}) \tag{4.22}$$

where $L_{msh} = \frac{2}{3}\frac{L_m}{N_s^2}$ and subscript 'sh' is used for shorted winding(s).

$$L_{bsbs} = L_{cscs} = \frac{N_s^2}{N_s^2}\left(L_{ls} + \frac{2}{3}L_m\right) = N_s^2 L_{mls} \tag{4.23}$$

As it can be seen from Eq. (4.22), the phase *as* self-inductance contains the unshorted self-inductance L'_{asas}, the mutual inductance between unshorted and shorted turns L_{assh}, and the shorted turns self-inductance L_{shsh}.

The stator mutual inductances will be

$$L_{asbs} = -\frac{1}{3}\frac{N_a N_s}{N_s^2}L_m = -\frac{1}{3}\frac{N_{us}}{N_s}L_m - \frac{1}{3}\frac{N_{sh}}{N_s}L_m = L'_{asbs} + L_{shbs} \tag{4.24}$$

$$L_{ascs} = L_{bsas} = L_{csas} = L'_{asbs} + L_{shbs},$$

$$L_{bscs} = L_{csbs} = -\frac{1}{3}L_m \tag{4.25}$$

The stator-to-rotor mutual inductances in Eqs.(4.15)–(4.17) will be

$$L_{asr} = L_{asar} = L_{asbr} = L_{ascr} = \frac{2}{3}\frac{N_a N_r}{N_s^2}L_m$$

$$= \frac{2}{3}\frac{N_{us}N_r}{N_s^2}L_m + \frac{2}{3}\frac{N_{sh}N_r}{N_s^2}L_m = L'_{asar} + L_{shar} \tag{4.26}$$

$$L_{bsr} = L_{bsar} = L_{bsbr} = L_{bscr} = L_{csar} = L_{csbr} = L_{cscr}$$

$$= \frac{2}{3}\frac{N_s N_r}{N_s^2}L_m \tag{4.27}$$

As in the previous section, assuming that stator windings have different numbers of turns, *dq0* axes inductances can be obtained for an inter-turn short circuit condition by using the newly

defined self- and mutual inductances. The transformations of ${L^{ss}}_{abc}$ to ${L^{ss}}_{qd0}$ and ${L^{sr}}_{abc}$ to ${L^{sr}}_{qd0}$ are

$$L_{qd0}^{ss} = \begin{bmatrix} L_{11}^{ss} & 0 & L_{13}^{ss} \\ 0 & L_{22}^{ss} & 0 \\ L_{31}^{ss} & 0 & L_{33}^{ss} \end{bmatrix} \text{ and}$$

$$L_{qd0}^{sr} = \begin{bmatrix} L_{11}^{sr} & 0 & 0 \\ 0 & L_{22}^{sr} & 0 \\ L_{31}^{sr} & 0 & 0 \end{bmatrix} \tag{4.28}$$

where $L_{11}^{ss} = \left(L_q^s + L_q^{ssh}\right) + \left(L_q^{sh} + L_q^{ssh}\right)$, $L_{22}^{ss} = L_d^s$, $L_{11}^{sr} = L_q^{sr} + L_q^{shr}$ and $L_{22}^{sr} = L_d^{sr}$.

Similarly, the results of transformation of rotor self- and mutual inductances can be simplified as

$$L_{qd0}^{rr} = \begin{bmatrix} L_{11}^{rr} & 0 & 0 \\ 0 & L_{22}^{rr} & 0 \\ 0 & 0 & L_{33}^{rr} \end{bmatrix} \text{ and}$$

$$L_{qd0}^{rs} = \begin{bmatrix} L_{11}^{sr} & 0 & 0.5L_{31}^{sr} \\ 0 & L_{22}^{sr} & 0 \\ 0 & 0 & 0 \end{bmatrix} \tag{4.29}$$

where $L_{11}^{rr} = L_q^r$ and $L_{22}^{rr} = L_d^r$. Matrix elements are given in Appendix A.

The stator and rotor flux linkages for the new model of a squirrel cage induction motors will be

$$\begin{bmatrix} \lambda_q^{sh} \\ \lambda_q^s \\ \lambda_d^s \\ \lambda_q^r \\ \lambda_d^r \end{bmatrix} = \begin{bmatrix} L_q^{sh} & L_q^{ssh} & 0 & L_q^{shr} & 0 \\ L_q^{ssh} & L_q^s & 0 & L_q^{sr} & 0 \\ 0 & 0 & L_d^s & 0 & L_d^{sr} \\ L_q^{shr} & L_q^{sr} & 0 & L_q^r & 0 \\ 0 & 0 & L_d^{sr} & 0 & L_d^r \end{bmatrix} \begin{bmatrix} i_q^{sh} \\ i_q^s \\ i_d^s \\ i_q^r \\ i_d^r \end{bmatrix} \tag{4.30}$$

The stator phase resistances are

$$r_{as} = \frac{N_a}{N_s} r_s = \frac{N_{us}}{N_s} r_s + \frac{N_{sh}}{N_s} r_s = r'_{as} + r_{sh} \tag{4.31}$$

$$r_{bs} = r_{cs} = r_s \tag{4.32}$$

where r_{sh} is the shorted winding(s) resistance. Stator qd resistance for new model will be

$$\begin{bmatrix} r_q^{sh} \\ r_q^s \\ r_d^s \end{bmatrix} = \begin{bmatrix} \frac{2}{3} r_{sh} & 0 & 0 \\ 0 & r_{11}^s & r_{12}^s \\ 0 & r_{21}^s & r_{22}^s \end{bmatrix} \tag{4.33}$$

The shorted portion of the stator winding (sh) is seen to only appear in the q-axis element. The matrix elements are given in Appendix A. Fig. 4.3 shows the motor model with an inter turn short circuit [8], which only effects part of the q-axis stator winding. r_{ext} is an external short circuit current limiting resistance.

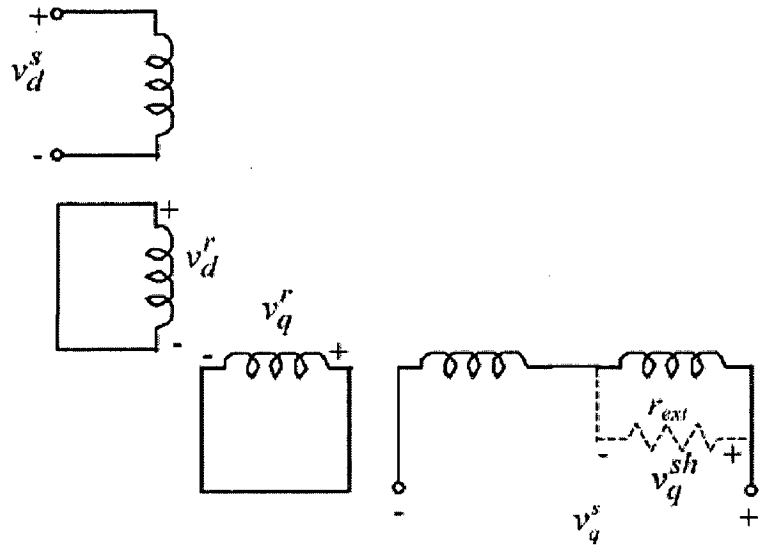

Fig.4.3.Motor Model with Inter Turn Stator Short Circuit.

Flux linkages may be obtained from Eq. (4.2) for a three wire system in the stationary reference frame to give

$$\lambda_q^{sh} = \int \left(v_q^{sh} - r_{sh}\, i_q^{sh}\right) dt,$$

$$\lambda_q^s = \int \left(v_q^s - v_q^{sh} - r_{11}^s i_q^s - r_{12}^s i_d^s\right) dt,$$

$$\lambda_d^s = \int \left(v_d^s - r_{21}^s i_q^s - r_{22}^s i_d^s\right) dt,$$

$$\lambda_q^r = \int \left(\omega_r \lambda_d^r - r_r^r i_q^r\right) dt,$$

$$\lambda_d^r = -\int \left(\omega_r \lambda_q^r + r_r^r i_d^r\right) dt \qquad (4.34)$$

Note that v_q^{sh} will be zero if the external resistance $r_{ext}$is zero.The current can be found by inverting Eq. (4.30).

4.5. Chapter Summary

In this chapter, a simulation model of induction motor with asymmetrical stator winding has been developed using the motor equations transformed from 3-phase to 2-phase stationary reference frame (qd axis). Then, the motor equations are so developed are modified to incorporate the effect of stator inter-turn fault and another simulation model of induction motor stator short circuit has been developed using these equations. The simulation results and the analysis of the characteristics of a induction motor with stator inter-turn fault are presented in the subsequent chapters.

CHAPTER 5

SIMULATION RESULTS OF STATOR FAULT INVESTIGATIONS

5.1 Simulation results of Induction motor model with stator Inter turn short circuit

The models developed have been simulated in Matlab/Simulink and the following simulation results are for a 2 hp motor whose parameters are given in Appendix A. The results are taken during acceleration from stand still to full speed. Figs. 5.1 and 5.2are results for acceleration from stand still to full speed at full load under normal conditions. Initially, motor currents are not symmetrical because of the starting transient. This introduces high negative sequence current until the motor reaches full speed.

a) *Torque(Nm) Vs Rotor speed*

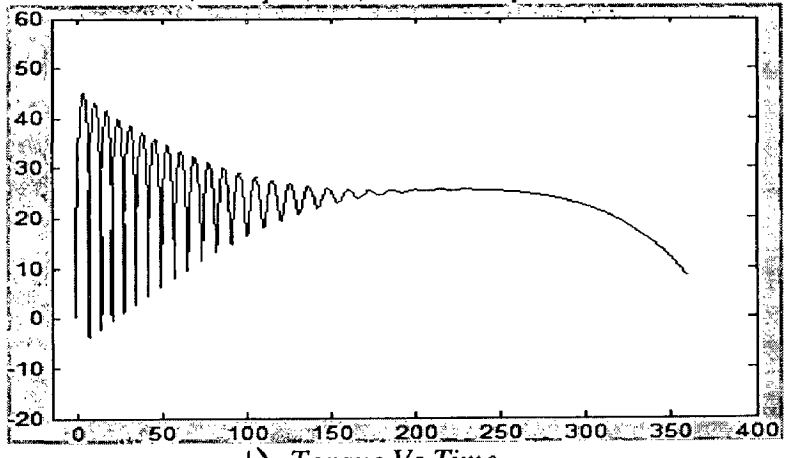

b) *Torque Vs Time*

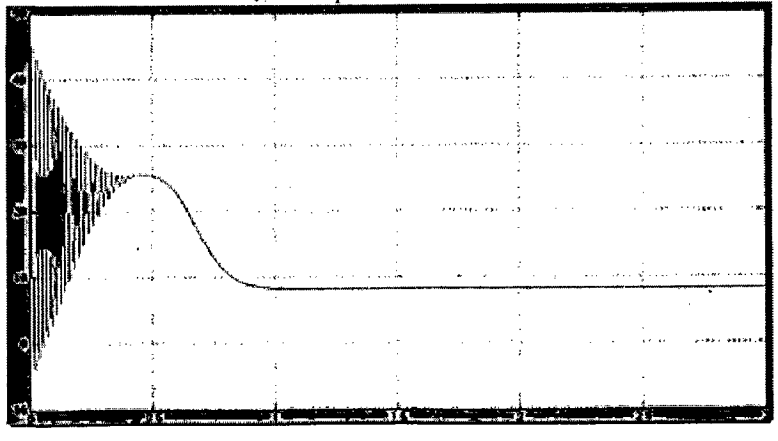

c) *Rotor speed Vs Time*

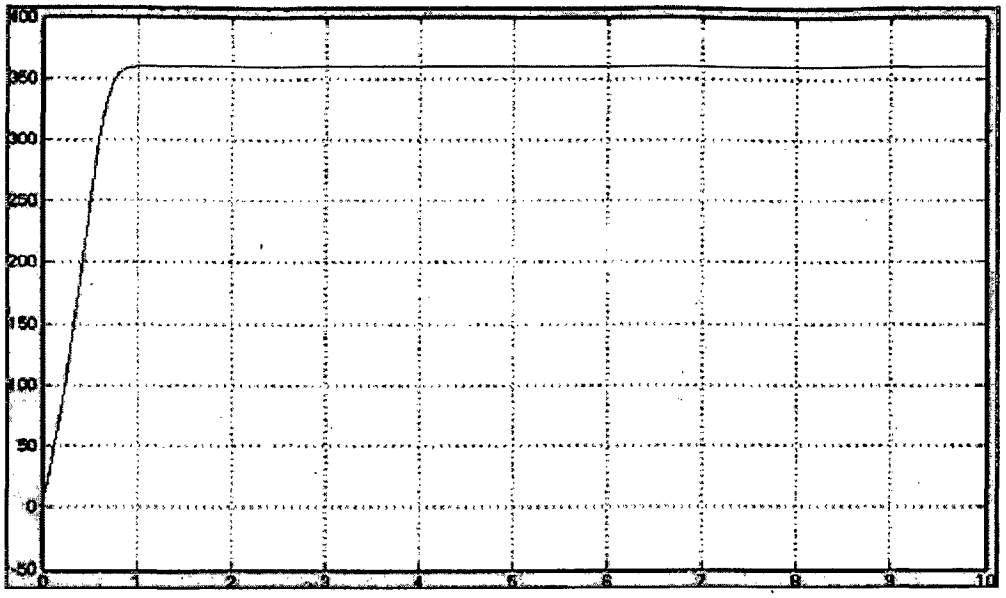

Fig. 5.1. Torque and speed variation under normal condition

a) *Positive Sequence Current*

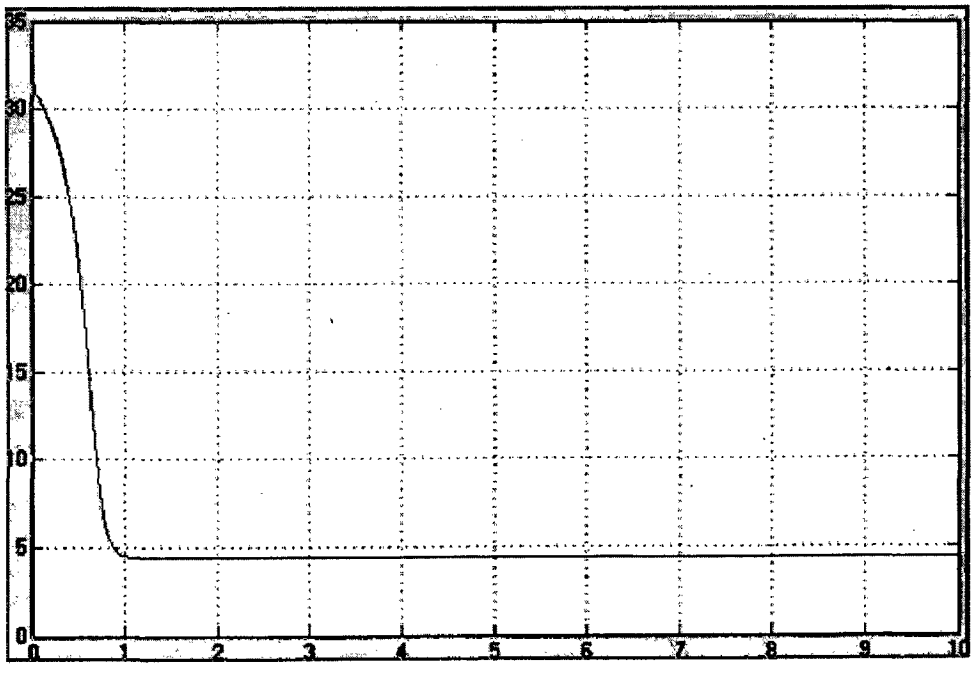

b) *Negative Sequence Current*

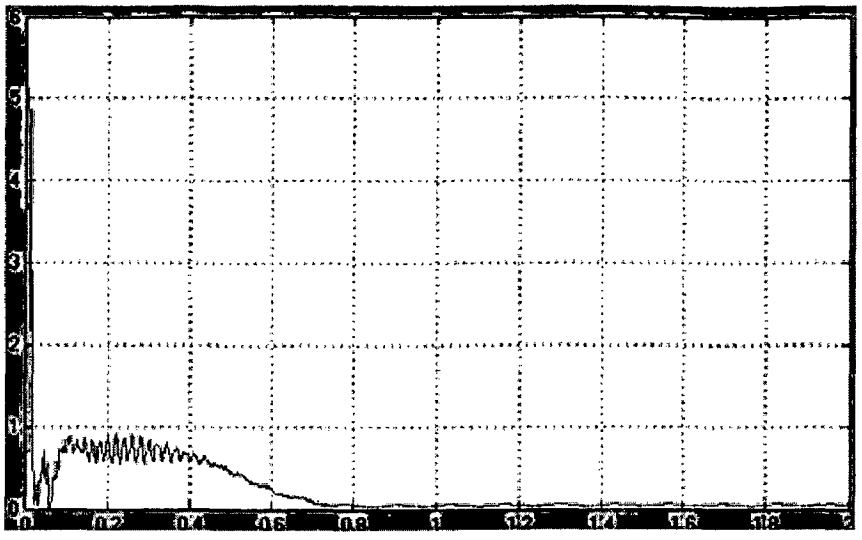

Fig. 5.2.Positive and negative sequence currents under normal condition.

Figs. 5.3and 5.5show the simulation results from stand still to full speed at full load with five turns shorted. The supply negative sequence current is around 0.35A. Because of stator asymmetry, the torque graph in Fig. 5.3 and 5.4shows the expected pulsation at twice supply frequency (2*fs*) even at steady state. This is because the negative sequence current introduces a braking torque in the motor. The short circuit current of 45 in the shorted turns seen in Fig. 5.5is 1.45 times the normal locked rotor current of 31 A.

a) *Torque(Nm) Vs Rotor speed*

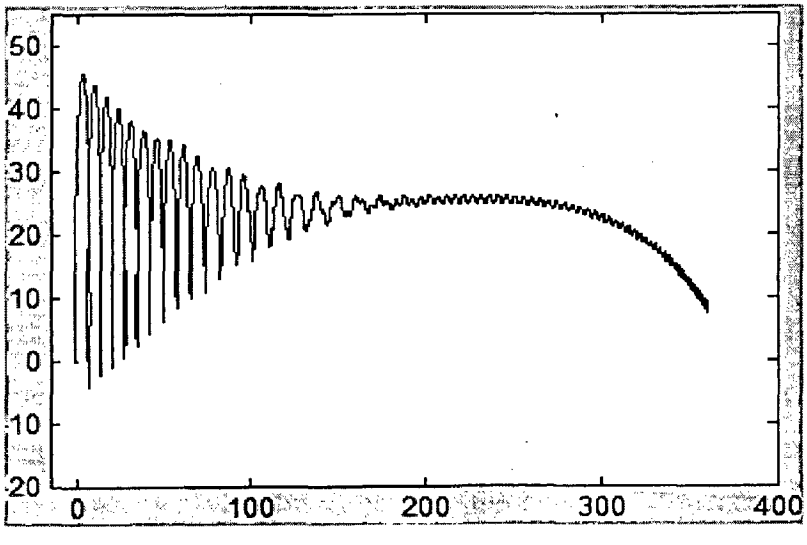

b) *Torque Vs Time*

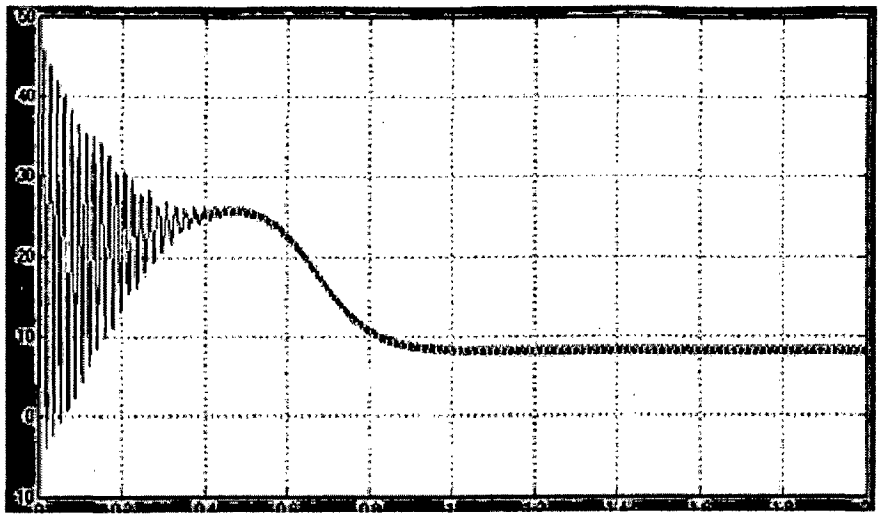

c) *Torque Pulsations:*

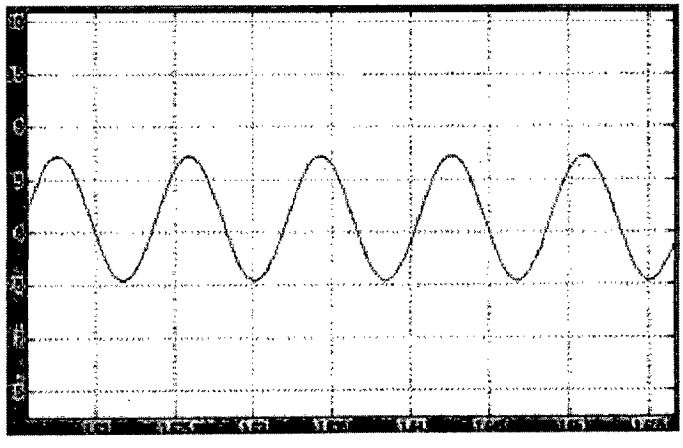

d) *Rotor speed Vs Time*

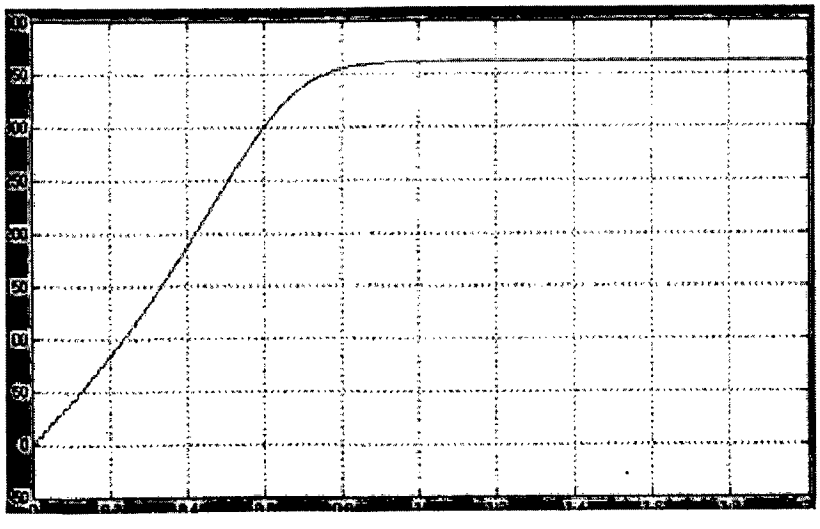

e) *Rotor speed pulsations:*

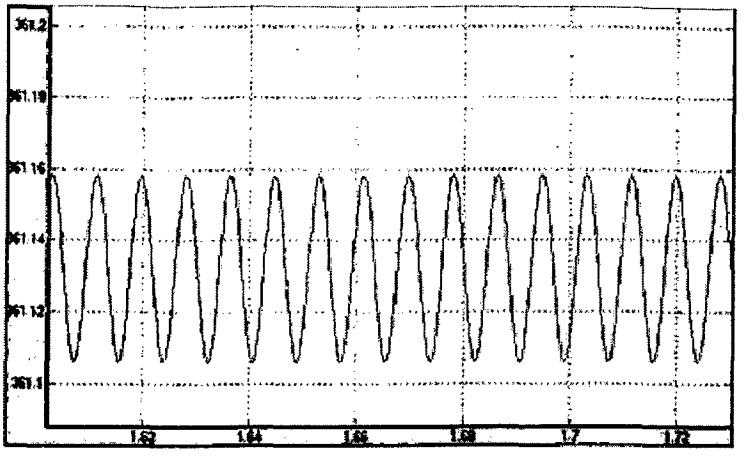

Fig. 5.3. Torque and speed variation with five turns shorted.

Fig.5.4. Different frequency components of Torque in an induction motor with Inter-turn fault:a)Fundamental frequency(60Hz), b)2nd harmonic, c)3rd harmonic, d)4th harmonic, e)5th harmonic.

a) *Positive Sequence current(A)*

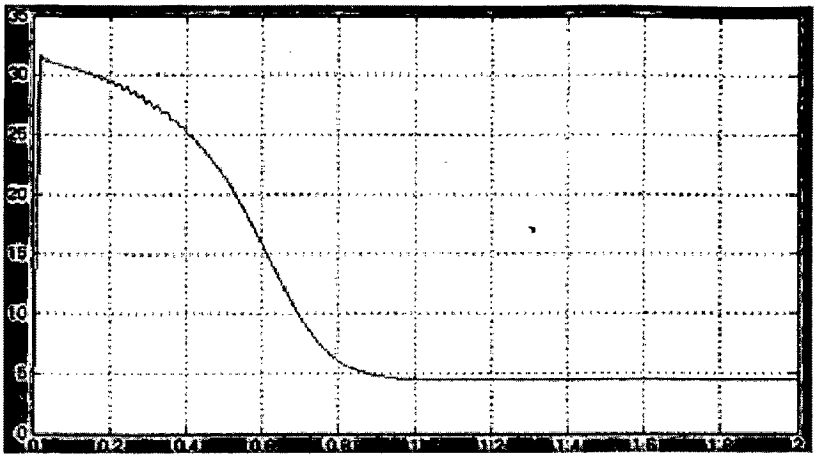

b) *Negative Sequence Current(A)*

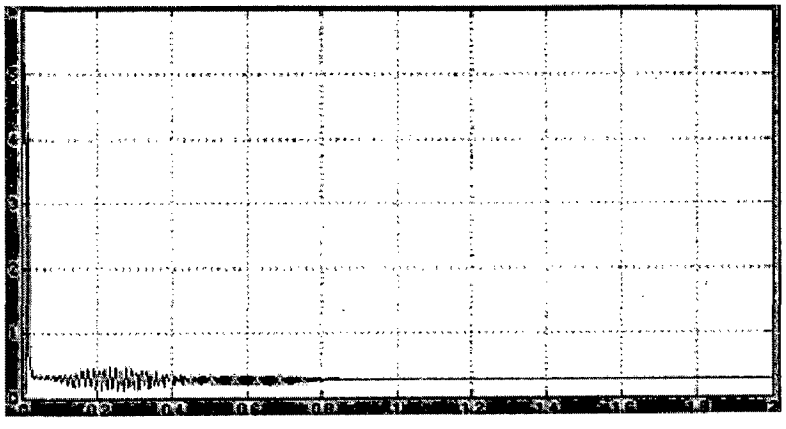

c) *Short Circuit Current(A)*

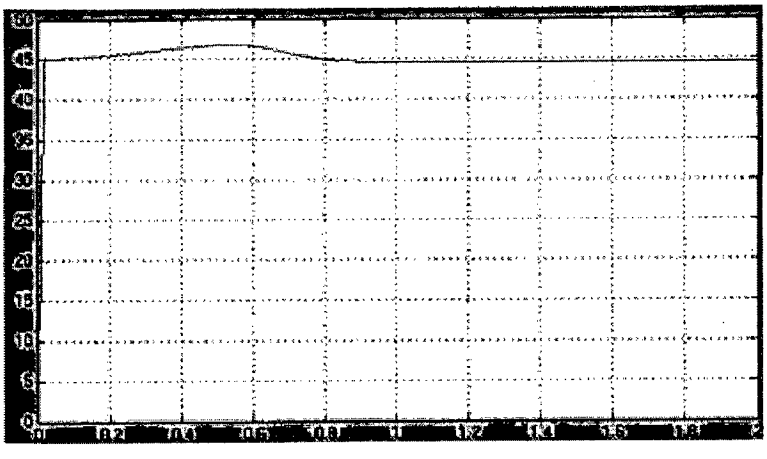

Fig. 5.5. Positive sequence, negative sequence, and short circuit currents for five turns shorted.

Figs. 5.6 and 5.7 are for same condition but with an external 1.5*ohm* resistance to limit short circuit current to avoid destruction of the motor. This limits short circuit current, and supply negative sequence current. The torque still has pulsation 2*fs* but is much smaller as seen inFig.5.6.

a) *Torque(Nm) Vs Rotor speed*

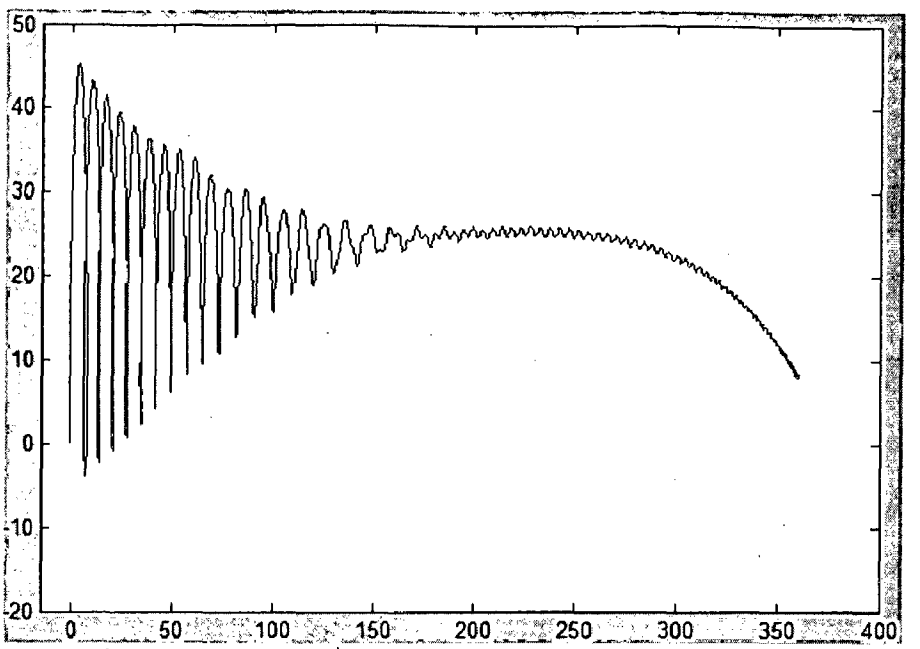

b) *Torque Vs Time*

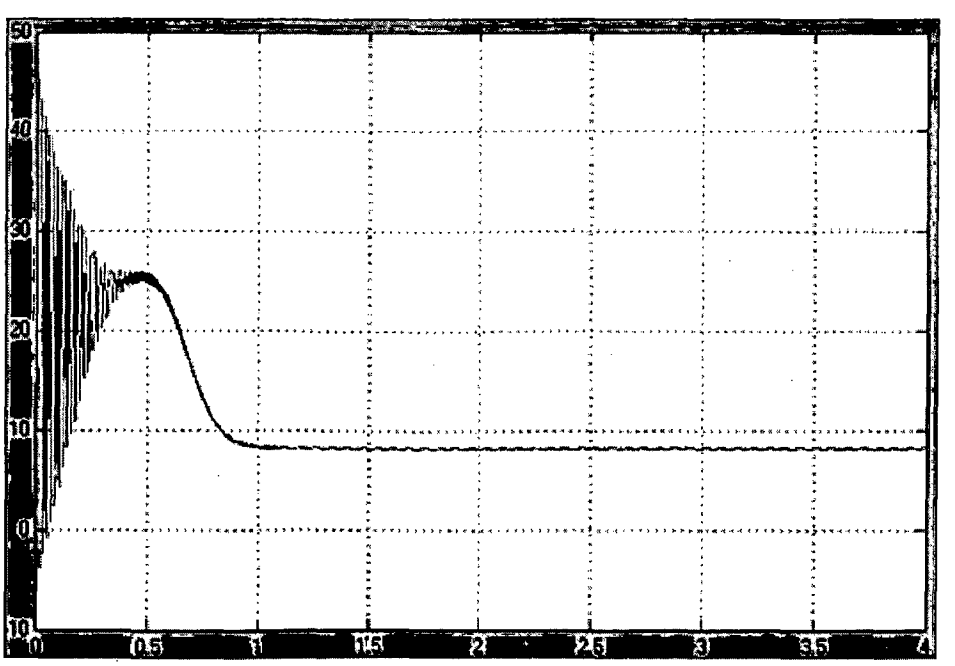

c) *Torque Pulsations:*

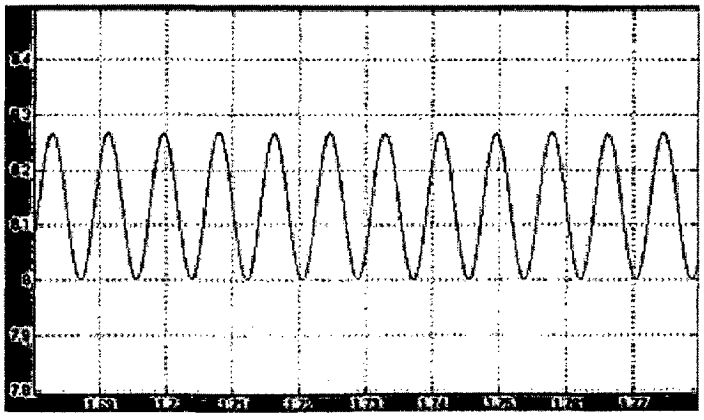

d) *Rotor speed Vs time*

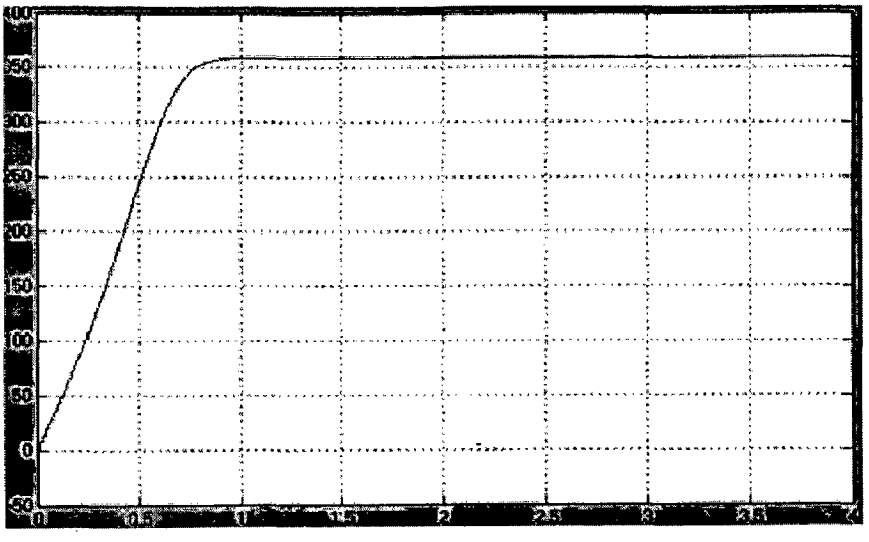

e) *Rotor Speed pulsations*

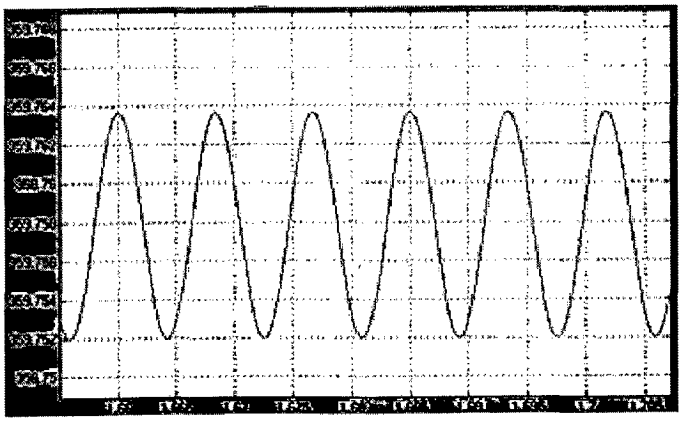

Fig. 5.6. Torque and speed variation with five turns shorted with 1.5ohm resistance.

a) *Positive Sequence current*

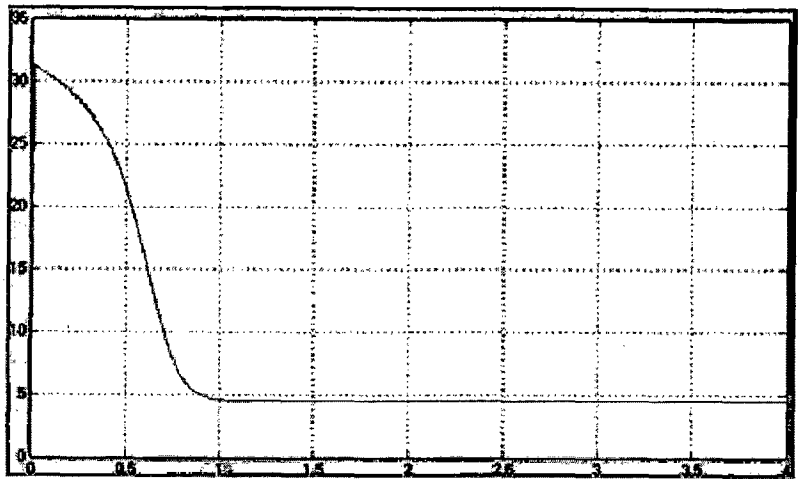

b) *Negative Sequence Current*

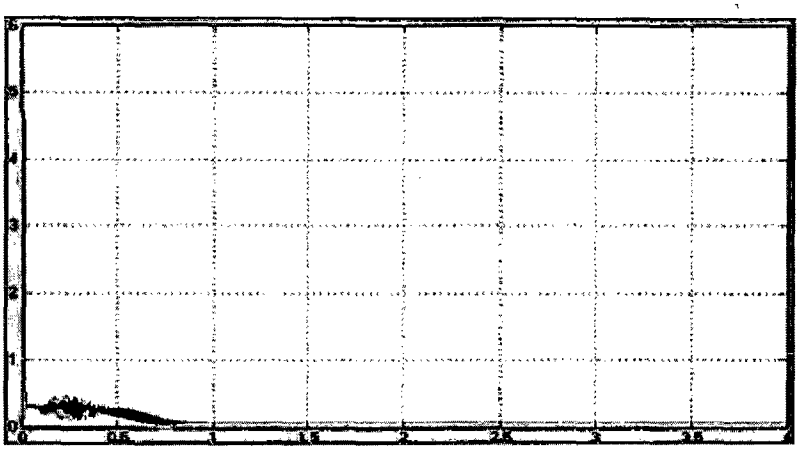

c) *Short Circuit Current*

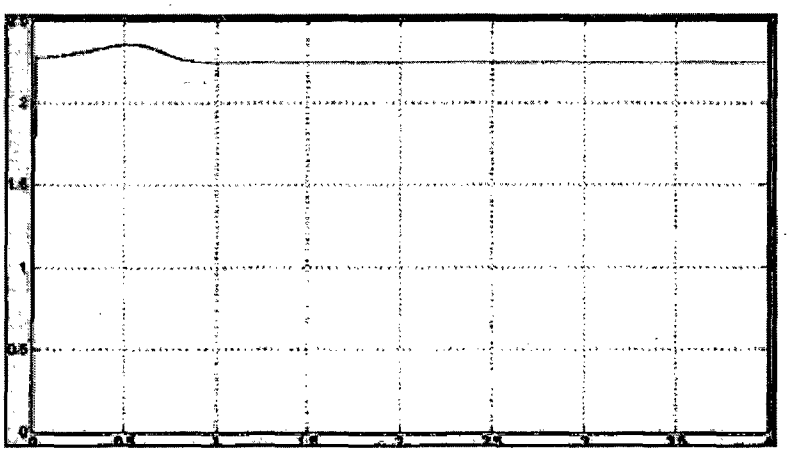

Fig. 5.7. Positive sequence, negative sequence and short circuit currents for five turns shorted with 1.5ohmresistance.

5.1.1. Effect of Number of shorted turns on the various characteristics of a induction motor

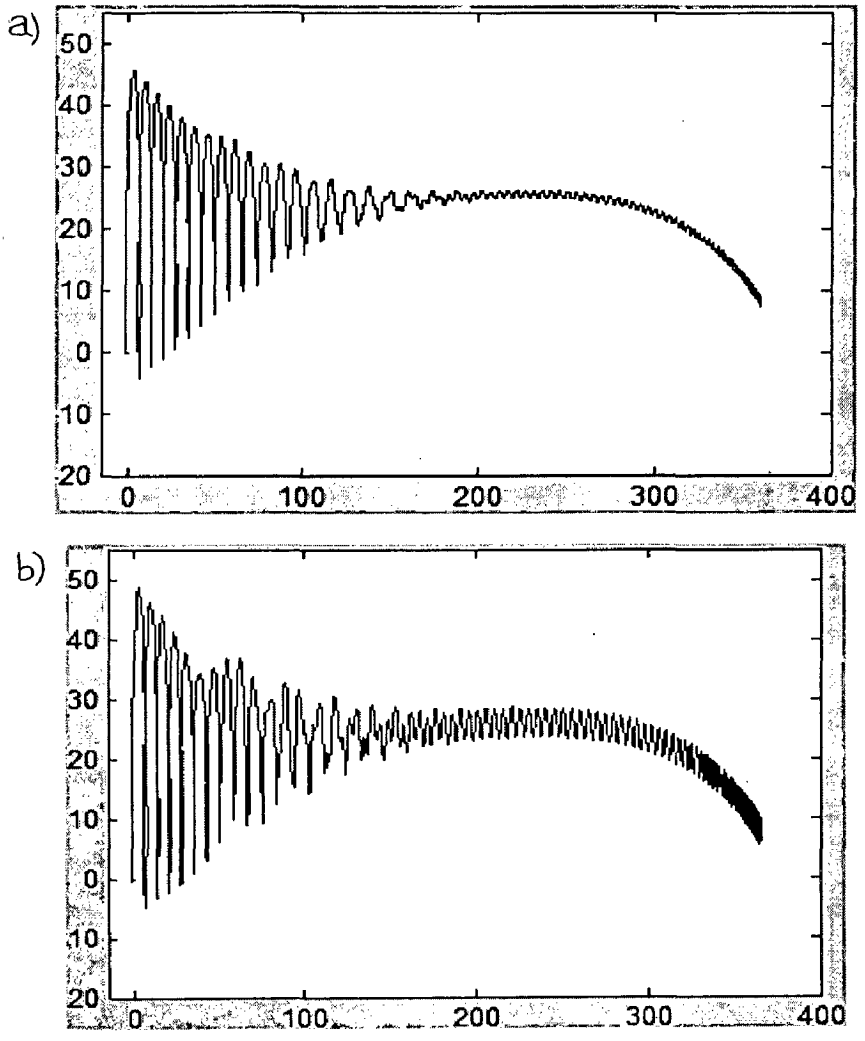

Fig.5.8. Torque-Speed characteristics when 5 turns and 20 turns of phaseA are shorted respectively

From Fig.5.8, when more number of turns are shorted in the phase A winding, the torque-speed characteristics shifts to the higher side compared to the torque-speed characteristic of a motor with less turns shorted. So, the motor approaches steady state i.e., $T = T_L$ at a higher speed. Also, since number of shorted turns is increased, the amount of asymmetry increases which increases the negative sequence current. Hence from Eq. (5.9), the twice the supply frequency oscillations in power increase resulting in the increase of torque pulsations. This can be observed from Fig.5.8.

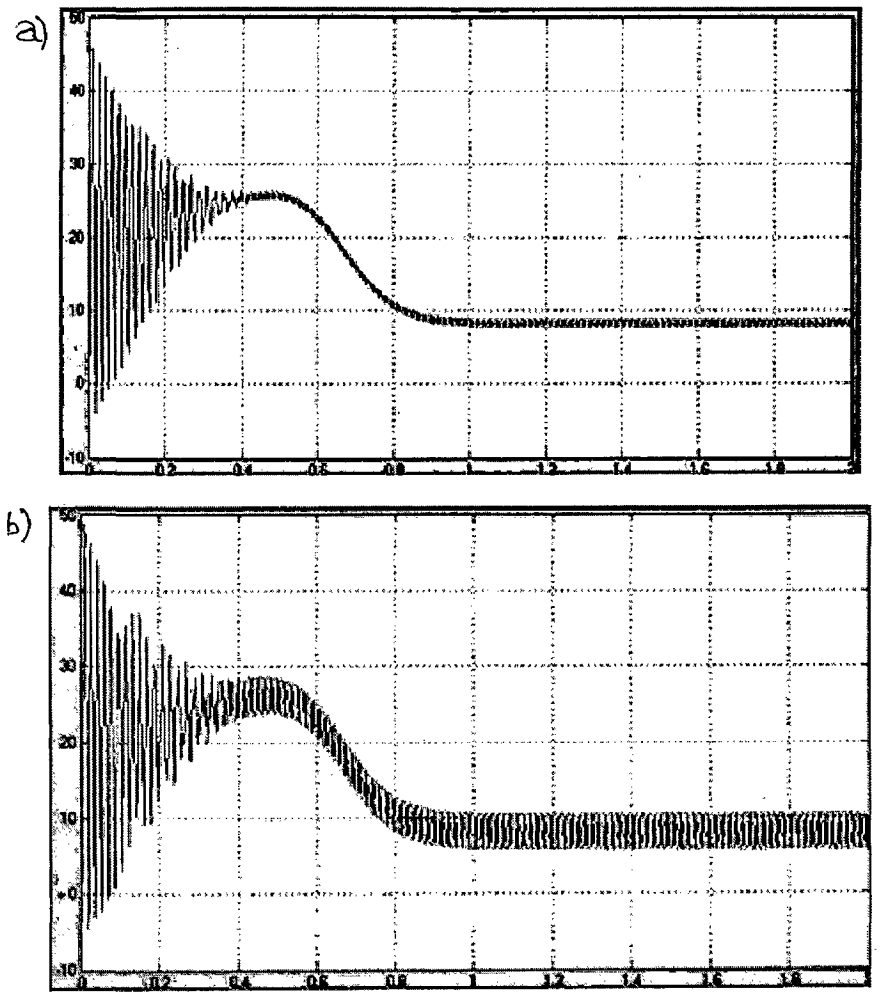

Fig.5.9. Torque characteristics when 5 turns and 20 turns of phaseA are shorted respectively

From Fig.5.9, as discussed earlier, when more number of turns are shorted, the torque characteristic follows a higher characteristic compared to the torque characteristic of a motor with less turns shorted which means at any particular instant, the torque of a motor with more shorted turns is higher than the torque of a motor with lesser shorted turns.

An increase in twice the supply frequency oscillations also occurs as the number of shorted turns is increased. This is due to the increase in the negative sequence current in Eq. (5.9).

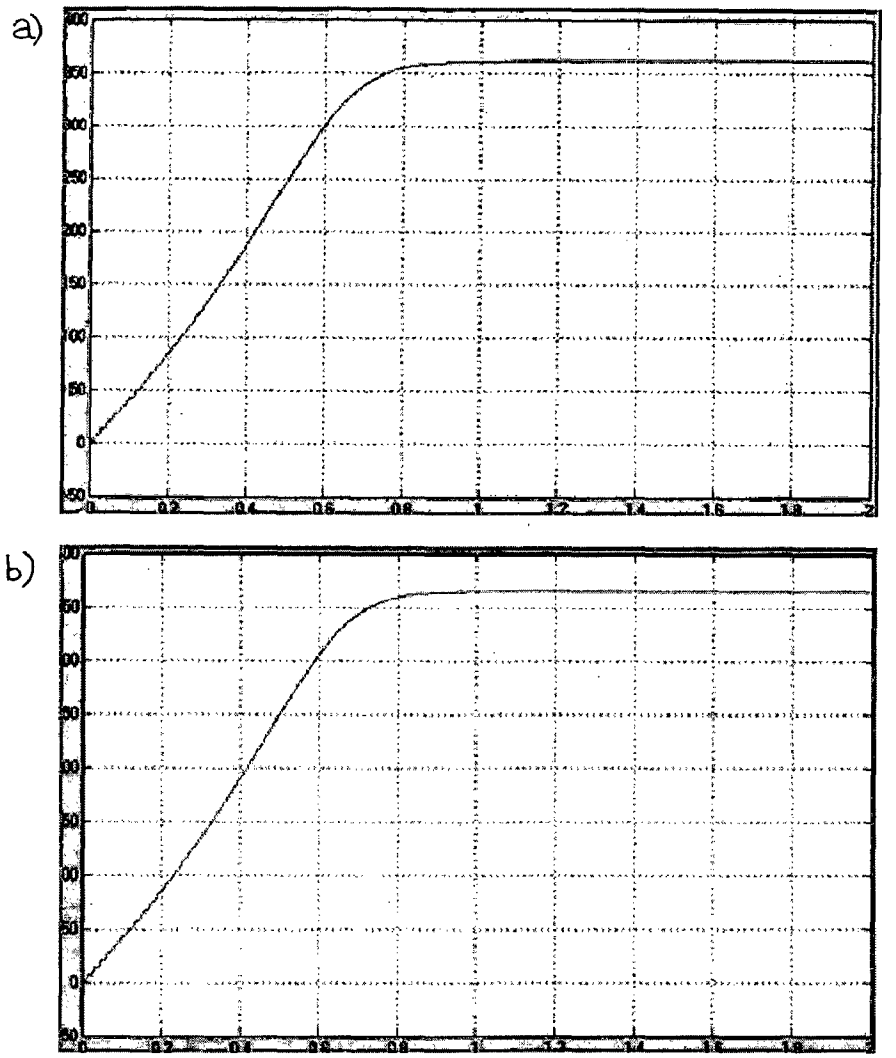

Fig.5.10. Speed characteristics when 5 turns and 20 turns of phaseA are shorted respectively

From Fig.5.10, as discussed earlier when there is an increase in the number of shorted turns in the winding of phase A, the torque-speed characteristics shifts to the higher side compared to the torque-speed characteristic of a motor with less turns shorted. So, the motor approaches steady state i.e., $T = T_L$ at a higher speed. This explains the increase in the speed from an inter turn fault with 5 shorted turns to inter turn fault with 20 shorted turns. The increase in the torque pulsations due to the increase in negative sequence current is reflected in the rotor speed pulsations.

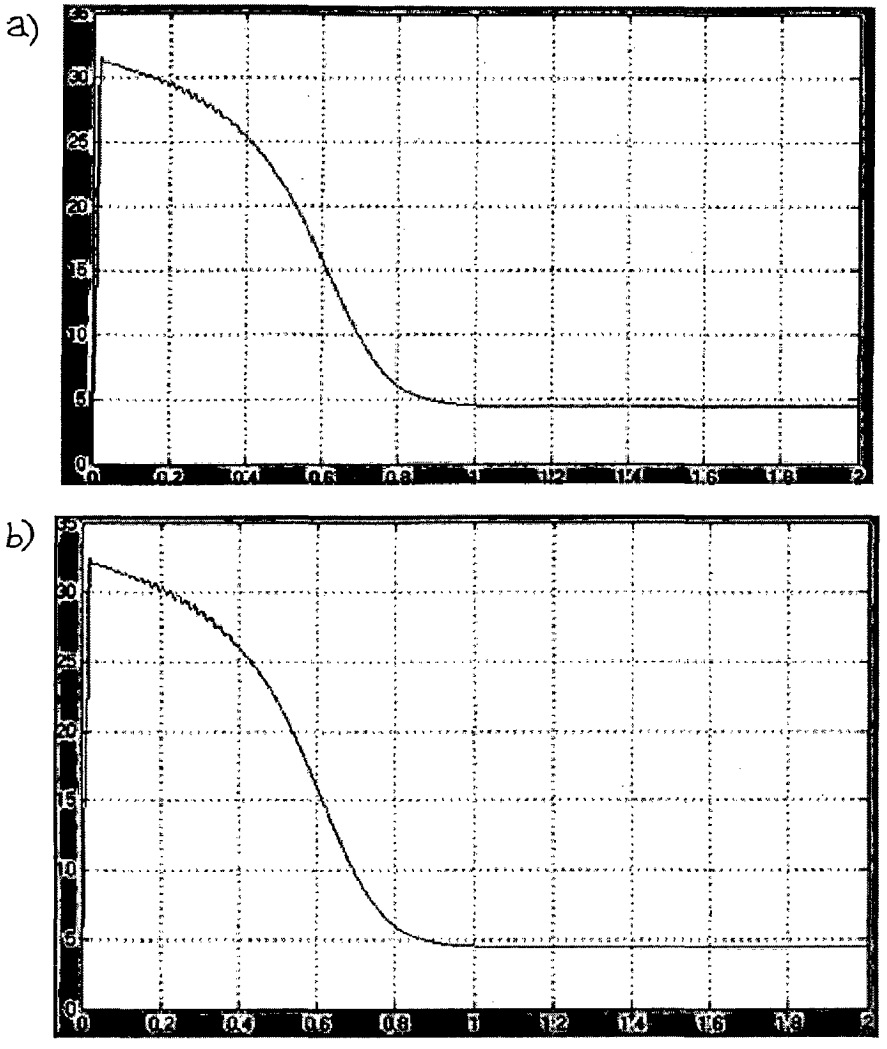

Fig.5.11. Positive Sequence current when 5 turns and 20 turns of phaseA are shorted respectively

It has been observed from Fig.5.5 that when an stator inter turn fault occurs there is negligible change in the positive sequence current compared to that of a healthy motor. The same is reflected in Fig.5.11, when the intensity of inter turn fault is increased by increasing the number of shorted turns there is no appreciable change in the positive sequence current.

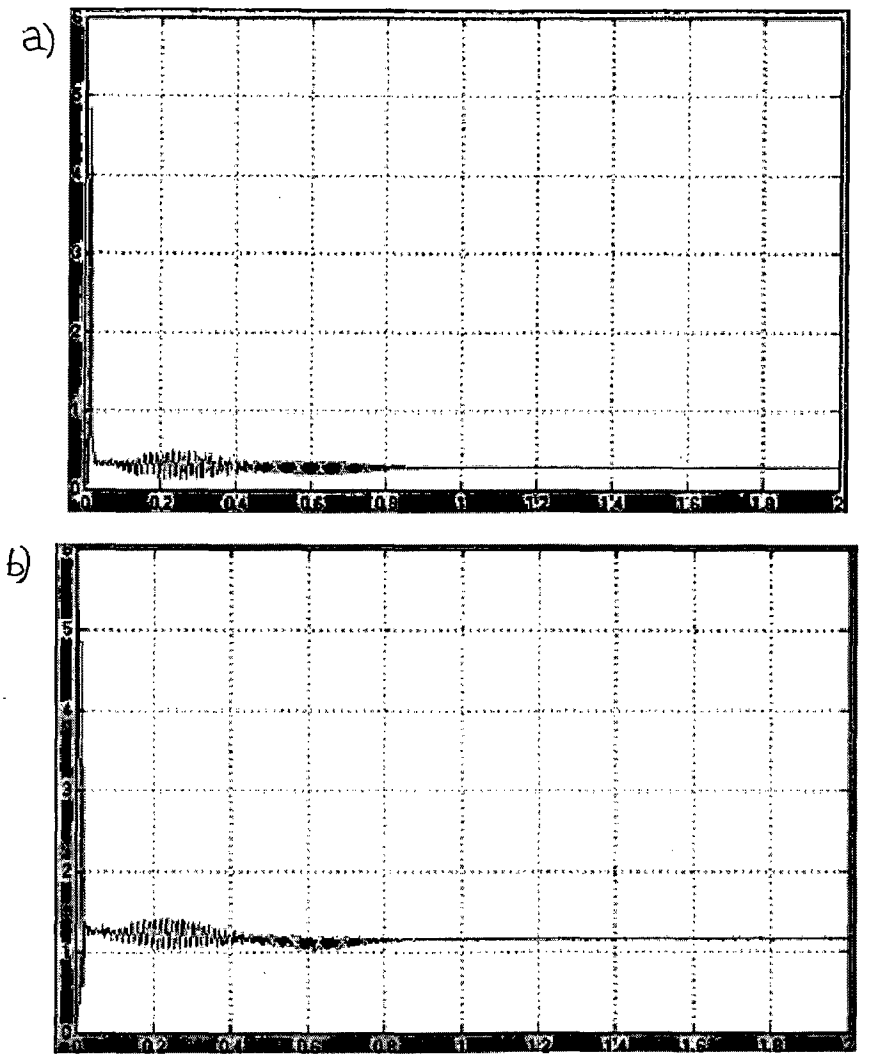

Fig.5.12. Negative Sequence current when 5 turns and 20 turns of phaseA are shorted respectively

From Fig.5.12, as number of shorted turns is increased, the amount of asymmetry created in the induction motor increases and hence the negative sequence current increases. The same is depicted in above fig. where the negative sequence current has increased from 0.25A to 1.2A.

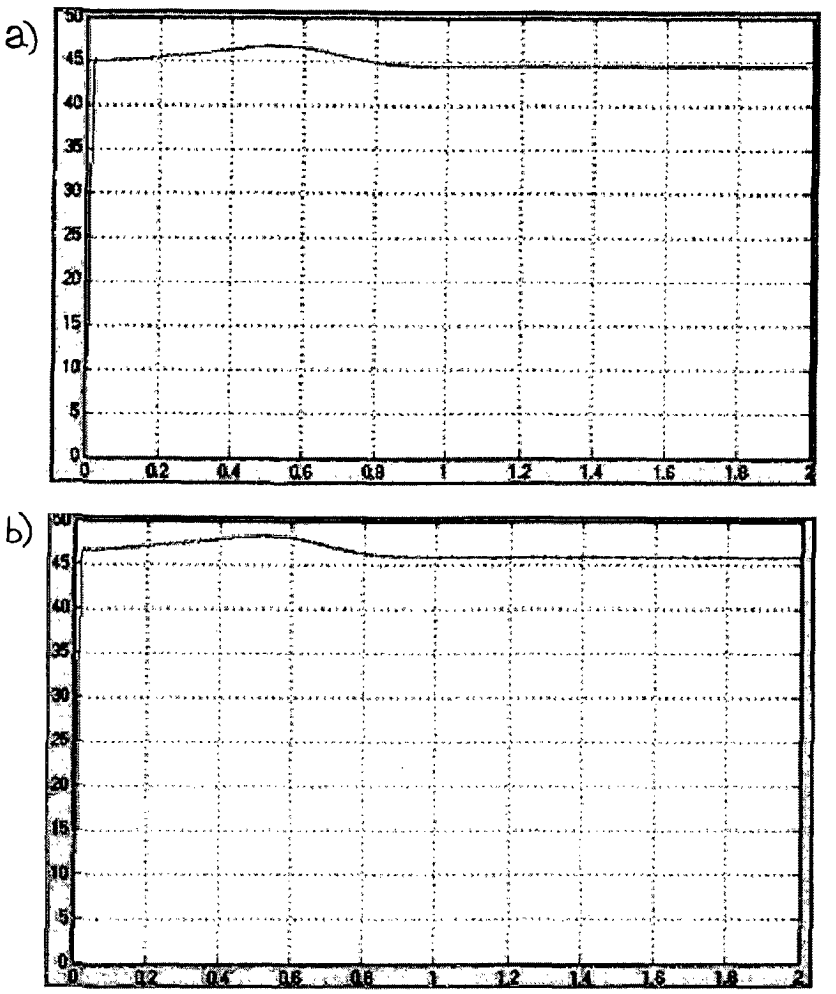

Fig.5.13. Short circuit current when 5 turns and 20 turns of phaseA are shorted respectively

In Fig.5.13, when the number of shorted turns in the winding of stator phase A is increased, the contribution of the short circuit current to the total phase current increases and hence the short circuit current increases.

5.2. Experimental Results of Stator Inter turn Fault depicting the presence of Negative sequence current and the effect of number of shorted turns

Motor Parameters: A 4-pole, 50Hz, 3hp, 440V, three phase squirrel cage induction motor with rated speed as 1480rpm and rated current as 3A. Its stator contains double layer lap winding with 36 slots and coil span of 7 slots.

Procedure: Experiments were done on the above three phase squirrel cage induction motor for stator inter turn fault analysis by short circuiting few of the coils in the winding of a single phase or two phases and the motor was then run using a balanced 3-phase voltage supply connected through a 3-phase auto transformer.

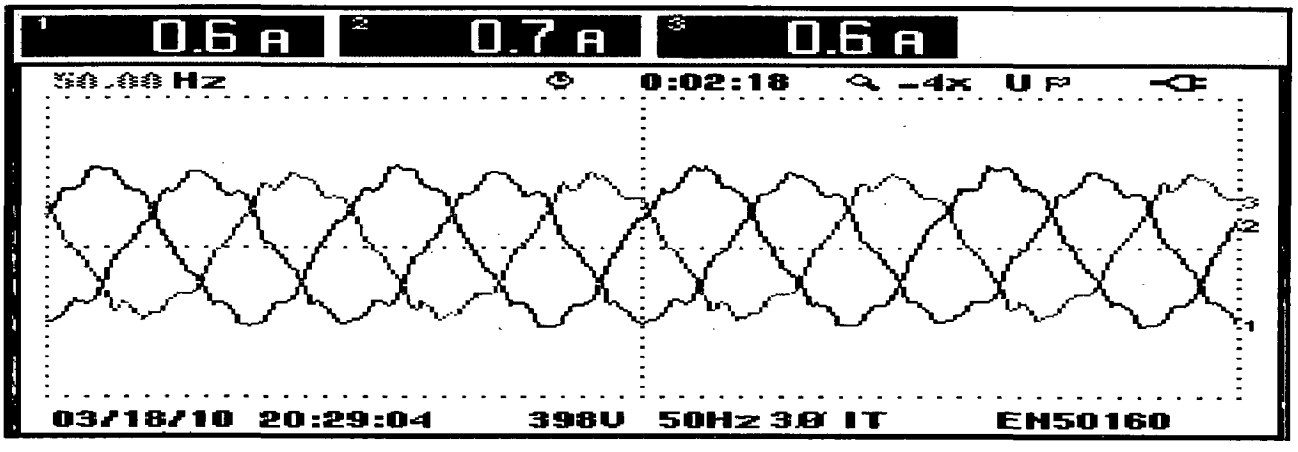

Fig.5.14. Motor operating at no load under healthy condition

From Fig.5.14, we can notice that under healthy condition the motor draws balanced currents.

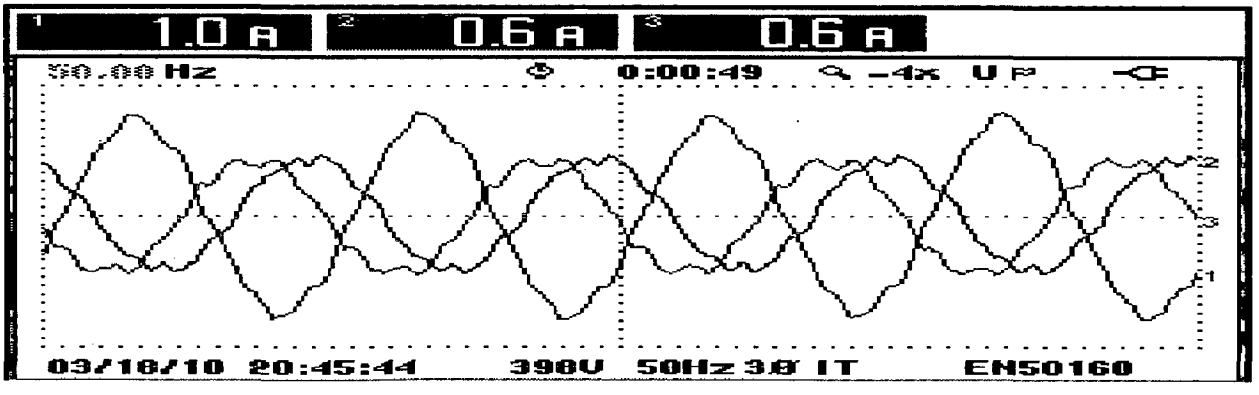

Fig.5.15. Motor operating at no load under one coil of phase A is short circuited

From Fig.5.15, It is observed that the phase A draws more current than other phases due to short circuit fault in phase A. Hence, motor under short circuit faults draws unbalance stator currents.

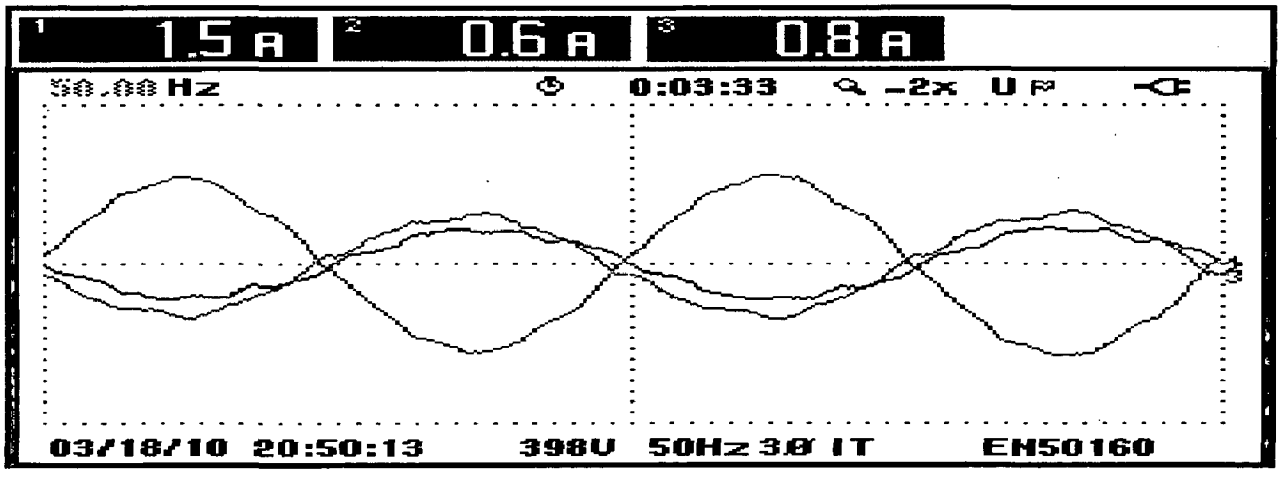

Fig.5.16. Motor operating at no load under coil 1 & coil 2 of phase A is short circuited.

From Fig.5.16, it is similar to the case when one coil was short circuited, but due to the presence of two shorted coils, the phase A current increases. It still draws unbalanced stator currents.

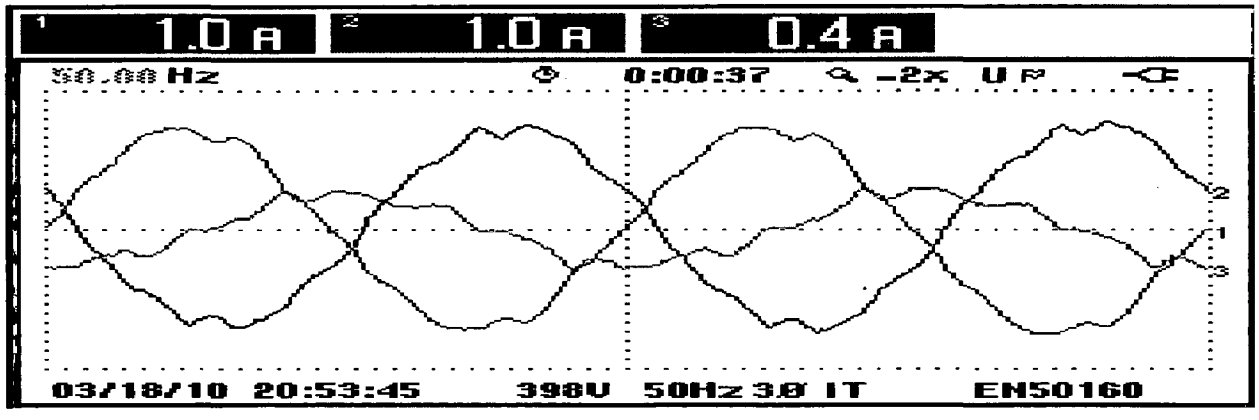

Fig.5.17. Motor operating at no load under one coil each in phase A and phase B are short circuited.

From Fig.5.17, due to the short circuit of a part of the winding in both phase A and phase B, motor draws unbalance stator currents similar to single phase short circuit. In this case, phase B current also increases.

Hence, from the above experimental study it is evident that when an inter turn fault is present in an induction motor, it draws unbalanced stator phase currents. This results in the occurrence of a significant amount of negative sequence current as justified by the equation,

negative sequence current, $i_2 = i_a + a^2 i_b + a i_c$ where i_a, i_b, i_c are the three stator phase currents.

In Fig.5.15, Δi_a = 0.4A, Δi_b = 0A, Δi_c= 0A

In Fig.5.16, Δi_a = 0.9A, Δi_b = 0A, Δi_c= 0.2A

In Fig.5.17, Δi_a = 0.4A, Δi_b = 0.4A, Δi_c= -0.2A

It can be stated from the above results that an inter turn short circuit affects the faulty phases to greater extent than the other phases.

5.3. Relation between shorted turns and negative sequence current

Results have also been obtained by simulation for different numbers of directly shorted turns (r_{ext} = 0). For r_{ext} =0 negative sequence current $I_n$is proportional to the number n of shorted turns

$$I_n \propto n \text{ or } I_n \cong kn \tag{5.1}$$

where k is constant.

Fig. 5.18 shows I_{rext} current in the external resistance andnumber of shorted turns relation with 0 and 0.2Ω external current limiting resistance. As it can be seen from figure short circuit current is almost independent of the number of shorted turns when external resistance is zero, at 2.6 times locked rotor current. This means that for a short circuit fault involving only few turns, the motor will run for a considerable time, from a few minutes to an hour, since the shorted turns can dissipate heat into adjacent turns. In addition, as their temperature rises, their resistance increases, and Fig. 5.18 shows that the current reduces quite rapidly with additional resistance within the short circuit path. Fig.5.19 presents relation between the number of shorted turns, external current limiting resistance, and negative sequence current.

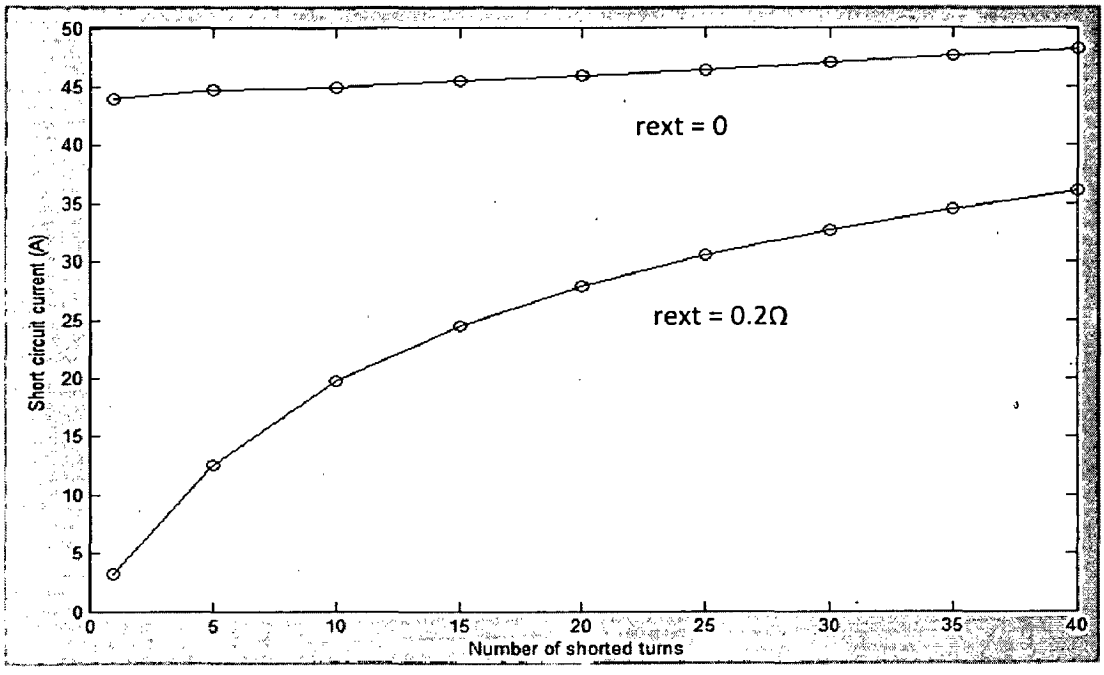

Fig.5.18 Short circuit current vs. shorted turns for different external resistance values (r_{ext}).

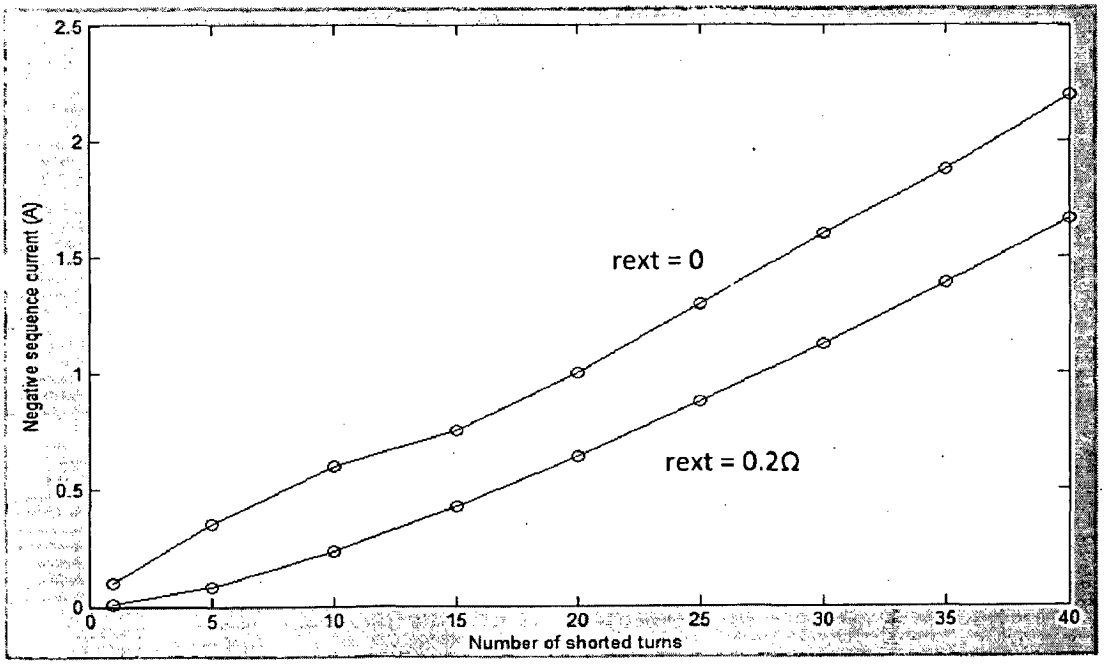

Fig.5.19 Negative sequence current vs. shorted turns for different external resistance values (r_{ext}).Short circuit current limited by 0 and 0.2Ω resistance.

5.4 Effect of unequal winding temperatures

If a motor is operated from an unbalanced voltage supply, the heating effect of unequal phase currents will cause resistive unbalance to develop between the phases, whose contribution to negative sequence current could be confused with a stator fault.

Assuming an additional temperature rise in only one motor phase, its effect may be obtained by considering an unbalance resistance r_{unb} in series with stator phase *as*. The maximum added resistance r_{unb} is 1ohm which is equivalent to a 61.5^0 C temperature rise. I_n is linearly proportional to r_{unb}(see Fig. 5.20).

$$I_n \propto r_{unb} \tag{5.2}$$

The relation between r_{unb} and negative sequence current can be defined [8] as

$$I_n = \frac{r_{unb}}{3} \frac{I_{sp}}{Z_n + (r_{unb}/3)} \tag{5.3}$$

where Isp is positive sequence current, $Zn = \left| r_s + \frac{r_r}{2-s_p} + j(X_s + X_r) \right|$,

and if $Zn >> r_{unb}/3$the above equation can be simplified to

$$I_n = \frac{r_{unb}}{3} \frac{I_{sp}}{Z_n} \tag{5.4}$$

under balanced supply conditions.

The relation between negative sequence and the number of shorted turns n is presented in [8] as

$$I_n = \frac{3}{8} \frac{n}{N_s} \frac{V_{sp}}{Z_s} \tag{5.5}$$

Where Vsp is the applied positive sequence voltage, Ns the total number of turns, n the number of shorted turn, and Zs=|rs+ jXs|. The relation between r_{unb} and n to give the same negative sequence current can be defined as

$$\frac{r_{unb}}{n} = \frac{9}{8} \frac{1}{N} \frac{Z_n}{Z_s} \frac{V_{sp}}{I_{sp}} \tag{5.6}$$

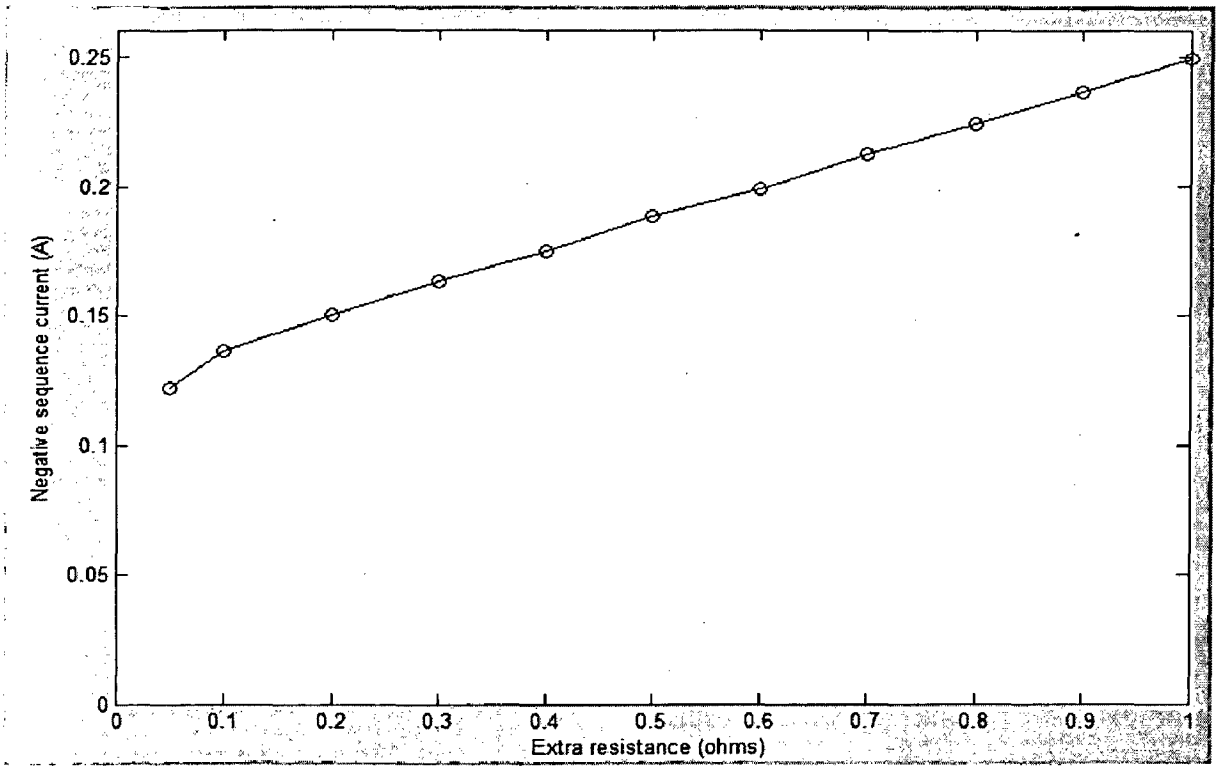

Fig. 5.20. Negative sequence current vs. extra series resistance r_{unb}

5.5 Effect of Voltage Unbalance on the characteristics of an Induction motor with Stator Inter turn fault

For the effect of voltage unbalance on the motor torque and power to be analyzed, voltage and currents are expressed in its symmetrical components. If the motor is supplied by unbalanced voltages, voltages and currents in a stationary reference frame are given by [64]:

$$v_{qds} = V_{sp}e^{j\omega_s t} + V_{sn}^{*}e^{-j\omega_s t}$$

$$i_{qds} = I_{sp}e^{j\omega_s t} + I_{sn}^{*}e^{-j\omega_s t} \tag{5.7}$$

In this reference frame, the instantaneous active power is calculated as follows:

$$p = \frac{3}{2}Re\left[v_{qds}i_{qds}^{*}\right] \tag{5.8}$$

By replacing voltages and currents, the power results in

$$p = \frac{3}{2}Re\left(V_{sp}I_{sp}^{*} + V_{sn}^{*}I_{sn}\right) + \frac{3}{2}Re\left(V_{sp}I_{sn}e^{j2\omega_s t}\right) + \frac{3}{2}Re\left(V_{sn}^{*}I_{sp}^{*}e^{-j2\omega_s t}\right) \quad (5.9)$$

The first term corresponds to the average power P_0, while the second and third terms contains the components at twice the supply frequency, produced by voltage and current unbalance. Hence, the motor power under voltage unbalance will present a pulsating component at twice the supply frequency. This oscillating power at twice the supply frequency results in a pulsating torque.

The positive sequence and negative sequence voltages obtained from Eq. (5.7) are applied to respective induction motor equivalent circuits as shown in Fig.5.21 [65]. where V1 is Positive sequence voltage, V2 is Negative sequence voltage, Ip is Positive sequence current, In is Negative sequence current, X1 is stator reactance, X'2 is rotor reactance referred to stator, R1 is stator resistance, R'2 is rotor resistance referred to stator, Xm is magnetizing reactance and S is slip.

The reduction of output power and motor torque due to unbalance voltage can be studied from Fig.5.21 and Fig.5.22 as follows [65].

$$P_m = I_p^2 R2\left[\frac{1-S}{S}\right] - I_n^2 R2\left[\frac{1-S}{2-S}\right] \text{ (per phase)}$$

$$T = R2\,\frac{\left[\frac{I_p^2}{S} - \frac{I_n^2}{2-S}\right]}{\omega_s} \text{ (per phase)} \quad (5.10)$$

Note the reduction in output power and torque due to the negative sequence current, where ω_s is the synchronous speed.

Using Eq. (5.10) and by equivalent circuits in Fig.5.21 the positive and negative sequence torque-speed curves may be plotted as

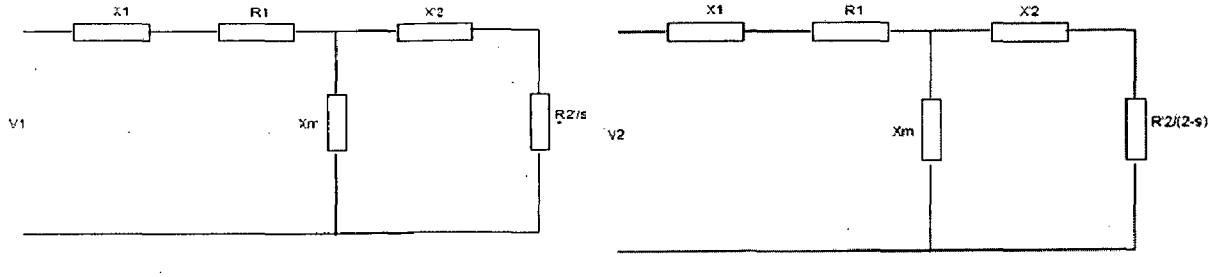

Fig.5.21. Positive and negative sequence equivalent circuits

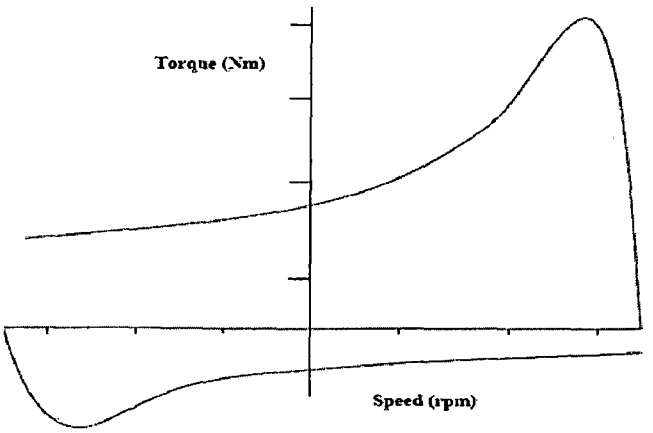

Fig.5.22. Torque-Speed characteristics when voltage unbalance is present

shown in Fig.5.22.The upper curve is the torque due to positive sequence component of current and the lower curve is the torque due to negative sequence component of current. The positive sequence torque resembles the torque of an induction motor operating from a balanced supply. Normal operation is between zero speed and synchronous speed. The counter rotating field produced by the negative sequence currents produces a negative sequence torque, with a peak in 3rd quadrant. The net shaft torque produced by the machine will be somewhat less than that produced by a balanced supply i.e. the entire envelope of the torque speed curve is reduced.

a) **HEALTHY CONDITION :Vas=265.59V, Vbs=265.59V, Vcs=265.59V**

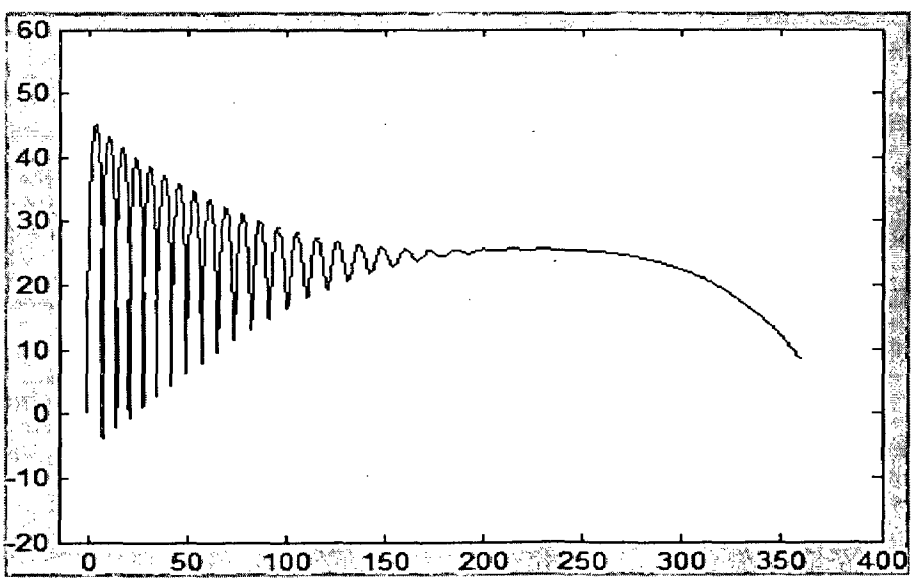

b) **Vas = 173.21V**, Vbs = 265.59V, Vcs = 265.59V

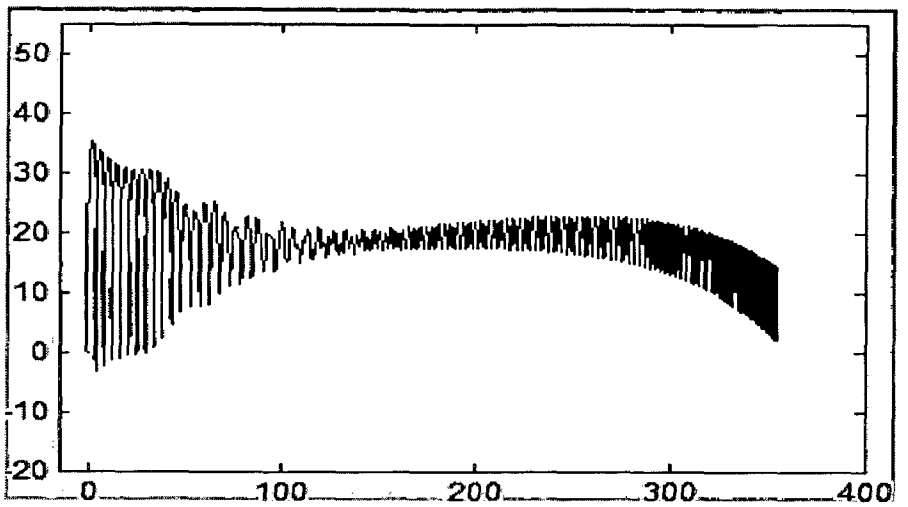

Fig.5.23. Torque-Speed characteristics in a) healthy condition (balanced voltages) and b) when the voltage of phase A is decreased.

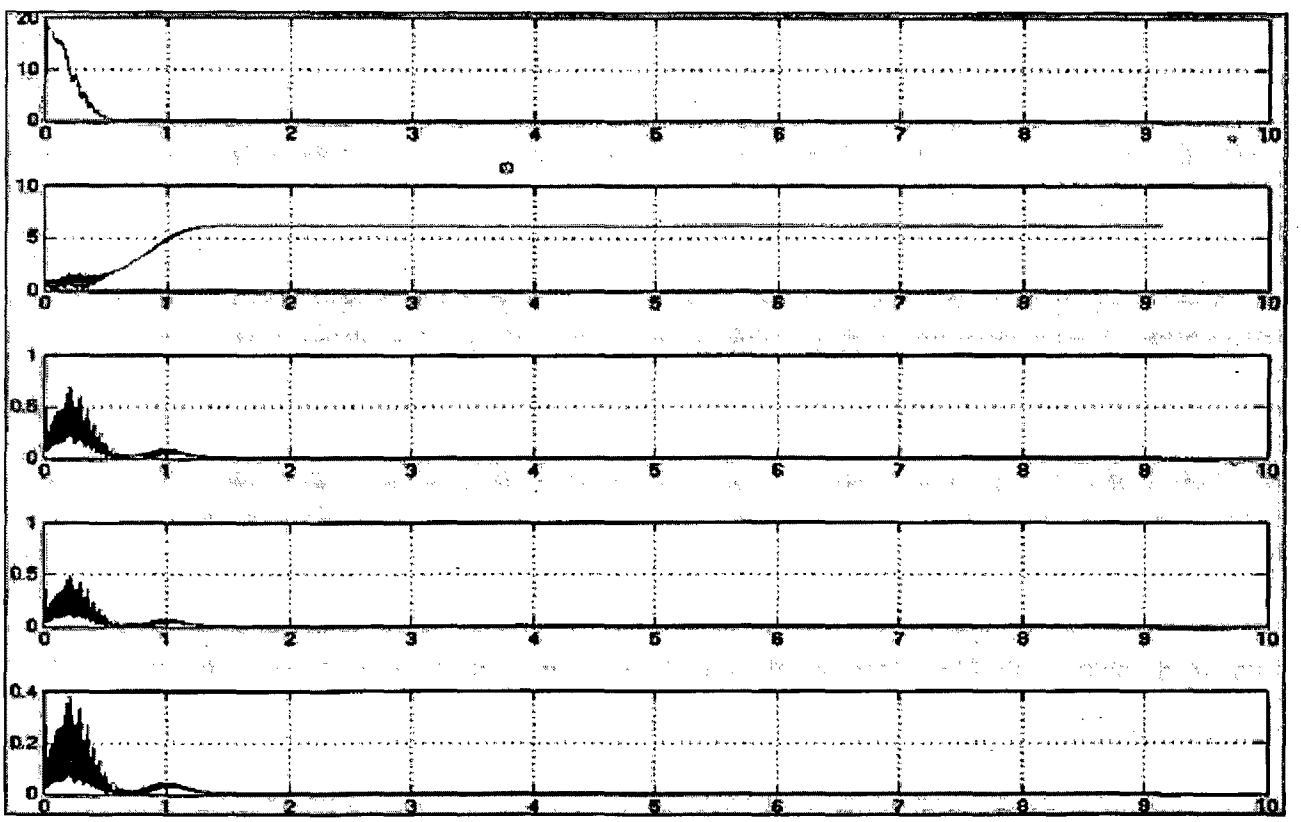

Fig.5.24. Different frequency components of Torque when Voltage Unbalance is present in an induction motor with Inter-turn fault:a) Fundamental frequency(60Hz), b) 2nd harmonic, c) 3rd harmonic, d) 4th harmonic, e) 5th harmonic.

Vas = 57.74V, Vbs = 265.59V, Vcs = 265.59V

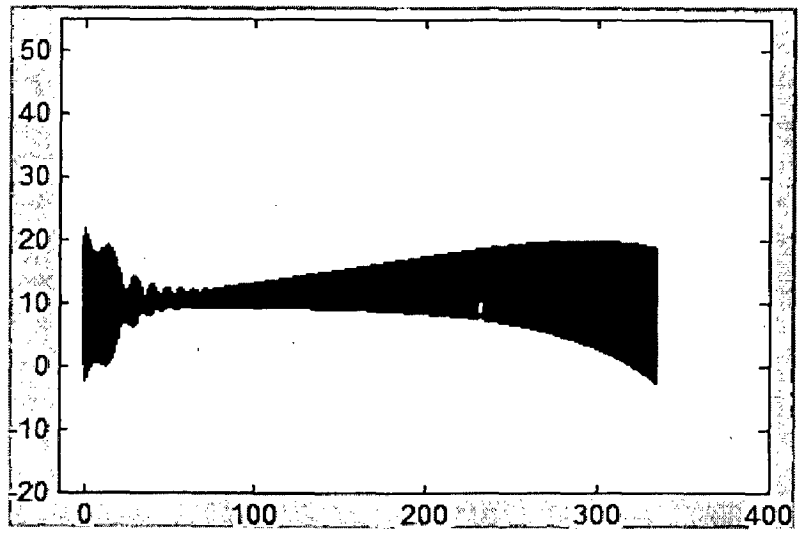

Fig.5.25. Torque-Speed characteristics as the voltage of phase A is decreased

From Fig. 5.23 and 5.25, as the voltage decreases, the resultant flux decreases and hence the torque-speed characteristics shifts to the lower side compared to the torque-speed characteristics of a healthy motor. So, the motor approaches steady state i.e., $T = T_L$ at a lower speed.

As voltage of one of the phases decreases, the voltage unbalance increases which increases the negative sequence component of voltage. The combined effect of voltage unbalance and inter turn fault increases the negative sequence current. Hence from Eq. (5.9), the twice the supply frequency oscillations in power increase resulting in the increase of torque pulsations. The phase sequence was also observed to be unchanged. This can be observed from Fig.5.23, Fig.5.24 and Fig.5.25.

a) **HEALTHY CONDITION: Vas=265.59V, Vbs=265.59V, Vcs=265.59V**

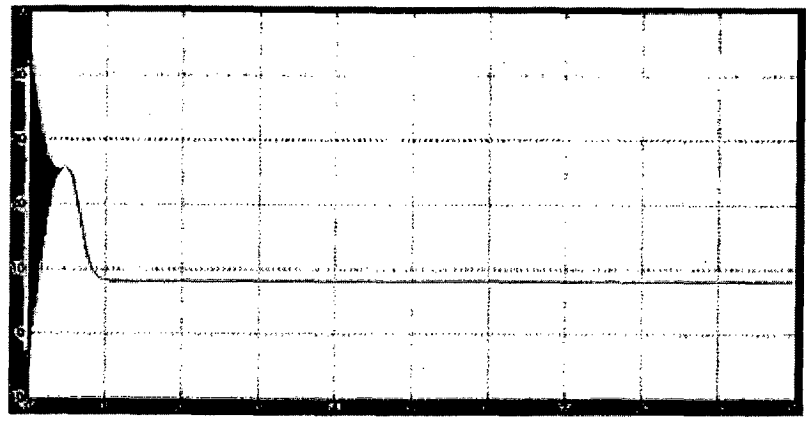

b) **Vas = 173.21V**, Vbs = 265.59V, Vcs = 265.59V

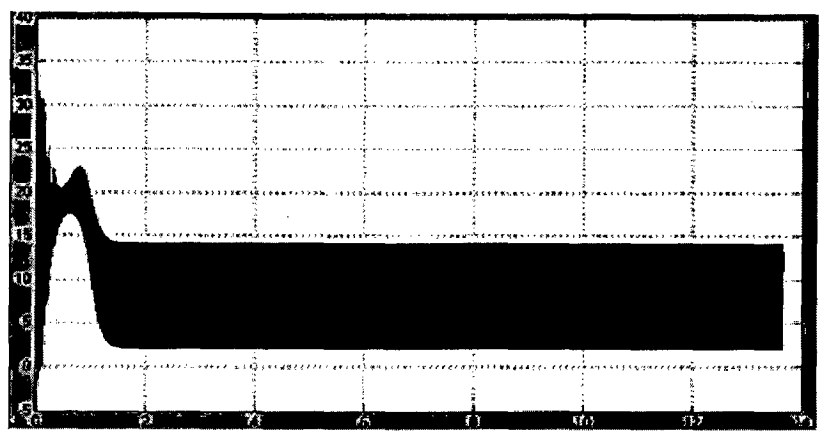

c) **Vas = 57.74V**, Vbs = 265.59V, Vcs = 265.59V

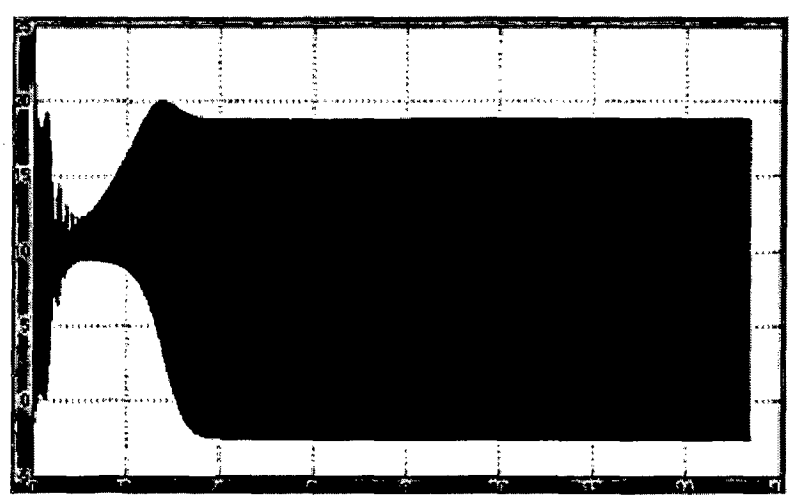

Fig.5.26. Torque characteristics as the voltage of phase A is decreased from healthy condition

From Fig.5.26, as discussed earlier when the voltage decreases, the resultant flux decreases and hence the torque characteristic follows a lower characteristic compared to the torque characteristic of a healthy motor which means at any particular instant, the torque of a motor with inter turn fault and voltage unbalance is less than the torque of a healthy motor. Here, the effect of voltage unbalance dominates the effect of inter turn fault and hence the above discussion is justified. But when the effect of inter turn fault dominates the effect of decrease in voltage, the torque characteristic follows a higher characteristic than the torque characteristic of a healthy motor i.e., at any particular instant, the torque of a motor with inter turn fault and voltage unbalance is more than the torque of a healthy motor.

An increase in twice the supply frequency oscillations occurs as voltage of one of the phases decreases. This is due to the increase in the negative sequence component of voltage and negative sequence current in Eq. (5.9) which are the consequences of voltage unbalance and of inter turn fault. Also, the rate at which the characteristics reach the steady state decreases as voltage decreases.

a) **HEALTHY CONDITION :Vas=265.59V, Vbs=265.59V, Vcs=265.59V**

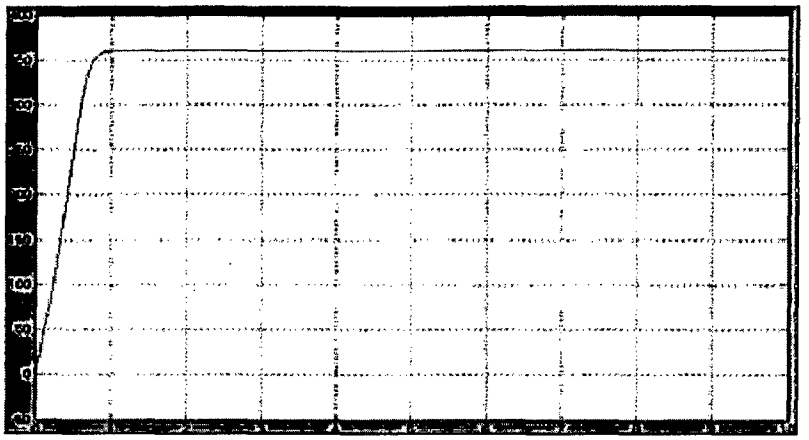

b) **Vas = 173.21V**, Vbs = 265.59V, Vcs = 265.59V

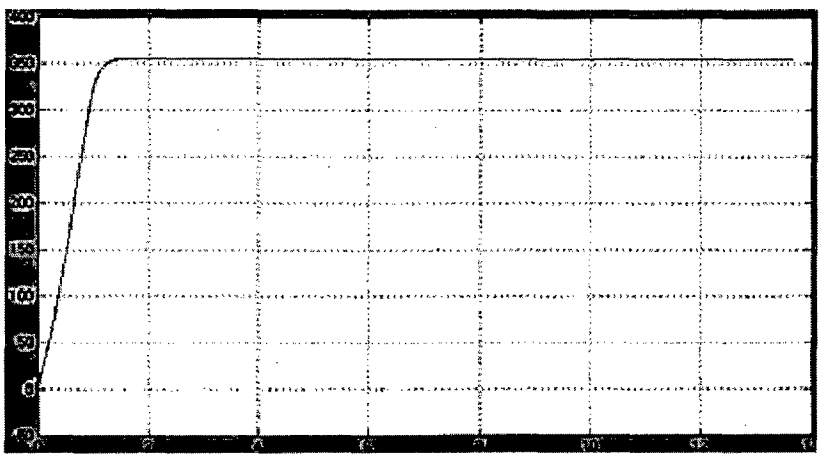

c) **Vas = 57.74V**, Vbs = 265.59V, Vcs = 265.59V

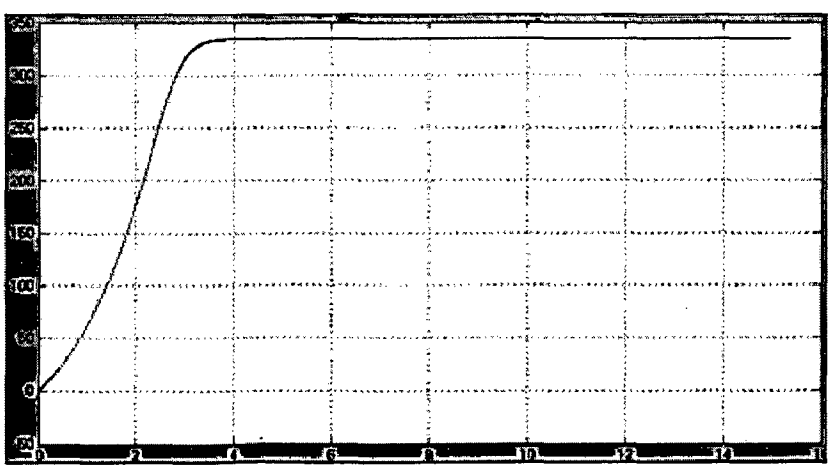

Fig.5.27. Speed characteristics as the voltage of phase A is decreased from healthy condition

From Fig.5.27, as discussed earlier, when there is a decrease in voltage, the resultant flux decreases and hence the torque-speed characteristics shifts to the lower side compared to the torque-speed characteristics of a healthy motor. So, the motor approaches steady state i.e., $T = T_L$ at a lower speed. This explains the decrease in the speed when the voltage of phase A is decreased to Vas = 173.21V. The increase in the torque pulsations due to the increase in voltage unbalance and negative sequence current is reflected in the rotor speed pulsations.

a) **HEALTHY CONDITION :Vas=265.59V, Vbs=265.59V, Vcs=265.59V**

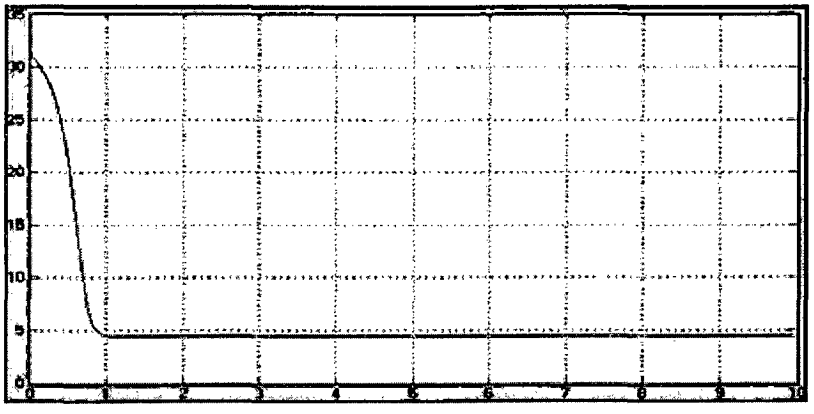

b) **Vas = 173.21V, Vbs = 265.59V, Vcs = 265.59V**

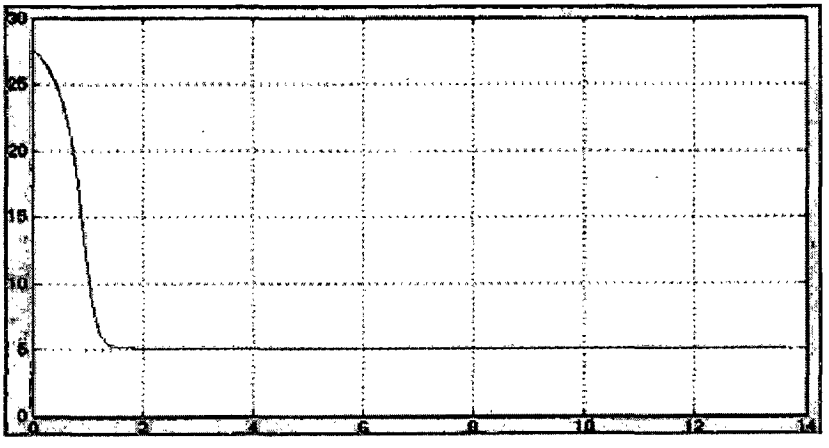

c) **Vas = 57.74V, Vbs = 265.59V, Vcs = 265.59V**

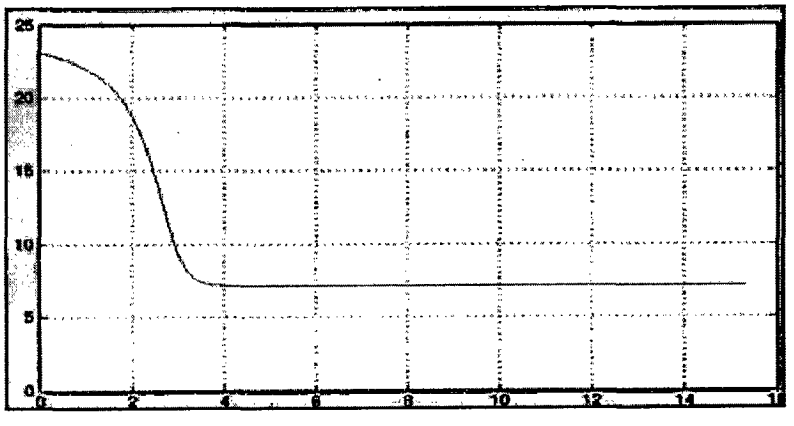

Fig.5.28. Positive Sequence current as the voltage of phase A is decreased from healthy condition

From Fig.5.28, the rate at which the positive sequence current reaches the steady state decreases as the voltage decreases. Also, the positive sequence current is observed to increase .

a) **HEALTHY CONDITION :Vas=265.59V, Vbs=265.59V, Vcs=265.59V**

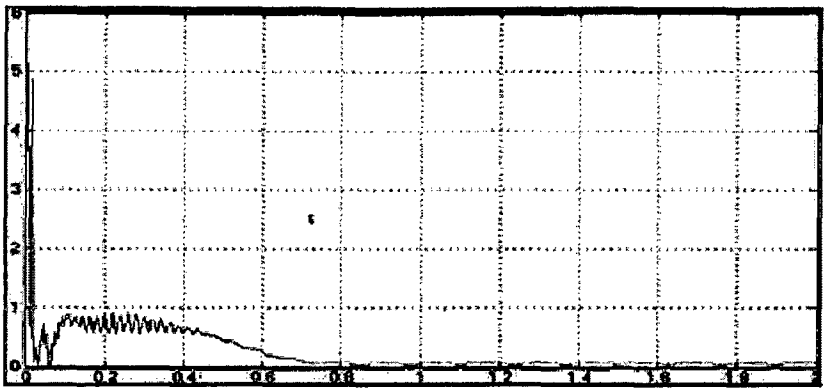

b) **Vas = 173.21V**, Vbs = 265.59V, Vcs = 265.59V

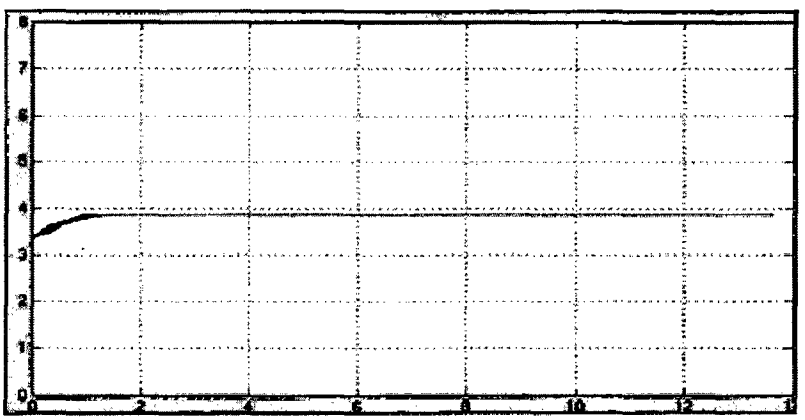

c) **Vas = 57.74V**, Vbs = 265.59V, Vcs = 265.59V

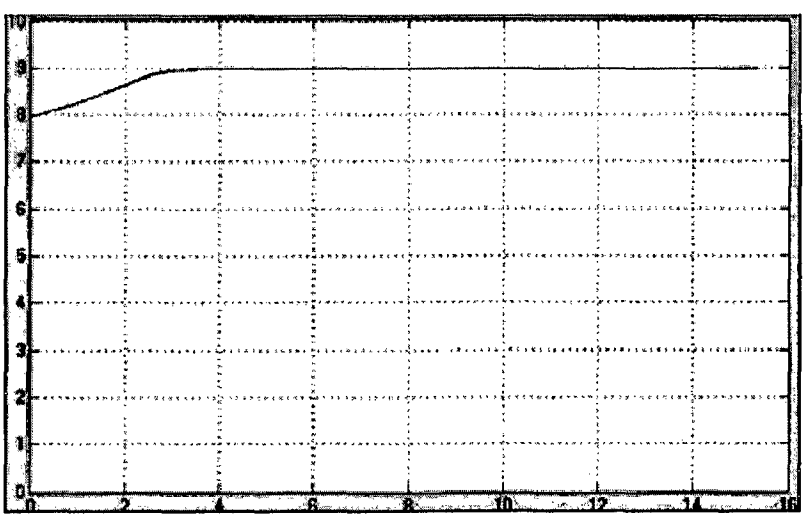

Fig.5.29. Negative sequence current as the voltage of phase A is decreased from healthy condition

From Fig.5.29, when inter turn fault is created by shorting 5 turns of the winding of phase A and the voltage of phase A is decreased, the amount of asymmetry created in the induction motor increases and hence the negative sequence current increases.

a) **Vas = 173.21V**, Vbs = 265.59V, Vcs = 265.59V

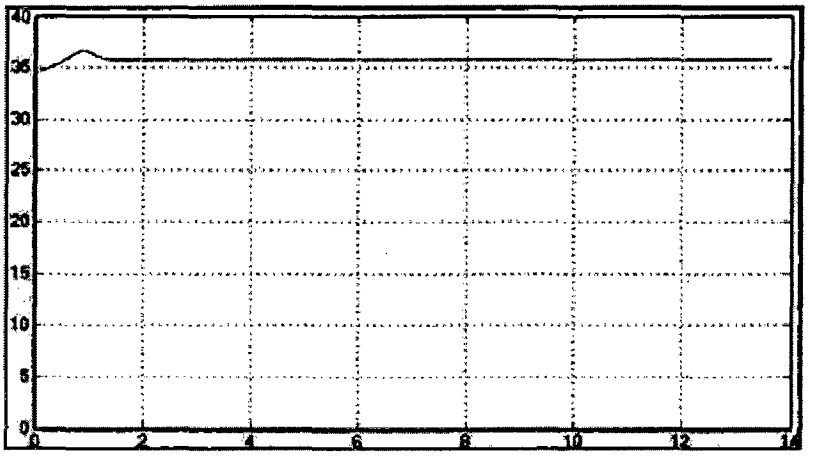

b) **Vas = 57.74V**, Vbs = 265.59V, Vcs = 265.59V

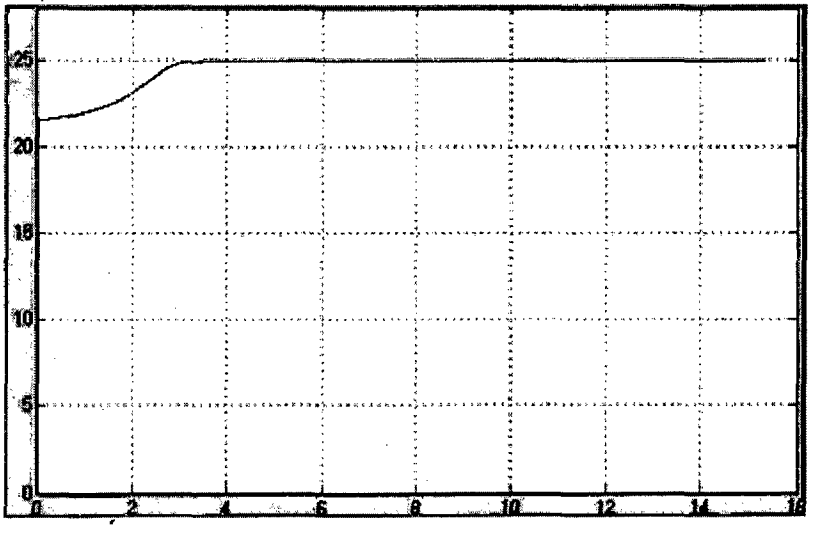

Fig.5.30. Short circuit current as the voltage of phase A is decreased

When few turns in the winding of phase A of the stator are shorted the short circuit current appears. So, it can be said that when the voltage of phase A is reduced, the short circuit current decreases. This is justified from the observation in Fig. 5.30.

5.5.1 Comparison of the effects of Voltage Unbalance and of Inter turn with Voltage Unbalance on the Induction Motor Characteristics

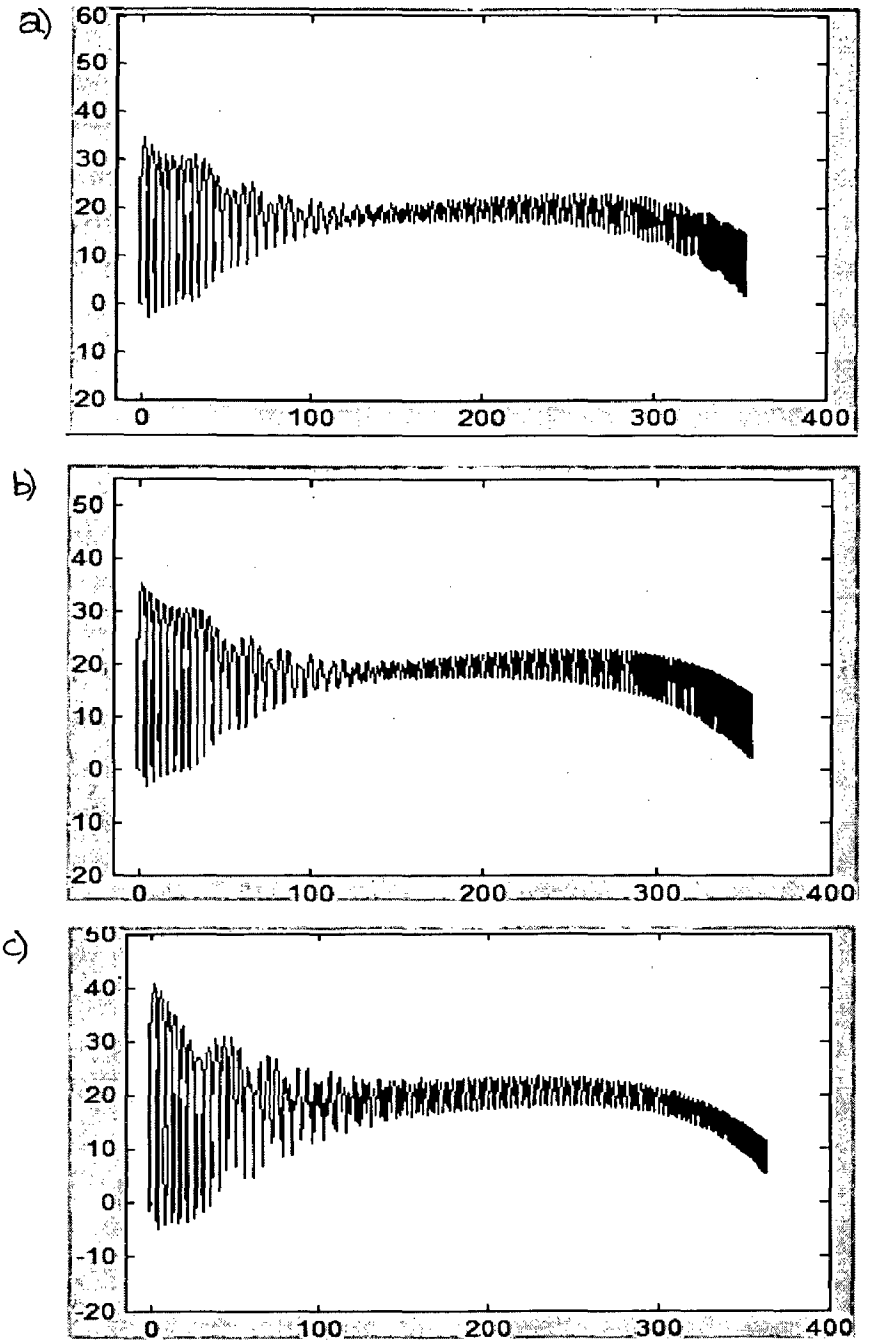

Fig.5.31. Torque-speed characteristics of a induction motor with only voltage unbalance, inter turn(Nsh = 5) with voltage unbalance and inter turn(Nsh = 40) with voltage unbalance , respectively when Vas = 173.21V.

From Fig.5.31, in the first two conditions, the torque-speed characteristic follows a lower characteristic compared to the torque-speed characteristics of a healthy motor because as the voltage decreases, the resultant flux decreases. Hence, the motor approaches the steady state at a lower speed. But, in the second condition due to the presence of inter turn fault the decrement in torque and speed is lesser. If the intensity of the inter turn fault is increased by increasing the number of shorted turns then the torque speed characteristic follows a higher characteristic and hence the motor approaches steady state at a higher speed. The twice the supply frequency torque pulsations arise as result of the negative sequence current and the negative sequence voltage.

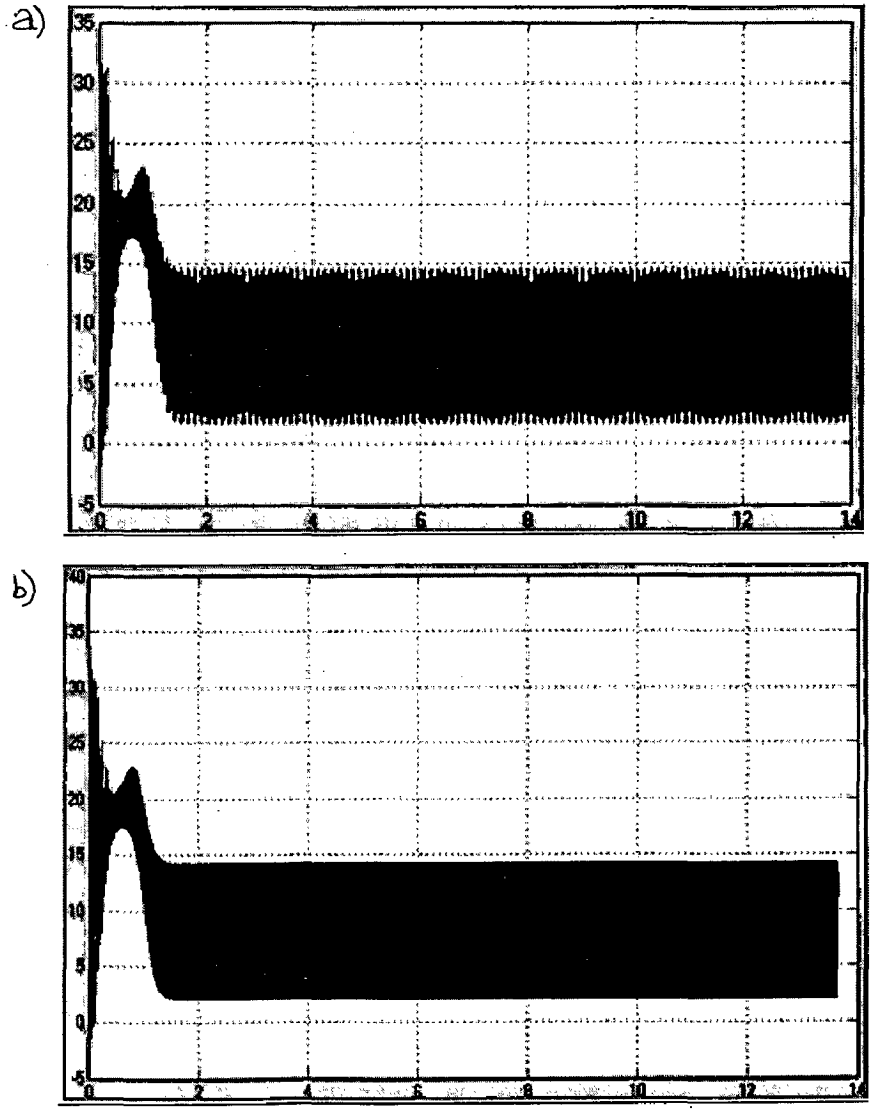

c)

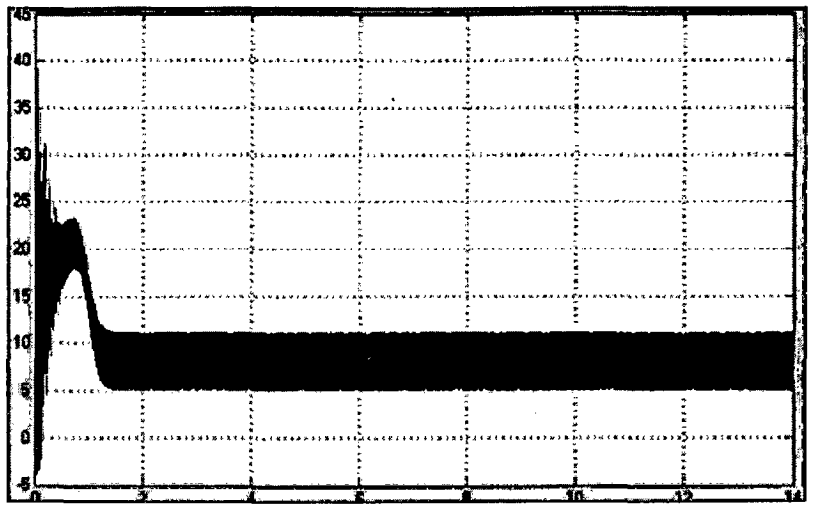

Fig.5.32. Torque characteristics of an induction motor with only voltage unbalance, inter turn (Nsh = 5) with voltage unbalance and inter turn(Nsh = 40) with voltage unbalance respectively when Vas = 173.21V.

From Fig.5.32, in the first two conditions, the torque characteristic is shifted to the lower side i.e. to reduced magnitude compared to the torque characteristics of a healthy motor. But, in the second condition due to the presence of inter turn fault the reduction in torque and speed is lesser. If the number of shorted turns are increased, the effect of inter turn dominates and then the torque characteristic follows a higher characteristic, the maximum torque also increases compared to that of a healthy motor.

a)

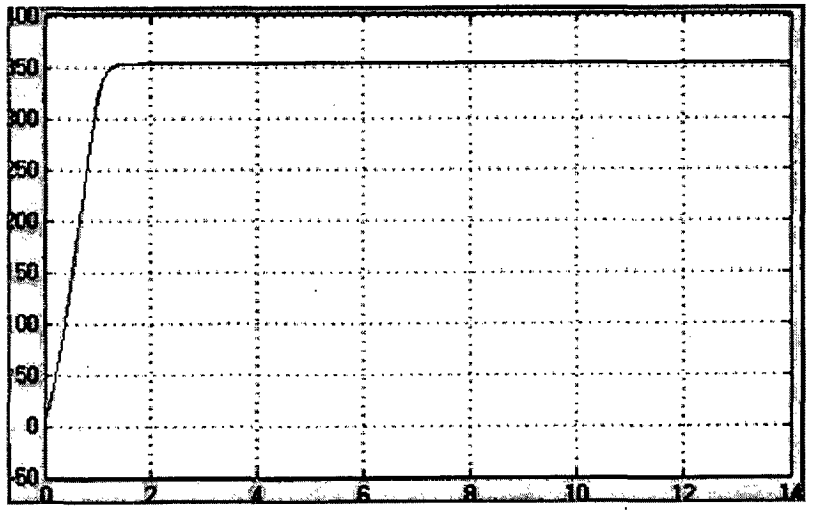

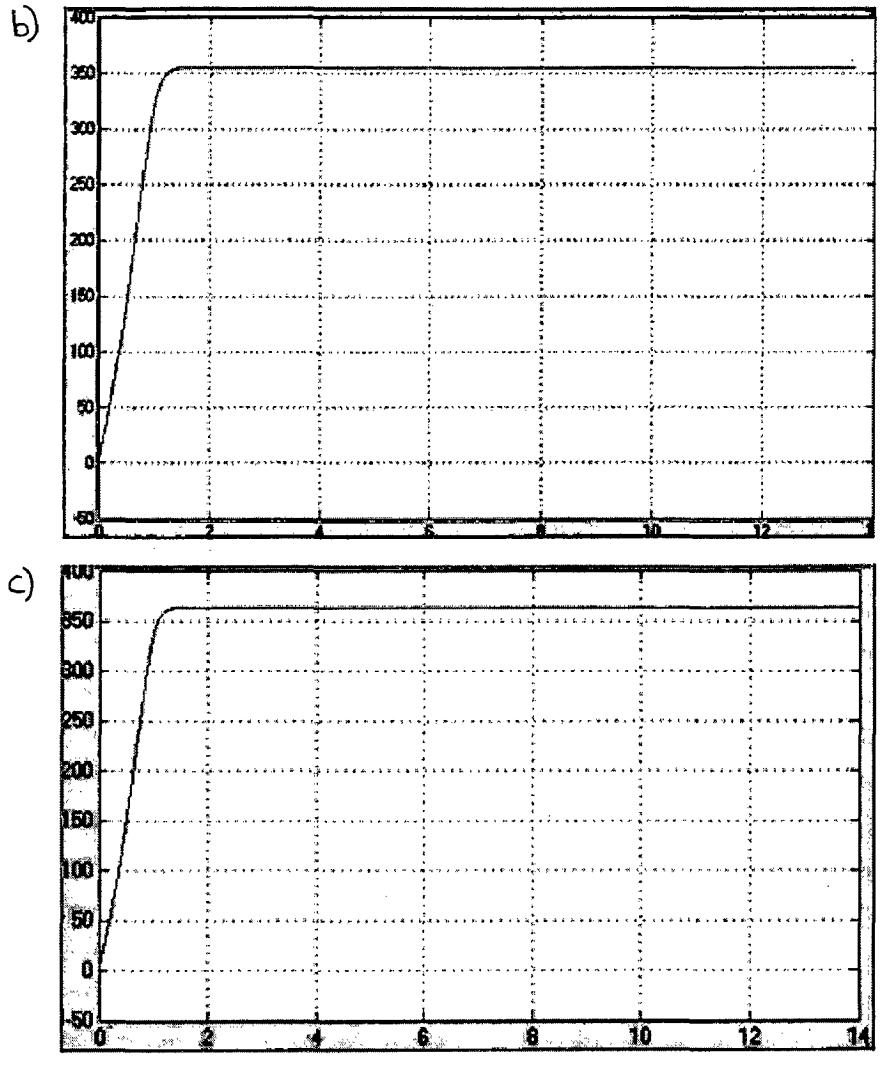

Fig.5.33. Speed characteristics of a induction motor with only voltage unbalance, inter turn (Nsh = 5) with voltage unbalance and inter turn(Nsh = 40) with voltage unbalance respectively when Vas = 173.21V.

From Fig.5.33, in the first two conditions, the motor approaches the steady state at a lower speed due to the reduction in the torque characteristic as a result of the decrease in phase a voltage. But, in the second condition due to the presence of inter turn fault the decrement in torque and hence the speed is lesser. If the intensity of the inter turn fault is increased by increasing the number of shorted as in the third case, then the torque speed characteristic follows a higher characteristic and hence the motor approaches steady state at a higher speed. The twice the supply frequency torque pulsations are also reflected in the speed.

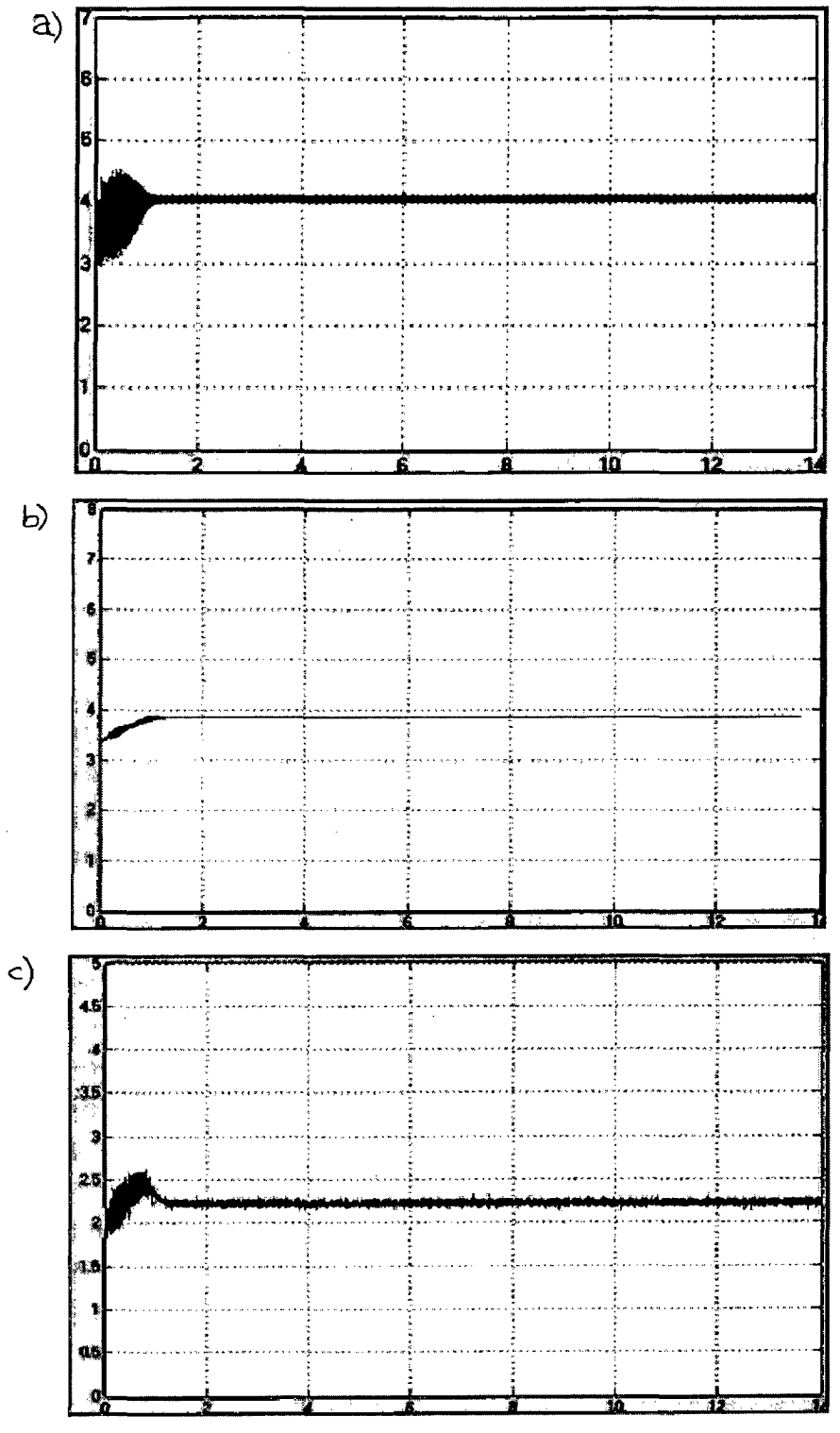

Fig.5.34. Negative sequence current of a induction motor with only voltage unbalance, inter turn (Nsh = 5) with voltage unbalance and inter turn(Nsh = 40) with voltage unbalance respectively when Vas = 173.21V.

From Fig.5.34, the negative sequence current is an indication of the amount of asymmetry. In the first case, the negative sequence current is around 4A, in the second case when only 5 turns were shorted and with the same phase A voltage of 173.21V the negative sequence current has slightly reduced to 3.85A and in the third case when 40 turns were shorted and with the same phase A voltage the negative sequence current has further reduced to around 2.2A. This can be explained by Fig.5.35 and Fig.5.36. In Fig. 5.35 when voltage of phase A was

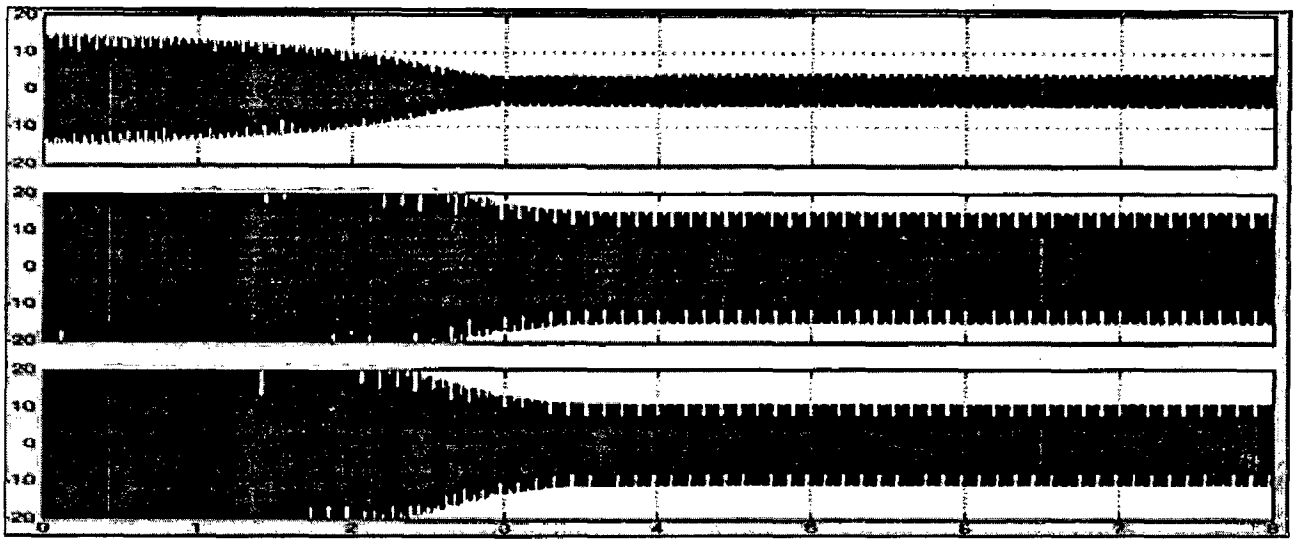

Fig.5.35 Stator phase A, phase B, phase C currents respectively when voltage unbalance is created with Vas=173.21V.

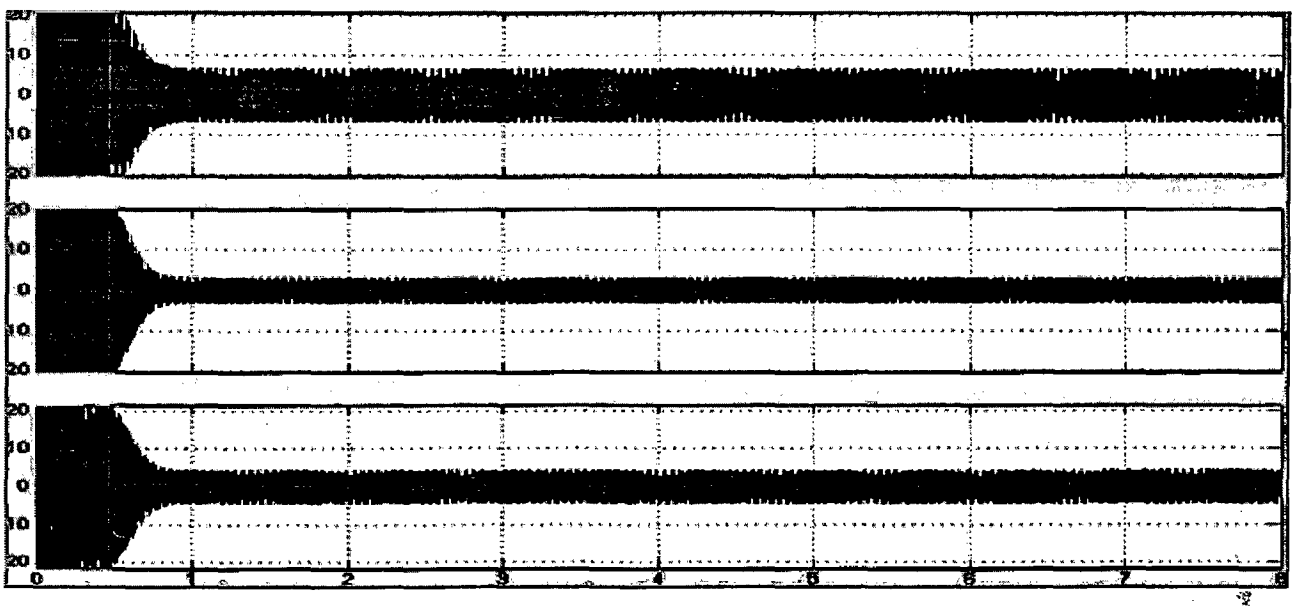

Fig.5.36. Stator phase A, phase B, phase C currents respectively when 40 turns of winding of phase A is shorted.

reduced to 173.21V and with no inter turn fault, the current in phases B and C have increased. Whereas in Fig.5.34 when only inter turn fault was created by shorting 40 turns of phase A winding, the current in phase A has increased with minor changes in the currents of phases B and C. The result in Fig.5.36 can also be justified by the experimental results in Fig.5.15, 5.16 and 5.17 where it was stated that an inter turn fault primarily affects the faulty phase. Hence, from all these observations we can conclude that the combined effect of voltage unbalance and inter turn fault has decreased the amount of asymmetry in the stator phase currents. Therefore, the negative sequence decreases when both voltage unbalance and inter turn fault are present.

Hence, it can be stated that negative sequence current in an induction motor with both voltage unbalance and inter turn fault is less compared to that in the case of only voltage unbalance or an inter turn fault. This result can be taken into consideration by the fault detection systems which monitor the negative sequence current to investigate the condition of the motor.

5.6. Effect of Inter turn fault and Voltage Unbalance with Inter turn fault on an Induction motor in running condition

The motor equations used in Chapter 4 to develop the models of asymmetrical induction motor and induction motor with inter turn fault are used to develop another model through which the fault can be created in the motor when it is already in running condition.

This model is simulated to observe the effects of Inter turn fault and Voltage Unbalance with Inter turn fault on an Induction motor in operating mode.

a) Torque vs Speed

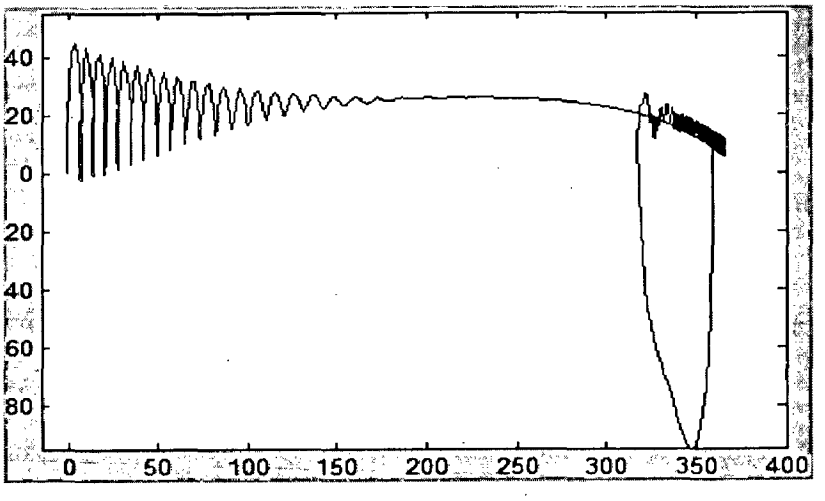

b) Torque vs Time

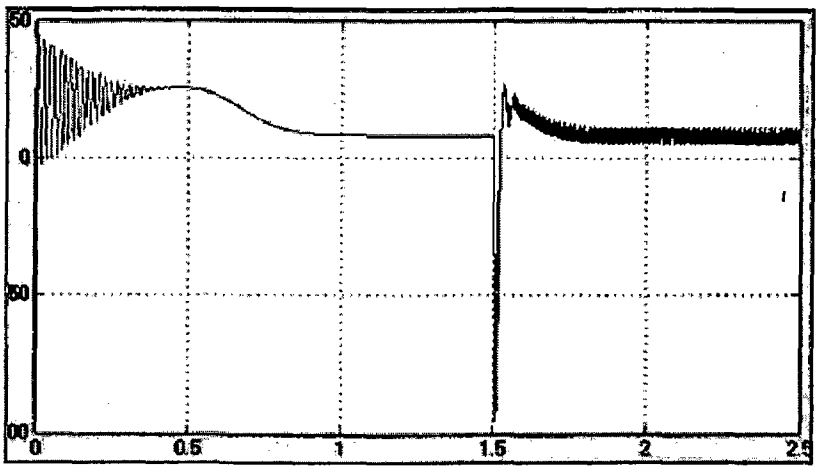

c) Speed vs Time

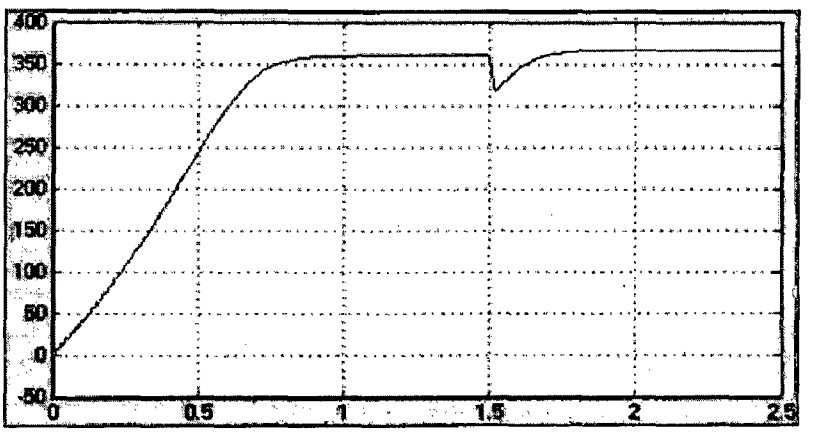

d) Positive sequence current

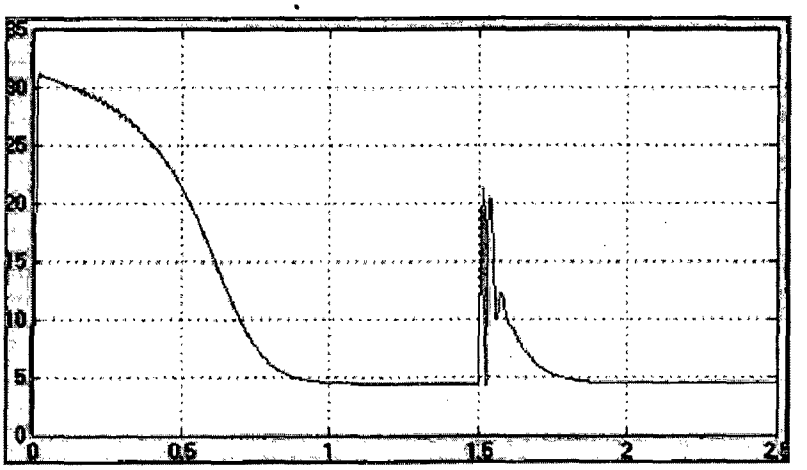

e) Negative sequence current

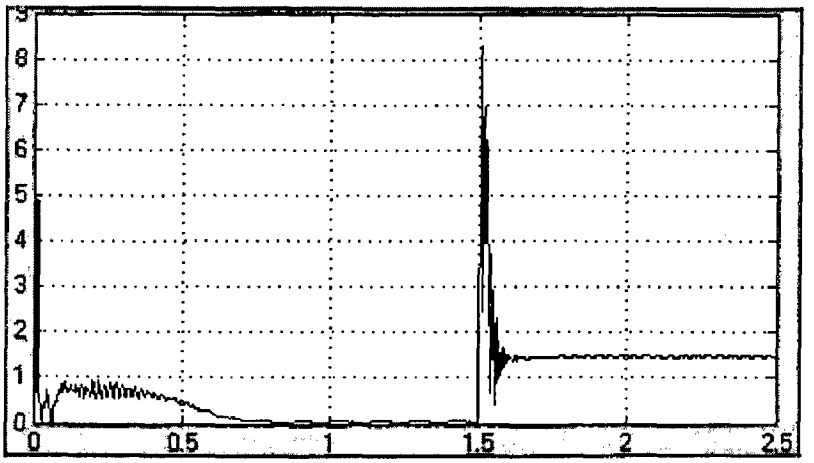

f) Short circuit current

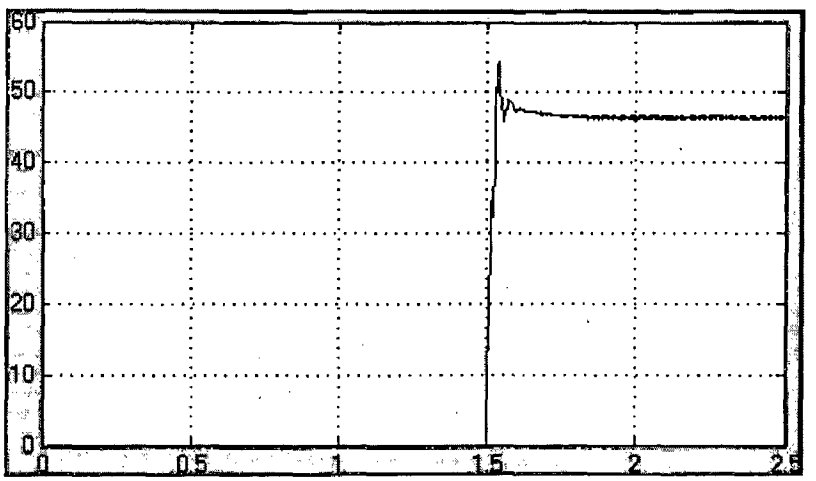

Fig.5.37. Various characteristics of an induction motor when 25 turns are shorted after 1.5sec.

From Fig.5.37, the induction motor follows similar characteristics as in Fig. 5.3-5.5.When an inter turn fault is present, the torque-speed characteristics shifts to the higher side compared to the torque-speed characteristics of a healthy motor. So, the motor approaches steady state i.e., $T = T_L$ at a higher speed.

Since few turns of phaseA winding are shorted a short circuit current arises and also, the stator draws unbalanced phase currents which results in a negative sequence current. From Eq. (5.9), the twice the supply frequency oscillations in power arise resulting in torque pulsations and hence speed pulsations.

a) Torque-Speed characteristic

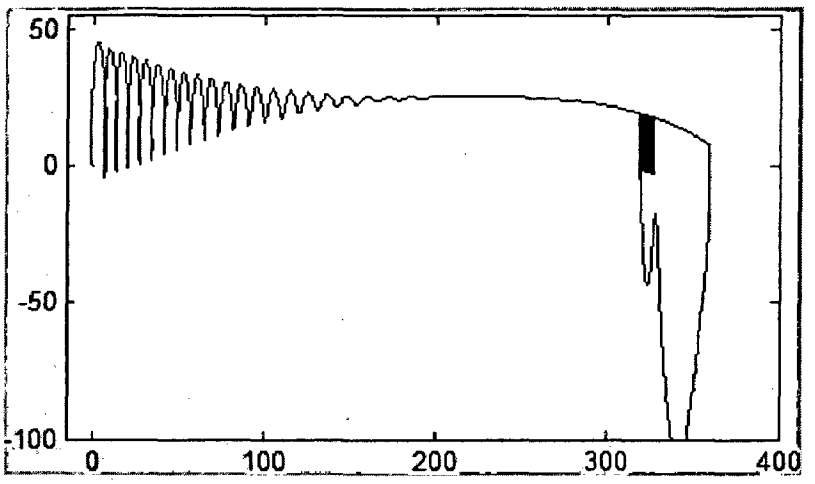

b) Torque vs Time

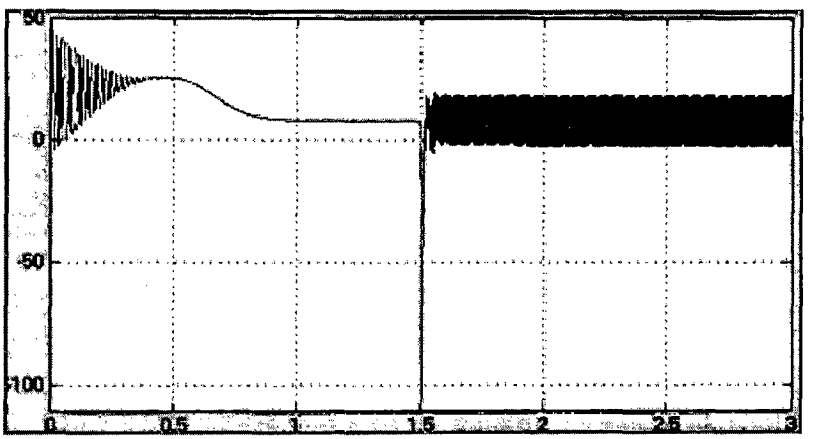

c) Speed vs Time

d) Positive sequence current

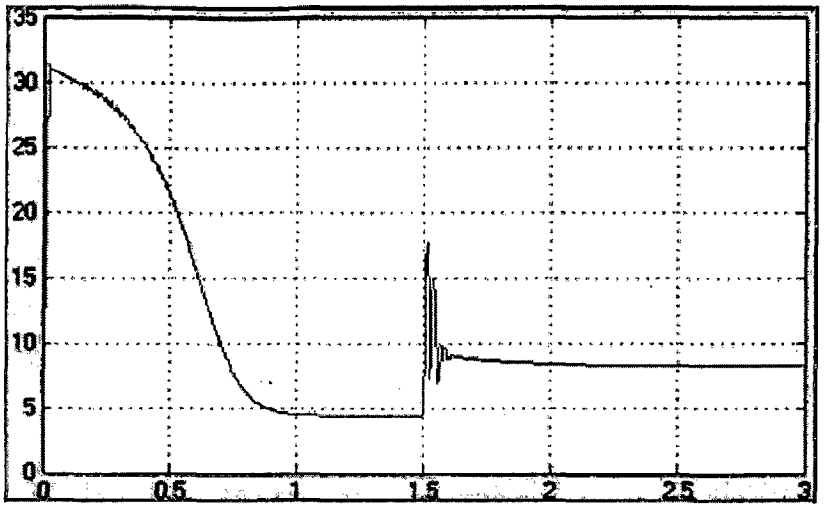

e) Negative sequence current

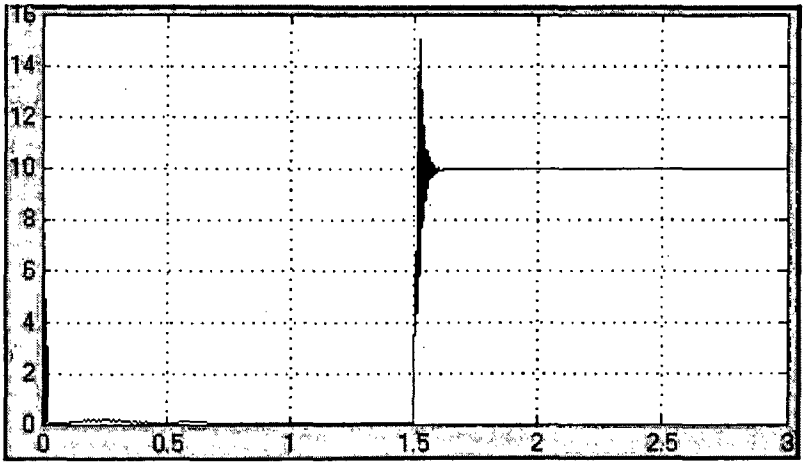

f) Short circuit current

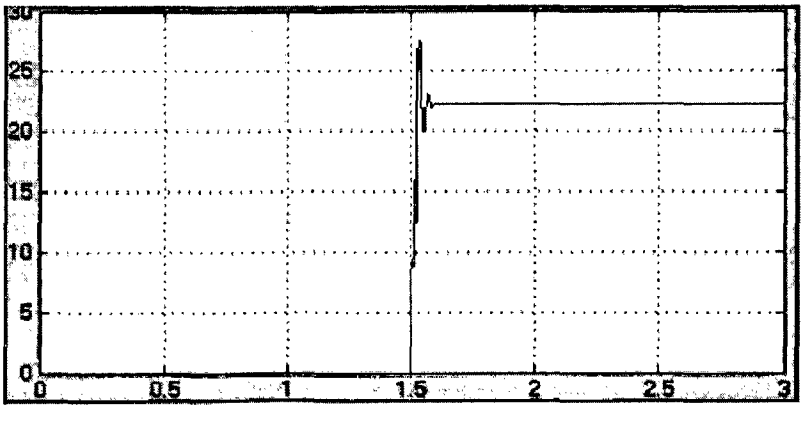

Fig.5.38. Various characteristics of an induction motor when 25 turns are shorted and Vas is reduced to 28.87V after 1.5sec.

From Fig.5.38, the induction motor follows similar characteristics as in Fig. 5.25-5.30. Due to the decrease in the stator voltage, the torque-speed characteristic follows a lower characteristic compared to that of a healthy motor and hence reaches the steady state at a lower speed.

5.7. Chapter Summary

In this chapter, the simulation results have been obtained from the developed model and the inter-turn fault analysis has been carried out. It has been observed that the Torque characteristic and hence, the speed contains twice the supply frequency oscillations due to the presence of a negative sequence current and the speed is found to increase. The variation of the negative sequence current and the short circuit current with the number of shorted turns at different values of external resistance has been observed and the effect of unequal winding temperature due to voltage unbalance on the negative sequence current has been observed to be similar to that of a stator inter-turn fault. An increase in the number of shorted turns increases the speed, negative sequence current and the short circuit current which were justified by the experimental results.

Also, various motor characteristics have been obtained when voltage unbalance is created in a single phase of a motor with an inter-turn fault. The following observations have therefore been made as the voltage of phase 'a' is decreased: torque and speed characteristic exhibits twice the supply frequency oscillations. The speed is observed to decrease as the torque follows a reduced magnitude characteristic. The negative sequence current continues to increase and the short circuit is observed to decrease. Also, the motor reaches its steady state much slowly as the one of the phase voltages is decreased.

A comparison of these results with that of a motor with only voltage unbalance showed that negative sequence current is less in the case of a motor with both voltage unbalance and inter turn fault. This observation can be used by the fault detection systems based on negative sequence current monitoring. Then, similar results were obtained using a model developed to incorporate the fault during running condition.

CHAPTER 6
CONCLUSIONS AND FUTURE SCOPE

6.1. Conclusions

Two models have been developed for analyzing an induction motor with stator faults. The models are based on general machine parameters so that it is not necessary to know detailed motor geometry or physical layout of the windings. The parameters for asymmetrical conditions have been presented. Inter-turn faults can be easily simulated by the model. Fault severity can be controlled by the number of shorted turns and an optional current limiting resistance to short circuit the windings. A third model was developed which can incorporate the fault when the motor is in operating condition.

The models have been used to study the relation between the number of shorted turns and negative sequence current, the effects of resistive unbalance between the phases due to the heating effect of unbalanced phase currents, and temperature effects on shorted turn resistance. Results confirm that negative sequence current and shorted number of turns are linearly dependant, and that resistive unbalance can produce comparable negative sequence current, so that fault detection algorithms should be able to distinguish between the effects of turn shorts and thermal unbalance. The results obtained for short circuit under limited short circuit current (by external resistance) reveal that sensitivity depends on number of shorted turns and short circuit current. The above results have been validated with experimental results.

The effect of voltage unbalance on the characteristics of an induction motor with inter turn fault has been observed. The variations in the various characteristics of the induction motor have been elaborately discussed. It has been suggested that the decrease in the negative sequence current in a motor with inter turn fault and voltage unbalance compared to that with only voltage unbalance should be taken into consideration by the fault detection systems based on negative sequence current monitoring.

6.2. Scope for Future Work

- Inter turn fault analysis has been carried out with the induction motor being directly connected to the 3-phase voltage supply. This should be extended to sophisticated drive systems excited from various power electronic sources.
- The negative sequence current has been monitored in order to analyze the inter turn faults and it has been shown that the unequal winding temperature caused due to voltage unbalance also has the same effect on negative sequence current. It is very essential that these two faults be accurately distinguished. For this purpose, several signal processing techniques can be used.
- Research trends show that AI techniques will have a greater role in electrical motor diagnostic system with advanced practicability, sensitivity, reliability, and automation. Diagnostic system based upon fuzzy neural will be very extensively used. Self-repairing electrical drives based upon genetic-algorithm-assisted neural and fuzzy neural systems will also be widely used in the near future. So, the future work should focus on implementing the various AI based fault monitoring techniques.
- In the present work, modelling and simulation have been used to investigate only stator faults. This can be extended to analyze various other faults of an induction motor.

REFERENCES

[1] P.J. Tavner and J Penman, "Condition Monitoring Of Electrical machines", UK: John Wiley& Sons Inc.,1987.

[2] N. Vilas Ghate, V. Sanjay Dudul and G. M. Dhole, "Generalized Model of Three-Phase Induction Motor for Fault Analysis", International Journal of Engineering Research and Industrial Applications Vol.01, No.IV, 2008 pp 113-127.

[3] H.C. Stanley, "An analysis of the induction machine", AIEE Trans. 57 (1938) 751_757.

[4] K. Himanshu Patel, "Steady State and Transient Performance Analysis of Three Phase Induction Machine using MATLAB Simulations", International Journal of Recent Trends in Engineering, Vol. 1, No. 3, May 2009.

[5] Vivek Pahwa and K. S. Sandhu, "Transient Analysis of three-phase induction machine using different reference frames", ARPN Journal of Engineering and Applied Sciences, Vol. 4, No. 8, October 2009.

[6] Abid Javed and Tahir Izhar, "An Improved Method for the Detection of Phase Failure Faults in Poly Phase Induction Machines", Electrical Engineering, 2009. ICEE '09. Third International Conference on , vol., no., pp.1-6, 9-11 April 2009.

[7] E.J. Akpama, O.I. Okoro and E. Chikuni, "Simulation of the Performance of Induction Machine under Unbalanced Source Voltage Conditions", The Pacific Journal of Science and Technology, Volume 11. Number 1, May 2010.

[8] M. Arkan , D. Kostic-Perovic , P.J. Unsworth , "Modelling and simulation of induction motors with inter-turn faults for diagnostics", Electric Power Systems Research 75 (2005) 57–66.

[9] B. Liang, B.S. Payne, A.D. Ball, S.D. Iwnicki, "Simulation and fault detection of three-phase induction motors", Mathematics and Computers in Simulation, Vol. 61, Issue 1, pp.1-15, November 2002.

[10] R. Ueda, T. Sonoda, K. Koga, M. Ichikawa, "Stability analysis in induction motor driven by V/f controlled general purpose inverter", IEEE Trans. Ind. Appl. 28 (2) (1992) 472_ 481.

[11] E. Levi, "Magnetizing flux saturation in variable speed inverter-fed induction motor drives", IEE Conference on Power Electronics and Variable Speed Drives, UK, 1994, pp. 78_ 83.

[12] M. Sokola, E. Levi, "Iron losses in current-controlled PWM inverter fed induction machines", IEEE MELECON96, Bari, Italy, 1996, pp. 361_ 364.

[13] L.M. Neto, J.R. Camacho, C.H. Salemo, "Analysis of a threephase induction machine including time and space harmonic effects: the ABC reference frame", IEEE Trans. Energy Conver. 14 (1) (1999) 80_ 85.

[14] H.A. Toliyat, A. Al-Nuiam, "Simulation and detection of dynamic air-gap eccentricity in salient-pole synchronous machines", IEEE Trans. Ind. Appl. 35 (1) (1999) 86_ 93.

[15] H.A. Toliyat, T.A. Lipo, "Transient analysis of cage induction machines under stator rotor bar and end ring faults", IEEE Trans. on Energy Conversion, Vol.10, No.2, (1995) 241_ 247.

[16] H.A. Toliyat, M.S. Arefeen, A.G. Parlos, "A method for dynamic simulation of air-gap eccentricity in induction machines", IEEE Trans. Ind. Appl. 32 (4) (1996) 910_ 917.

[17] G.M. Joksimovic, J. Penman, "The detection of inter-turn short circuit in the stator windings of operating motors", IEEE Trans. Ind. Electron. 47 (5) (2000) 1078_ 1084.

[18] S.A. Al Kaazaz, "Intelligent Diagnostic and Monitoring of Electrical Drives", A Ph.D. Thesis under the supervision of Dr. S.P.Gupta & Dr. Vinod Kumar, Professors, Department of Electrical Engineering, IIT Roorkee, 1997-2001.

[19] W.V. Lyon, "Transient Analysis of Alternating Current Machinery", Wiley and Sons, New York, 1954.(Book)

[20] A.J.M. Cardoso, S.M.A. Cruz, D.S.B. Fonseca, "Inter-turn stator winding fault diagnosis in three-phase induction motors by Park's vector approach", IEEE Trans. Energy Convers. 14 (3) (1999) 595.

[21] R.M. Tallam, T.G. Habetler, R.G. Harley, Transient Model for Induction Machines with Stator Winding Turn Faults, in: Proceedings of the IEEE Industry Applications Conference 35th Annual Meeting- World Conference on Industrial Applications of Electrical Energy, Rome, Italy, October 2000, 2000.

[22] J.E. Brown, O.I. Butler, A general method of analysis of three phase induction motors with asymmetrical primary connections, Proc. IEE 100 (1953) 25–34.

[23] C.S. Jha, S.S. Murthy, Generalised rotating-field theory of woundrotor induction machines having asymmetry in stator and/or rotor windings, Proc. IEE 120 (8) (1973).

[24] X. Luo, Y. Liao, H.A. Toliyat, T.A. Lipo, Multiple coupled circuit modelling of induction machines, IEEE Trans. Ind. Appl. 31 (2) (1995) 311–317.

[25] H.A. Toliyat, T.A. Lipo, Transient analysis of cage induction machines under stator, rotor bar end ring faults, IEEE Trans. Energy Convers. 10 (2) (1995) 241–247.

[26] G.M. Joksimovic, J. Penman, The detection of inter-turn short circuits in the stator windings of operating motors, IEEE Trans. Ind. Electron. 47 (5) (2000) 1078–1084.

[27] S. Williamson, K. Mirzoian, Analysis of cage induction motors with stator winding faults, IEEE Trans. Power Apparatus Syst. PAS-104 (7) (1985) 1838–1842.

[28] A. Consoli, T.A. Lipo, Orthogonal axis models for asymmetrically connected induction machines, IEEE Trans. Power Apparatus Syst. PAS-101 (12) (1982) 4518–4526.

[29] A.K. Wallace, E.S. Ward, A. Wright, Sources of harmonic currents in slip-ring motors, Proc. IEE 121 (12) (1974).

[30] Peter Vas, "Parameter estimation, condition monitoring, and diagnosis of electrical machines", Clarendon Press Oxford., 1993.

[31] A. H. Bonnet and G. C. Soukup, "Cause and analysis of stator and rotor failures in three-phase squirrel case induction motors," IEEE Transactions Industry Application, Vol., 28, No.4, pp. 921-937, July/August, 1992.

[32] IAS Motor Reliability Working Group, "Report of large motor reliability survey of industrial and commercial installation, part I," IEEE Transactions on Industry Applications, vol. IA-21, pp. 853-864, July/Aug., 1985.

[33] J. Sottile and J.L. Kohler, "An on-line method to detect incipient failure of turn insulation in random-wound motors," IEEE Transactions on Energy Conversion, vol. 8, no. 4, pp. 762-768, December, 1993.

[34] T. A. Lipo, Introduction of AC machine design, Wisconsin Power Electronics Research Center, 2nd edition, 2004.

[35] S. F. Farag, R. G. Bartheld, and W. E. May, "Electronically enhanced low voltage motor protection and control," IEEE Transactions on Industry Applications, Vol. 29, No. 1, pp. 45-51, Jan./Feb., 1994.

[36] J. T. Boys and M. J. Miles, "Empirical thermal model for inverter-driven cage induction machines," IEE Proc., Electric Power Application, Vol. 141, pp. 360-372, 1994.

[37] K. D. Hurst and T. G. Habetler, "A thermal monitoring and parameter tuning scheme for induction machines," in Conf. Rec. IEEE IAS'97, pp. 136-142, New Orleans, LA, USA, October, 1997.

[38] S. B. Lee and T. G. Habetler, "An online stator winding resistance estimation technique for temperature monitoring of line-connected induction machines," IEEE Transactions on Industry Applications, Vol. 39, No. 3, pp. 685-694, May/June, 2003.

[39] W. L. Roux, R. G. Harley, and T. G. Habetler, "Detecting rotor faults in permanent magnet synchronous machines," in Conf. Rec. SDEMPED'03, pp. 198-203, Atlanta, GA, USA, August, 2003.

[40] J. R. Stack, T. G. Habetler, and R. G. Harley, "Bearing fault detection via autoregressive stator current modeling," IEEE Transactions Industry Applications, Vol. 40, No. 3, pp. 740-747, May/June, 2004.

[41] M. A. Cash, "Detection of turn faults arising from insulation failure in the stator windings of AC machines," Doctoral Dissertation, Dept. of Electrical and Computer Engineering, Georgia Institute of Technology, USA, 1998.

[42] D. E. Schump, "Predict motor failure with insulation testing," Pulp and Paper Industry Technical Conference'97, pp.48-50, Cincinnati, OH, USA, June, 1997.

[43] D. E. Schump, "Reliability testing of electric motors," IEEE Transactions on Industry Applications, Vol. 25, No. 3, pp. 386-390, May/June, 1989.

[44] R. Maier, "Protection of squirrel-cage induction motor utilizing instantaneous power and phase information," IEEE Transactions on Industry Applications, Vol. 28, No. 2, pp. 376-380, March/April, 1992.

[45] J. Cros and P. Viarouge, "Synthesis of high performance PM motors with concentrated windings," IEEE Transactions on Energy Conversion, Vol. 17, No. 2, pp. 248- 253, June, 2002.

[46] G. B. Kliman, W. J. Premerland, R. A. Koegl, and D. Hoeweler, "A new approach to on- line turn fault detection in AC motors," in Conf. Rec. IEEE IAS'96, Vol. 1, pp.687-693, San Diego, CA, USA, October, 1996.

[47] F. C. Trutt, J. Sottile, and J. L. Kohler, "Online condition monitoring of induction motors," IEEE Transactions on Industry Applications, Vol. 38, No. 6, pp. 1627-1632, Nov./Dec., 2002.

[48] J. Penman, H. G. Sedding, B. A. Lloyd, and W. T. Fink, "Detection and location of interturn short circuits in the stator windings of operating motors," IEEE Transactions on Energy Conversion, Vol. 9, No. 4, pp. 652-658, December, 1994.

[49] D. G. Dorrell, W. T. Thomson, and S. Roach, "Analysis of air-gap flux, current, and vibration signals as function of a combination of static and dynamic eccentricity in 3-phase induction motors", IEEE Transactions on Industry Applications, Vol. 33, Jan./Feb., pp. 24-34, 1997.

[50] S. Wu, and T.W.S. Chow, "Induction machine fault detection using SOM-based RBF neural networks", IEEE Transactions on Industrial Electronics, Vol. 51, No. 1, February, pp. 183-194, 2004.

[51] M. Bradford, "Unbalanced magnetic pull in a 6-pole induction motor," IEEE Proceedings, Vol. 115, No. 11, pp. 1619-1627, 1968.

[52] P. F. Allbrecht, J. C. Appiarius, and R. M. McCoy, et al, "Assessment of the reliability of motors in utility applications – updated," IEEE Transactions on Energy Conversion, Vol. 1, No. 1, pp. 39-46, 1986.

[53] S. Nandi and H. A. Toliyat, "Condition monitoring and fault diagnosis of electrical machines – a review," in Proc. 34th Annual Meeting of the IEEE Industry Applications, pp. 197-204, 1999.

[54] R. Randy Schoen, G. Thomas Habetler, Farrukh Kamran and G. Robert Bartheld, "Motor bearing damage detection using stator current monitoring", IEEE Transactions on Industry Applications, Vol. 31, No 6, pp. 1274-1279, 1995.

[55] P. Eschmann, L. Hasbargen, K. Weigand, "Ball and roller bearings: Their theory, design, and application" (London: K G Heyden), 1958.

[56] J. Riddle, "Ball bearing maintenance", Norman, OK: University of Oklohama Press, 1955.

[57] Y. Han and Y. H. Song, "Condition Monitoring Techniques for Electrical Equipment—A Literature Survey", IEEE Transactions on Power Delivery, Vol. 18, No. 1, January 2003.

[58] Arfat Siddique, G. S. Yadava and Bhim Singh, "A Review of Stator Fault Monitoring Techniques of Induction Motors", IEEE Transactions on Energy Conversion, Vol. 20, No. 1, March 2005.

[59] Mohamed A. Awadallah, "Application of AI Tools in Fault Diagnosis of Electrical Machines and Drives—An Overview", IEEE Trans. on Energy Conversion, Vol. 18, No. 2, June 2003.

[60] D.W. Novotny, T.A. Lipo, "Vector Control and Dynamics of AC Drives", Clarendon Press, Oxford, 1996.

[61] P. Krause, O. Wasynczuk, S.D. Sudhoff, "Analysis of Electric Machinery", IEEE Inc, 1995, ISBN 0-7803-1101-9.

[62] P. Vas, "Vector Control of AC Machines", Oxford Science Publications, 1999.

[63] C.M. Ong, "Dynamic Simulation of Electric Machinery", Prentice Hall PTR, 1998, ISBN 013-723785-5.

[64] G.R. Bossio, C.H. De Angelo, P.D. Donolo, A.M. Castellino, G.O. Garcia, "Effects of voltage unbalance on IM power, torque and vibrations", Seventh IEEE Int. Symp. on Diagnostics for Electric Machines, Power Electronics and Drives (SDEMPED 2009), Carge`se, France, August–September 2009.

[65] K.V Vamsi Krishna, "Effects of Unbalanced Voltage on Induction Motor Current and its Operation Performance," Lecon Systems.

LIST OF PUBLICATIONS

[1] S. Hari Kishan, S.P. Gupta, "Effect of voltage unbalance and stator inter turn short circuit on the characteristics of an induction motor", International Conference on Advances in Electrical, Electronics and Computer Science Engineering, EEC 2012, Dehradun, India. (Status: Accepted).

APPENDIX

A.1. Matrix elements for induction motor with different numbers of stator turns

The *qd0* resistances elements are:

$$r_{11}^s = \frac{2}{3}\left(r_{as} + \frac{1}{4}r_{bs} + \frac{1}{4}r_{cs}\right)$$

$$r_{12}^s = \frac{\sqrt{3}}{6}(r_{bs} - r_{cs})$$

$$r_{13}^s = \frac{1}{3}(2r_{as} - r_{bs} - r_{cs})$$

$$r_{22}^s = \frac{1}{2}(r_{bs} + r_{cs})$$

$$r_{33}^s = \frac{1}{3}(r_{as} + r_{bs} + r_{cs}) \qquad \text{------(A.1.1)}$$

$r_{21}^s = r_{12}^s$, $r_{23}^s = -\frac{1}{2}r_{12}^s$, $r_{31}^s = \frac{1}{2}r_{13}^s$, and $r_{32}^s = -r_{12}^s$, where $r_{as} = \frac{N_a}{N_s}r_s$, $r_{bs} = \frac{N_b}{N_s}r_s$, and $r_{cs} = \frac{N_c}{N_s}r_s$, when $N_a = N_b = N_c = N_s$, $r_{11}^s = r_{22}^s = r_{33}^s = r_s$ and $r_{12}^s = r_{13}^s = r_{21}^s = r_{23}^s = r_{31}^s = r_{32}^s = 0$.

A.2. The stator qd0 self- and mutual inductances

L_{qd0}^{ss} matrix elements are:

$$L_{11}^{ss} = \frac{2}{3}(L_{asas} + .25L_{bsbs} + .25L_{cscs} - L_{asbs} - L_{ascs} + .5L_{bscs})$$

$$L_{12}^{ss} = \frac{1}{2\sqrt{3}}(L_{bsbs} - L_{cscs} - L_{asbs} + L_{ascs})$$

$$L_{13}^{ss} = \frac{2}{3}(L_{asas} - .5L_{bsbs} - .5L_{cscs} + .5L_{asbs} + .5L_{ascs} - L_{bscs})$$

$$L_{21}^{ss} = \frac{1}{\sqrt{3}}(.5L_{bsbs} - .5L_{cscs} - L_{asbs} + L_{ascs})$$

$$L_{22}^{ss} = \frac{1}{2}(L_{bsbs} + L_{cscs} - 2L_{bscs})$$

$$L_{23}^{ss} = \frac{1}{\sqrt{3}}(-L_{bsbs} + L_{cscs} - L_{asbs} + L_{ascs})$$

$$L_{33}^{ss} = \frac{1}{3}(L_{asas} + L_{bsbs} + L_{cscs} + 2L_{asbs} + 2L_{ascs} + 2L_{bscs})$$

and $L_{31}^{ss} = \frac{1}{2}L_{13}^{ss}$, and $L_{32}^{ss} = \frac{1}{2}L_{23}^{ss}$. ----------(A.2.1)

When $N_a = N_b = N_c$,
$N_{asas} = N_{bsbs} = N_{cscs}$ and $N_{asbs} = N_{ascs} = N_{bscs}$.

By using Eqs.(2.7)–(2.13) it can be shown that

$$L_{12}^{ss} = L_{13}^{ss} = L_{21}^{ss} = L_{23}^{ss} = L_{31}^{ss} = L_{32}^{ss} = 0 \text{ and } L_{11}^{ss} = L_{22}^{ss} = \bar{L}_{ls} + \bar{L}_m,\ L_{33}^{ss} = \bar{L}_{ls}.$$

A.3. The stator-to-rotor qd0 mutual inductances

Because of rotor symmetry, the coefficients of stator-to-rotor mutual inductances can be simplified as

$N_{asar} = N_{asbr} = N_{ascr} = N_{asr}$, $N_{bsar} = N_{bsbr} = N_{bscr} = N_{bsr}$, and $N_{csar} = N_{csbr} = N_{cscr} = N_{csr}$,

and the transformation result is

$$L_{11}^{sr} = L_{asr} + .25L_{bsr} + .25L_{csr}$$

$$L_{12}^{sr} = \frac{\sqrt{3}}{4}(L_{bsr} - L_{csr})$$

$$L_{22}^{sr} = \frac{3}{4}(L_{bsr} + L_{csr})$$

$$L_{31}^{sr} = .5L_{asr} - .25L_{bsr} - .25L_{csr}$$

$L_{21}^{sr} = L_{12}^{sr}$, and $L_{32}^{sr} = -L_{12}^{sr}$. ----------(A.3.1)

When $N_a = N_b = N_c = N_s$,

$L_{asar} = L_{asbr} = L_{ascr} = L_{bsar} = L_{bsbr} = L_{bscr} = L_{csar} = L_{csbr} = L_{cscr}$ and mutual inductances will be

$L_{11}^{sr} = L_{22}^{sr} = \frac{N_r}{N_s} L_m$ and $L_{12}^{sr} = L_{21}^{sr} = L_{31}^{sr} = L_{32}^{sr} = 0.$

A.4. The rotor qd0 self- and mutual inductances

The rotor self- and mutual inductances are

$$L_{11}^{rr} = L_{22}^{rr} = L_{lr} + \frac{3}{2} L_{mar} = L_{lr} + \frac{N_r^2}{N_s^2} L_m$$

$$L_{33}^{rr} = L_{lr} \qquad \text{----------(A.4.1)}$$

A.5. Matrix elements for induction motor with inter-turn stator short circuit

The stator *qd* self- and mutual inductances:

From (7.2.1), the stator *qd* self- and mutual inductances can be defined as follows:

$$L_{11}^{ss} = \frac{2}{3}(L_{asas} + .5L_{bsbs} - 2L_{asbs} + .5L_{bscs})$$

$$= \frac{2}{3}\left[(L'_{asas} + .5(L_{bsbs} + L_{bscs}) - 2L'_{asbs}) + (L_{assh} - L_{shbs})\right] + \frac{2}{3}\left[L_{shsh} + (L_{assh} - L_{shbs})\right]$$

$$= (L_q^s + L_q^{ssh}) + (L_q^{sh} + L_q^{ssh})$$

$$L_{22}^{ss} = \frac{1}{2}(L_{bsbs} + L_{cscs} - 2L_{bscs}) = L_{bsbs} - L_{bscs}$$

$$= L_{ls} + L_m = L_d^s \qquad \text{-----(A.5.1)}$$

The stator-to-rotor *qd* mutual inductances:

From (7.3.1), the stator-to-rotor *qd* mutual inductances can be defined as follows:

$$L_{11}^{sr} = L_{asr} + .25L_{bsr} + .25L_{csr} = L_{asr} + .5L_{bsr}$$

$$= (L'_{asr} + .5L_{bsr}) + L_{shar} = L_q^{sr} + L_q^{shr}$$

$$L_{22}^{sr} = \frac{3}{4}(L_{bsr} + L_{csr}) = \frac{3}{2}L_{bsr} = L_d^{sr} \qquad \text{------(A.5.2)}$$

The rotor self- and mutual inductances and resistances will be the same as before.

A.6. Motor parameters

Line voltage - 460V

Full load linecurrent–4.7A

Horse power - 2 hp

Rated speed at60 Hz - 1752 rpm

Number of poles - 4

Total number of turns per phase – 252

Stator winding resistance - 4.05ohms

Stator leakage inductance - 13.97mH

Rotor resistance (stator referred) - 2.6*ohms*

Rotor leakage inductance(stator referred) - 13.97mH

Magnetising inductance - 538.68mH

Rotor inertia - 0.06 kgm^2